

68-10

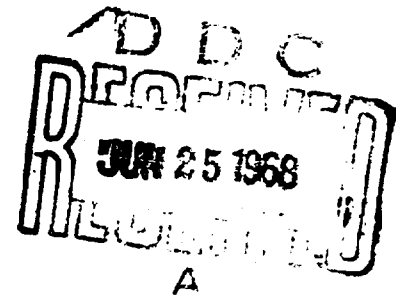
AD 670519

17,51854

RING-STIFFENED ORTHOTROPIC CIRCULAR CYLINDRICAL
SHELL UNDER HYDROSTATIC PRESSURE

by

Kempner, Joseph, Misovec, A. P. and Herzner, F. C.



POLYTECHNIC INSTITUTE OF BROOKLYN

DEPARTMENT
of
AEROSPACE ENGINEERING
and
APPLIED MECHANICS

Reproduced From
Best Available Copy

MAY, 1968

DISTRIBUTION OF THIS
DOCUMENT IS UNLIMITED

Reproduced by the
CLEARINGHOUSE
for Federal Scientific and Technical
Information

PIBAL REPORT No. 68-10

131

Contract No. Nonr 839(39)
Project No. NR 064-167

RING-STIFFENED ORTHOTROPIC CIRCULAR CYLINDRICAL
SHELL UNDER HYDROSTATIC PRESSURE

by

Kempner, Joseph, Misovec, A.P. and Herzner, F.C.

Polytechnic Institute of Brooklyn

Department of

Aerospace Engineering and Applied Mechanics

May 1968

PIBAL Report No. 68-10

Reproduction in whole or in part is permitted for any purpose of the United States Government. Distribution of this document is unlimited.

Reproduced From
Best Available Copy

ABSTRACT

A ring-reinforced, orthotropic circular cylindrical shell subjected to external hydrostatic pressure loading is investigated. The stresses and deflections throughout the shell are determined by a shell theory which considers the combined and separate effects of large rotations, transverse shear deformation, initial deflections and Flugge type thickness terms. The ring deformations are described by both a deep ring theory and a plane strain analysis. The results are used in the development of pertinent design formulae. Numerical results applicable to a typical glass-reinforced-plastic shell indicate that the nonlinear effects may be accurately provided for by using a perturbation solution. Hill's criterion for yielding of an orthotropic material as well as an analysis to approximate the actual stresses in the constituent materials of a nonhomogeneous shell are also applied.

LIST OF SYMBOLS

A	parameter measuring higher order effects in governing differential equation, Eq. (2.4)
\bar{A}, \bar{B}	arbitrary constants of integration in Lamé analysis of ring, Eqs. (3.10)
$A_x, A_\varphi, B_x, B_\varphi, C_\varphi, C_x, C_{xz}$	constants in elastic law relating stress resultants to strains and curvature change, Eqs. (2.13)
A_f	cross-sectional area of ring frame, Eq. (3.3)
B	parameter measuring coupling of beam column effect with transverse shear effect, Eq. (2.4)
$C_{1,2,3,4}$	arbitrary constants of integration of solution to governing differential equation of deflection, Eq. (4.7)
D_x	axial flexural rigidity of shell, Eq. (2.17)
D_x^*	modified flexural rigidity (includes Flugge and nonhomogeneous effects), Eq. (A.28)
E_x, E_φ	moduli of elasticity in axial and circumferential directions, respectively
$E_{\varphi^*}, E_\varphi^*$	modified elastic constants, Eq. (A.28)
E_{sf}, E_{Rf}	circumferential and radial elastic moduli of ring, respectively
F_s	circumferential force acting over ring cross section, Eq. (3.3)

F_1, F_2, F_3, F_4, F_5	functions of shell material, geometry and load, Eqs. (4.12)
G_{xz}	transverse shear modulus
G_{xz}^*	modified shear modulus, Eq. (A.28)
$K_{1,2,3}$	constants measuring ratio of ring deflection to interaction pressure corresponding to ring theory, isotropic and orthotropic Lamé analyses, respectively
L	length of unsupported shell between rings, Fig. 1
L_f	center to center distance between rings, Fig. 1
L_e	effective width of shell plating, Eq. (6.10)
M_x	axial bending moment per unit circumferential length
N_x	axial force per unit circumferential length
N_ϕ	circumferential force per unit axial length
Q	transverse shear force per unit circumferential length
Q_f	Q evaluated at the frame (i.e., at $x = \pm L/2$)
\bar{Q}_f	equivalent radial line load (per unit circumferential length) on ring, Eq. (6.2)

\bar{p}_h	equivalent line load on section of shell in contact with frame, Eq. (6.6)
\bar{p}_c	$= \bar{Q}_f + \bar{Q}_n$
\bar{R}	radius of datum circle in ring, Fig. 1
R	radial coordinate, Fig. 1
R_o, R_i	radii of outer and inner ring surfaces, respectively, Fig. 1
R_o', R_i'	radii of interior surfaces of outer and inner flanges of ring, respectively, Fig. 1
R_c	radius of surface of contact between ring and shell, Fig. 1
$W(x)$	nondimensional shell deflection parameter, Eqs. (5.3)
W_m, W_f	W at midbay and frame, respectively
$Y_x, Y_\varphi, Y_z, Y_{zx}$	axial, circumferential, radial and transverse shear yield stresses, respectively
z	radial ring coordinate measured positive inward from ring datum circle, Fig. 1
a	mean shell radius, Fig. 1
$a_x, a_{x\varphi}, b_{\varphi x}$ b_x, d_x	constants in elastic law relating stress resultants to strains and curvature change
b_c	faying width of ring, Fig. 2
b'	width of ring, Eq. (3.3)

b_w	width of ring web
b_o, b_i	widths of outer and inner flanges of ring, respectively, Fig. 2
b_o'	$b_o - b_w$
b_i'	$b_i - b_w$
c'	nondimensional geometric ring parameter, Eq. (3.4)
d	depth of the ring cross section, Fig. 2
f	plastic potential function of the stresses, Eq. (7.1)
$g_1(x), \dots, g_4(x)$	characteristic functions of shell differential equation, Eqs. (4.8)
g_{1f}, \dots, g_{4f}	characteristic function evaluated at $x = L/2$
h	shell wall thickness, Fig. 1
h_o, h_i	radial distances from datum circle to outer and inner surfaces of ring, respectively, Fig. 1
p	external hydrostatic pressure
p_o, p_o', p_i, p_i'	pressures acting on ring surfaces, Fig. 2
p^*	axisymmetric buckling pressure of an unstiffened orthotropic circular cylindrical shell under axial pressure, Eq. (6.15)
p_{cr}	axisymmetric buckling load of ring supported orthotropic circular cylindrical shell under hydrostatic pressure (6.16)

P_c	interaction pressure between ring and shell, Eq. (6.4)
$p_y(x,z), p_{y_1}(x,z)$	pressures required for shell to yield at the position (x,z) predicted by Hill's criterion and maximum stress criterion, respectively,, Eq. (7.3)
$p_{y_a}(x,z)$	approximate value of $p_y(x,z)$, Eq. (7.4)
$p_{y_0}(x), p_{y_1}(x,0)$	pressure at which yielding has penetrated through half the shell thickness, Eq. (7.5)
ds_0, ds_1	lengths of infinitesimal line element in shell wall prior to and after loading, respectively
t_o, t_i	thicknesses of outer and inner flanges of ring, respectively
u_m	axial displacement of shell median surface
u	axial displacement of point in shell wall
w	inward radial deflection of shell median surface measured from median surface prior to loading
w_0	initial deflection of median surface

w_R	inward radial displacement of ring outer surface, Fig. 1
w_s	inward radial displacement of length of shell in contact with ring
w_p	particular solution of governing differential equation
x, z	axial and inward radial coordinates measured from the median surface of the deformed shell at midbay, Fig. 1
x'	value of x at position of minimum bending stress, Eq. (6.9)
z_1	parameter
Δ	Inward initial deflection at midbay
Δ_0	initial deflection for which shell particular solution vanishes, Eq. (4.2b)
Δ_1	initial deflection for which the shell deforms without bending, Eq. (4.10c)
Δ_2	initial deflection for which interaction pressure vanishes, Eq. (6.4)
$\theta_{1,2,3,4,5}$	constants depending on yield stresses and Poisson ratios of shell material
$\Lambda(x)$	nondimensional shell curvature parameter, Eq. (5.3)

Λ_m, Λ_f	values of Λ at midbay and at frame, respectively
$\bar{\Lambda}, \Lambda^*$	ring-shell interaction parameters
ψ	parameter measuring higher order effects in governing differential equation
ψ_{cr}	values of ψ at buckling load
α	parameter measuring Flugge effect, Eq. (2.4)
$\alpha_c, \beta_c^*, \lambda^*$	nondimensional ring-shell interaction parameters
β_c	b_c/L_f
γ	measure of the beam-column effect, Eq. (2.4)
γ_{cr}	value of γ for which shell buckles
$\bar{\gamma}$	nondimensional load parameter, Eq. (2.4)
γ_{xz}	transverse shear strain
δ	$= h/2a$
δ^*	internal or external ring indicator
$\epsilon_x, \epsilon_\varphi$	axial and circumferential strain components, respectively
$\epsilon_{x_0}, \epsilon_{\varphi_0}$	axial and circumferential median surface strain components, respectively, Eq. (2.12)

ϵ_s	circumferential strain in the length of shell in contact with the ring
ϵ_R	radial ring strain
(ζ_0, ξ_0) (ζ_1, ξ_1)	inward radial and axial coordinates, measured from midbay at the median surface of a perfect cylindrical shell, to points on the shell before (zero subscript) and after (one subscript) deformation, Eqs. (A.1), (A.1)
$\eta_{1,2}$	real and imaginary components of roots of characteristic equation, Eq. (4.5)
η_1^i	$= -i\eta_1$
θ	shell flexibility parameter $\{= L^4[hE_\phi^*/4a^2D_x^*]^{1/4}\}$, Eq. 1
$\lambda_{1,2,3,4}$	roots of characteristic equation
λ	nondimensional ring material parameter, Eq. (4.4)
λ^*	nondimensional ring shell interaction parameter
$\nu_{x\phi}, \nu_{\phi x}, \nu$	Poisson ratios of shell material
$\nu_{\phi x}^*$	modified Poisson ratio, Eq. (2.17)
$\nu_{R_{sf}}, \nu_{\epsilon_{Kf}}, \nu_f$	ring Poisson ratios
ξ	nondimensional measure of the transverse shear effect

σ_x, σ_φ

axial and circumferential shell normal stresses

$\sigma_{x_b}, \sigma_{\varphi_b}$

axial and circumferential bending stresses

σ_r, σ_φ

radial and circumferential normal stresses in ring, respectively

σ'_{φ_M}

shell circumferential membrane stress due to axial bending

τ_{xz}

transverse shear stress

φ

circumferential cylindrical coordinate

ω

axial rotation (measured with respect to initially deformed cylinder)

1. INTRODUCTION

Attempts to design submersible vehicles capable of extended lateral excursions at great depths have led to extensive research on ring-reinforced cylindrical shells constructed of filament wound composites. This material is relatively easy to fabricate and possesses a much higher strength-to-weight ratio than the commonly used metals. The shells (and ring-supports) are formed by winding strong glass fibers about a cylindrical mandrel and either impregnating or preimpregnating them with an epoxy resin.

For many applications the shell material as described above may be considered as orthotropic and nonhomogeneous through the thickness. For deep-submergence vehicles the shell thickness must be relatively large in order to withstand severe pressures. Observed shell failures indicate that transverse shear may be a significant factor of the collapse mechanism (Ref. 1). Furthermore, built-in outward initial deflections may enable the designer to utilize the "beam-column" effect to strengthen the shell. Thus, the analysis presented here considers the separate and combined influence of these effects on the stress state of the shell.

Numerical results demonstrate that the more accurate calculation of the cross-sectional area of the shell (which increases the axial stress resultant) is the only significant thick shell correction. It is found that the stresses do change when transverse shear is considered. However, the comparison made with the three-dimensional elasticity analysis developed in Ref. 2 indicates that no improvement is obtained by permitting transverse shear deformations.

Because of the low radial yield stresses of the composite, yielding (as described by Hill's orthotropic criterion) can begin well in advance of experimentally obtained collapse loads. The elastic region is thus confined to relatively low pressures. This, in turn, keeps the deflection small enough to avoid any significant beam-column effects. Initial deflections, on the other hand may be large enough to cause substantial beam-column effects even at relatively low pressures. Thus, initial deflections could affect the stresses and hence change the value of the load for which yielding begins.

To obtain accurate estimates of the stresses in the constituent materials it is necessary to consider the nonhomogeneous nature of the structure. When the stresses are thus obtained and utilized in a maximum stress yield criterion, the yield pressures obtained are reasonably close to the experimental collapse pressure.

The deformation of the reinforcing frames are, in general, adequately described by ring theory (which permits only circumferential stress). However, the frames of interest here are constructed of an orthotropic material for which radial deformations may become significant. For this reason a more accurate plane strain analysis is performed, in addition to the ring analysis, and a comparison is made for internal frames of rectangular cross section. Excellent agreement is found for a particular ring considered in this work.

Designers of present day submersibles are familiar with the formulae first developed for thin, isotropic metal shells by van Sanden and Gunther (Ref. 3), which were later modified by Viterbo (Ref. 4), and finally by Pulos and Salerno (Ref. 5). The results presented here represent an ex-

tension of the work of Ref. 5 in that the formulae obtained therein for use of metal shells are modified to include more complicated filament wound composite shells. These include solutions for various stresses, points of minimum bending, ring-shell interaction pressure, axisymmetric buckling loads, effective width of shell plating, stress in the reinforcing rings, yield pressure and the location at which yielding begins.

2. Governing Shell Equations

The differential equations of equilibrium of a circular cylindrical, orthotropic, ring-supported shell subjected to hydrostatic pressure loading are found to be [see Fig. 1 and Appendix A; Eqs. (A.20), (A.31) and (A.33)]

$$w_{,xxxx} + 4(\theta/L)^2 (A/B) w_{,xx} + 4(\theta/L)^4 w/B = (4\gamma\xi/B) w_{o,xxxx} - [4\gamma(\theta/L)^2/B] w_{o,xx} + 8(\theta/L)^2 \gamma [1 - (\nu_{\phi\phi}^*/2)(1+\delta)]/aB(1+\delta) \quad (2.1)$$

$$\omega_{,x} = \{Bw_{,xx} - 4\xi(\theta/L)^2 w + 8\gamma\xi [1 - (\nu_{\phi\phi}^*/2)(1+\delta)]/a(1+\delta) - 4\gamma\xi w_{o,xx}\}/(1+2\alpha\xi) \quad (2.2)$$

The associated conditions at the shell boundaries $x = \pm L/2$ are

$$w = w_s = w_R \quad (2.3a)$$

$$\omega = 0 \quad (2.3b)$$

In Eqs. (2.1) to (2.3) w is the inward deflection of the shell median surface from the initially deformed shape and ω is the additional rotation of the median surface normal about a circumferential tangent; w_R is the inward radial ring displacement at the contact surface between the ring and the shell and w_s is the inward deflection of the section of shell in contact with the ring.

Also,

$$A = \gamma - \xi + \alpha \quad B = 1 - 4\gamma\xi \quad (C/L)^4 = hE_{\varphi}^*/4a^2D_x^*$$

$$\gamma = \bar{\gamma} = -N_x/4D_x^*(\theta/L)^2 \quad \xi = (\theta/L)^2 D_x^*/hG_{xz}^*$$

$$\alpha = a\delta^3 E_{\varphi x}^*/3D_x^*(\theta/L)^2 \quad \delta = h/2a \quad (2.4)$$

The quantities E_{φ}^* , D_x^* , $E_{\varphi x}^*$ and G_{xz}^* represent standard stiffness parameters of a shell whose material properties vary through the shell thickness h [see Eqs. (A.28)]; a is the average radius and L is the length of the unsupported shell (see Fig. 1). N_x is the axial stress resultant, which for this problem was found to be closely approximated by the constant (see Eq. A.26)

$$N_x = - (pa/2)(1 + \delta)^2 \quad (2.5)$$

The parameters γ , ξ , α and δ represent the effects described in the introduction:

1. $\bar{\gamma} \neq 0$, $\gamma \equiv 0$ Beam-Column effects neglected
2. $\xi \equiv 0$ Transverse shear deformations neglected
3. $\alpha \equiv \delta \equiv 0$ Plugge thickness terms neglected.

Hence, in the analysis which follows it is possible to evaluate the individual and combined nature of these effects. In Appendix A the necessary procedures required to reduce the governing equations (2.1 and 2.2) both to those obtained in Ref. 1 and to those deduced in Ref. 6 are discussed.

6.

Since condition (2.3a) depends upon the ring support, the ring-shell interaction problem will be investigated before a solution is attempted.

3. RING-SHELL INTERACTION

The rings considered are assumed to be constructed of a linearly elastic homogeneous material and to have cross sections of the generalized "I" type. If a ring is assumed to resist its loading with only a circumferential stress, the corresponding strain is

$$\epsilon_s = -w_R/(\bar{R} - Z) \quad (3.1)$$

where w_R is the radial displacement (positive inward); \bar{R} is the radius of a datum circle. Z is the radial coordinate measured positive inward from the datum circle. The circumferential stress is given by

$$\sigma_s = E_{sf}\epsilon_s = -(E_{sf}w_R)/(\bar{R} - Z) \quad (3.2)$$

E_{sf} is the modulus of elasticity in the circumferential direction. The corresponding hoop force is

$$F_s = \int_{-h_0}^{h_i} \sigma_s b(Z) dZ = -E_{sf}A_f c' (w_R/\bar{R}) \quad (3.3)$$

where $b(Z)$ is the width of the ring at Z ; h_0 and h_i are the radial distances from the datum circle to the outer and inner ring surfaces, respectively, and A_f is the ring cross-sectional area. The nondimensional parameter c' is defined by

$$c' = \frac{\bar{R}}{A_f} \int_{-h_0}^{h_i} b(Z)/(\bar{R} - Z) dZ \quad (3.4)$$

and depends only upon the geometry of the ring cross section. Appendix B, taken from Ref. [7], evaluates c' for different types of 'I' ring cross sections.

The hoop force F_s acting on the ring is easily obtained by cutting the ring in half and finding F_s necessary to maintain equilibrium (Fig. 2b). This leads to

$$F_s = \bar{R} \left[p_o' b_o' \left(1 + \frac{h_o - t_o}{R} \right) + p_i b_i \left(1 - \frac{h_i}{R} \right) - p_o b_o \left(1 + \frac{h_o}{R} \right) - p_i' b_i' \left(1 - \frac{h_i - t_i}{R} \right) \right] \quad (3.5a)$$

where

$$b_o' = b_o - b_w \quad (3.5b)$$

$$b_i' = b_i - b_w \quad (3.5c)$$

b_w is the web width, b_o and b_i are the outer and inner flange widths, respectively; and t_o and t_i are the thicknesses of the outer and inner flanges, respectively. p_o , p_o' , p_i , p_i' denote pressures; the subscripts o and i denote the outer and inner flanges, respectively, while the prime superscript denotes the surface of the flange nearest to the datum circle (see Fig. 2).

If the frame acts on the inner shell surface,

$$p_i = p_i' = p_o' = 0 \quad (3.6a)$$

$$p_o = p_c \quad (3.6b)$$

$$b_c = b_o \quad (3.6c)$$

If the frame acts on the outer shell surface,

$$p_i' = p_o' = p_o = p. \quad (3.7a)$$

$$p_i = p_c \quad (3.7b)$$

$$b_c = b_i \quad (3.7c)$$

p_c is the interaction or contact pressure between the ring and the shell. b_c is the faying width of the contact surface between the ring and the shell.

If F_s is eliminated between Eqs. (3.5a) and (3.3), a relation between the radial ring displacement and pressure loads is found

$$w_R = - \bar{R} [p_o' R_o' b_o' + p_i R_i b_i - p_o R_o b_o - p_i' b_i' R_i'] / (E_{sf} A_f c') \quad (3.8a)$$

where

$$R_o' = R_o - t_o \quad (3.8b)$$

$$R_i' = R_i + t_i \quad (3.8c)$$

and R_o and R_i are the radii to the outer and inner ring surfaces, respectively.

A more accurate description of an orthotropic ring of rectangular cross section may be obtained by permitting radial strains in addition to hoop strain via a Lamé plane strain analysis. The field equations necessary to describe such ring deformations are

$$\epsilon_R = -w_{R,R} \quad (3.9a)$$

$$\epsilon_S = -w_R/R \quad (3.9b)$$

$$\epsilon_R = (\sigma_R - \nu_{Rsf} \sigma_S)/E_{Rf} \quad (3.9c)$$

$$\epsilon_S = \frac{1}{1} (\sigma_S - \nu_{SRf} \sigma_R)/E_{sf} \quad (3.9d)$$

$$(R\sigma_R)_{,R} - \sigma_S = 0 \quad (3.9e)$$

R is the radial coordinate measured from the center line of the ring, E_{Rf} , E_{sf} , ν_{Rsf} , ν_{SRf} are the elastic constants of the ring. The solution is

$$\sigma_R = E_{Rf} [-\bar{A}(\lambda + \nu_{SRf})R^{\lambda-1} + \bar{B}(\lambda - \nu_{SRf})R^{-\lambda-1}]/(1 - \nu_f^2) \quad (3.10a)$$

$$\sigma_S = E_{sf} [-\bar{A}(\lambda \nu_{Rsf} + 1)R^{-\lambda-1} + \bar{B}(\lambda \nu_{Rsf} - 1)R^{\lambda-1}]/(1 - \nu_f^2) \quad (3.10b)$$

$$w_R = \bar{A}R^\lambda + \bar{B}R^{-\lambda} \quad (3.10c)$$

where, for an internal frame

$$\bar{A} = [P_c (1 - \nu_f^2) R_o^{1-\lambda}] / [E_{Rf} (\lambda + \nu_{sRf}) \{1 - (R_i/R_o)^{2\lambda}\}] \quad (3.10d)$$

$$\bar{B} = [P_c (1 - \nu_f^2) R_o^{1+\lambda}] / [E_{Rf} (\lambda - \nu_{sRf}) \{(R_o/R_i)^{2\lambda} - 1\}] \quad (3.10e)$$

$$\lambda^2 = E_{sf} / E_{Rf} \quad (3.10f)$$

$$\nu_f^2 = \nu_{sRf} \nu_{Rs_f} \quad (3.10g)$$

Thus, for an internal frame the relation between interaction pressure and the radial displacement of the frame outer surface is expressed by

$$\begin{aligned} (E_{sf} w_R / P_c R_o) &= \{\lambda^2 (1 - \nu_f^2) [(\lambda - \nu_{sRf}) + (\lambda + \nu_{sRf}) (1 - d/R_o)^2] \\ &\quad \div \{(\lambda + \nu_{sRf}) (\lambda - \nu_{sRf}) [1 - (1 - d/R_o)^{2\lambda}]\} = K_3 \end{aligned} \quad (3.11)$$

where d is the depth of the ring cross section.

For an isotropic material

$$(E_{sf} w_R / P_c R_o) = \{[(1 - \nu_f) + (1 + \nu_f) (1 - d/R_o)^2] / [1 - (1 - d/R_o)^2]\} = K_2 \quad (3.12)$$

For an internal, rectangular cross section frame, ring theory gives [see Eq. (2.8)]

$$(E_{sf} w_R / P_c R_o) = - (2 - d/R_o) / \{(d/R_o) [2 + (1/6) (d/R_o)^2 (1 - d/R_o)^2]\} = K_1 \quad (3.13)$$

A comparison of the two solutions may be obtained from Eqs. (3.12) and (3.13)

$$1 - (K_2/K_1) \approx \nu \left(\frac{d}{R} \right) + O \left[\left(\frac{d}{R} \right)^2 \right] \quad (3.14)$$

Thus, for thin isotropic rings the two solutions are in very good agreement. Furthermore, when the orthotropic Lamé solution is compared with the ring solution, the agreement is even better for the particular shell examined in this work.

The radial ring displacement and shell deflection must be matched at the shell boundaries. Because the shell theory used here cannot describe the radial changes in stresses that occur in the shell region in contact with the ring, that length of the shell is treated separately with a simple analysis. Since the ring and shell are bonded together, and classical ring theory does not provide for distortion of the ring flanges, the assumption is made that the portion of the shell in contact with the ring does not bend. With this assumption, equilibrium of radial forces leads to (see Fig. 2c)

$$b_c N_s - 2Q_f a + [(1+\delta)p\delta^* + (1+\delta-2\delta^*)p_c]ab_c = 0 \quad (3.15)$$

where

$$\delta^* = \begin{cases} 1 & \text{for internal frame} \\ 0 & \text{for external frame} \end{cases}$$

(continued on next page)

$$b_c = \begin{cases} b_o & \text{for internal frame} \\ b_i & \text{for external frame} \end{cases} \quad (3.16)$$

and from Eq. (A.27b) and the above assumption

$$\frac{w_s}{a} = - (N_s - v_{\phi x}^* N_x) / h E_{\phi}^* \quad (3.17)$$

Combining Eqs. (3.15) and (3.17) to eliminate N_s yields

$$w_s = (a^2 / h E_{\phi}^*) [(1+\delta) p \delta^* + p_c (1+\delta-2\delta^*) - (2Q_f / b_c) + v_{\phi x}^* (N_x / a)] \quad (3.18)$$

The matching conditions are that

$$w_R = w_s \quad (3.19a)$$

$$w_s = w_f \quad (3.19b)$$

Equation (3.19a) is used to satisfy the boundary condition Eq. (A.20b). Eq. (3.19a), combined with Eqs. (3.18) and (3.13), leaves an expression for the interaction pressure in terms of quantities which can be determined from the shell solution

$$p_c = (\alpha_c / \beta_c^*) \{ -(2Q_f / b_c) + v_{\phi x}^* (N_x / a) + p [(1+\delta) \delta^* + \lambda^*] \}$$

where

$$\lambda^* = (\beta_c / \alpha_c) (1 - \delta^*) [(A_f / b_c R_c) - 1]$$

$$\beta_c = b_c / L_f$$

$$\alpha_c = (E_{\varphi_f} A_f c' a^2) / (E_{\varphi}^* h L_f \bar{R} R_c)$$

$$L_f = L + b_c$$

$$R_c = \begin{cases} R_o & \text{for internal frame} \\ R_i & \text{for external frame} \end{cases}$$

$$\beta_c^* = (2\delta^* - 1) (\alpha_c + \beta_c) - \alpha_c \delta \quad (3.20)$$

The N_x term in Eq. (3.17) corresponds to the "Viterbo effect" (Ref. 4) in that it accounts for the two-dimensional nature of the stresses in the straight section of the shell adjacent to the ring.

4. SOLUTION OF GOVERNING SHELL EQUATIONS

The solution of Eqs. (2.1) and (2.2) subject to boundary condition Eqs. (2.3) can now be obtained. Lunchick and Short, Ref. (8) suggested that the initial deflections encountered in isotropic metal shells could be approximated by a simple parabolic function which would ensure constant axial curvature. This form is assumed here; thus

$$w_0 = \Delta[1 - 4(x/L)^2] \quad (4.1)$$

where Δ is a constant equal to the largest value of w_0 (at midbay). With the type of initial deflection described in Eq. (4.1), a particular solution to Eq. (2.1) is

$$w_p = 8(\gamma\Delta - \bar{\gamma}\Delta_p)/\theta^2 \quad (4.2a)$$

where

$$\Delta_p = -L^2[1 - (\nu_{\phi}^*/2)(1 + \delta)]/4a(1 + \delta) \quad (4.2b)$$

If the complementary solution of Eq. (2.1) is assumed to have the form

$$w \sim e^{\lambda x} \quad (4.3)$$

The characteristic equation becomes

$$\lambda^4 + 4(\theta/L)^2 (A/B) \lambda^2 + 4(\theta/L)^4/B = 0 \quad (4.4)$$

with the four roots

$$\lambda_{1,2,3,4} = \pm (\theta/L) \sqrt{2/B} \sqrt{-\psi \pm \sqrt{\psi^2 - 1}} \quad (4.5a)$$

or

$$\lambda_{1,2,3,4} = \pm 2(\theta/L) (\eta \pm i\eta_2) \quad (4.5b)$$

where

$$\eta_{1,2} = \sqrt{1 \mp \psi} / (2\sqrt{B}) \quad (4.5c)$$

$$\psi = A/\sqrt{B} \quad (4.5d)$$

Numerical results demonstrate that for the range of ξ and α of interest in this report, the shell reaches a yield condition while γ , ξ and α are in the region defined by $\psi^2 < 1$. Moreover, in this region the following special cases can be obtained:

1. Neglect beam-column effect by setting $\gamma = 0$
2. Neglect transverse shear effect by setting $\xi = 0$
3. Neglect Flugge type corrections by setting $\alpha = 0$ and $\delta = 0$.

Therefore, the only solution considered in this work will satisfy the inequalities $0 < \psi^2 < 1$ and $B > 0$. The final form of the solution depends on whether:

$$B \begin{matrix} \geq \\ < \end{matrix} 0 \quad (4.6a)$$

$$\psi = 0 \quad (4.6b)$$

or

$$0 < \psi^2 < 1 \quad (4.6c)$$

Thus, the solution of Eq. (2.1) can be written in the real form

$$w(x) = w_p \left[1 + \sum_{i=1}^4 c_i g_i(x) \right] \quad (4.7)$$

where

$$g_1(x) = \sinh(2\eta_1 \theta x/L) \cos(2\eta_2 \theta x/L)$$

(continued on next page)

$$g_2(x) = \sinh(2\eta_1 \theta x/L) \sin(2\eta_2 \theta x/L)$$

$$g_3(x) = \cosh(2\eta_1 \theta x/L) \sin(2\eta_2 \theta x/L)$$

$$g_4(x) = \cosh(2\eta_1 \theta x/L) \cos(2\eta_2 \theta x/L) \quad (4.8)$$

c_i represents four arbitrary constants of integration. Symmetry demands that (see Fig. 1)

$$c_1 = c_3 = 0 \quad (4.9)$$

The constants c_2 and c_4 are determined by using the boundary conditions defined by Eqs. (2.3) in conjunction with Eqs. (3.18), (3.20), (A.34), (A.35), (4.2), (4.7) (4.8), and (4.9). Hence,

$$c_4 = -\Lambda^* (\gamma \Delta - \bar{\gamma} \Delta_1) / (\gamma \Delta - \bar{\gamma} \Delta_p) \quad (4.10a)$$

where

$$\Lambda^* = \beta_c^* B G_2 / \{ B \beta_c^* + G_1 (1 - \beta_c) [\beta_c^* + (1 + \delta - 2\delta^*) \alpha_c] / \beta_c \} \quad (4.10b)$$

$$\Delta_1 = \Delta_p + L^2 \{ [1 + (1 + \delta - 2\delta^*) (\alpha_c / \beta_c^*)] [\delta^* - (v_{\varphi x} / 2) (1 + \delta)]$$

$$+ \alpha_c \lambda^* / [\beta_c^* (1 + \delta)] \} / 4\alpha (1 + \delta) \quad (4.10c)$$

Also,

$$c_2/c_4 = [(G_4/G_2) + \psi]/4B\eta_1\eta_2 \quad (4.11)$$

where

$$G_1 = [(4/\theta)(g_{30}^2 + g_{10}^2)] / [(B_1/\eta_1)(g_{30}g_{20} + g_{10}g_{40}) + (B_2/\eta_2)(g_{30}g_{40} - g_{10}g_{20})] \quad (4.12a)$$

$$G_2 = [(B_1/\eta_1)g_{10} + (B_2/\eta_2)g_{30}] / [(B_1/\eta_1)(g_{30}g_{20} + g_{10}g_{40}) + (B_2/\eta_2)(g_{30}g_{40} - g_{10}g_{20})] \quad (4.12b)$$

$$G_3 = \{ (1/\eta_2)(g_{40}g_{30} - g_{10}g_{20})(B_1 + 4\xi\psi) - (1/\eta_1)(g_{30}g_{20} + g_{10}g_{40})(B_2 + 4\xi\psi) \} / [(B_1/\eta_1)(g_{30}g_{20} + g_{10}g_{40}) + (B_2/\eta_2)(g_{30}g_{40} - g_{10}g_{20})] \quad (4.12c)$$

$$G_4 = [(B_1/\eta_2)g_{30} - (B_2/\eta_1)g_{10}] / [(B_1/\eta_1)(g_{30}g_{20} + g_{10}g_{40}) + (B_2/\eta_2)(g_{30}g_{40} - g_{10}g_{20})] \quad (4.12d)$$

$$B_1 = 1 - 2\xi[2\xi - 2\alpha - (1-2\psi)] \quad (4.12e)$$

$$B_2 = 1 - 2\xi[2\xi - 2\alpha + (1+2\psi)] \quad (4.12f)$$

$$g_{10}, g_{20}, g_{30}, g_{40} = g_1(L/2), g_2(L/2), g_3(L/2), g_4(L/2) \quad (4.12g)$$

The function G_3 is presented prematurely here in order to list the complete set of G_i , which is used subsequently. The functions are similar to those plotted as functions of γ and θ for the isotropic case [see Ref. 5 and App. D, Eqs. (D12)], where the effects of transverse shear and Flügge terms were not considered (i.e., $\xi = \delta = \alpha = 0$). When these effects are accounted for, these functional relationships change in that $G_i = G_i(\gamma, \theta, \xi, \delta, \alpha)$.

It is interesting to note that in their work on isotropic shells Luncheon and Short, Ref. (8), neglected transverse shear effects and found a "critical" initial deflection parameter such that the shell deforms without bending (i.e., $\omega_{,x} = 0$). This parameter, modified here to include orthotropic effects and thick-shell terms, which results from consistently maintaining Flügge accuracy, is now given by Δ_1 [Eq. (4.10c)].

The deflection may now be expressed as

$$w = [8(\gamma\Delta - \bar{\gamma}\Delta_p)/\theta^2] \{ 1 - [(\gamma\Delta - \bar{\gamma}\Delta_1)/(\gamma\Delta - \bar{\gamma}\Delta_p)] [g_4(x) + (g_2(x)/4B\eta_1\eta_2) (\frac{G_4}{G_2} + \psi)] \Lambda^{\frac{1}{2}} \} \quad (4.13)$$

and the change in curvature as

$$\begin{aligned} \omega_{,x} = & - (32\Lambda^{\frac{1}{2}}/L^2) (\gamma\Delta - \bar{\gamma}\Delta_1) \{ - [(\psi \frac{G_4}{G_2} + 1)/2 + \xi (\frac{G_4}{G_2} + \psi)] [g_2(x)/4B\eta_1\eta_2] \\ & + (\frac{G_4}{2G_2} - \xi) g_4(x) \} / (1 + 2\alpha\xi) \end{aligned} \quad (4.14)$$

The shear stress resultant at the frame is obtained by combining Eqs. (A.27c), (4.10), (4.13) and (2.3b). Hence,

$$Q_f/N_x = \frac{4G_1\Lambda^*}{8G_2L} [(\gamma/\gamma)\Delta - \Delta_1] \quad (4.15)$$

5. STRESSES IN SHELL

The stress-displacement relations are obtained by combining Eqs. (A.5), (A.21) and (A.23); hence,

$$\sigma_x = [E_x / (1 - \nu^2)] [\epsilon_{x_0} - \nu_{\varphi x} w / (a - z) - z \omega_{,x}] \quad (5.1a)$$

$$\sigma_\varphi = [E_\varphi / (1 - \nu^2)] [-w / (a - z) + \nu_{x\varphi} (\epsilon_{x_0} - z \omega_{,x})] \quad (5.1b)$$

From Eqs. (2.11a) and (2.17)

$$\epsilon_{x_0} = (1/a_x) [N_x + a_{x\varphi} (w/a) + b_{x\omega} \omega_{,x}] \quad (5.2)$$

It should be noted that the entire analysis to this point can be applied to a shell which is inhomogeneous through the thickness. In an actual filament wound composite shell, the elastic constants are discontinuous functions of the thickness coordinate z ; hence, the actual stresses are discontinuous functions of this coordinate. In the present analysis the less complex state of stress in an equivalent homogeneous material will be computed. The stresses in the actual (nonhomogeneous) shell are approximated in Appendix E, in which suitable multipliers (stress concentration factors) are utilized.

Equations (5.1) and (5.2) combine to yield, for a homogeneous material,

$$\frac{\sigma_x h}{N_x} = 1 - \frac{4\delta^2 \nu_{\varphi x}}{1 - 2\delta (\frac{z}{h})} (\frac{z}{h}) W - (\frac{\delta}{3} + \frac{2z}{h}) \Lambda \quad (5.3a)$$

$$\frac{\sigma_\varphi h}{N_x} = \nu_{\varphi x} \left\{ 1 - \frac{(h/a)}{\nu_{x\varphi}} \left[\frac{1 + 2\delta (\frac{\nu^2}{1 - \nu^2}) (\frac{z}{h})}{1 - 2\delta (\frac{z}{h})} \right] W - (\frac{\delta}{3} + \frac{2z}{h}) \Lambda \right\} \quad (5.3b)$$

where

$$W(x) = E_x w(x) / N_x \quad (5.3c)$$

$$\Lambda(x) = [E_x h^2 / 2(1 - \nu^2) N_x] \omega_{,x} \quad (5.3d)$$

The shear stress is assumed to be parabolically distributed across the shell thickness, i.e.,

$$\tau_{xz} = \frac{3}{2} (Q/h) [1 - 4(z/h)^2] \quad (5.4)$$

Thus, the maximum shear stress occurs at the median surface. At the frame, this stress is

$$\frac{\tau_{xz} h}{N_x} = \frac{6G_1 \Lambda^*}{LBG_2} [(\gamma/\bar{\gamma})\Delta - \Delta_1] \quad (5.5)$$

The direct stresses can be separated into their membrane and bending components; thus,

$$\left(\frac{\sigma_x h}{N_x}\right)_{\text{membrane}} = 1 - \delta\Lambda/3 \quad (5.6a)$$

$$\left(\frac{\sigma_\phi h}{N_x}\right)_{\text{membrane}} = v_{\phi x} [1 - (h/a)W/v_{x\phi} - \delta\Lambda/3] \quad (5.6b)$$

$$\left(\frac{\sigma_x h}{N_x}\right)_{\text{bending}} = - (4\epsilon^2 v_{\phi x} W + \Lambda) (2z/h) \quad (5.6c)$$

$$\left(\frac{\sigma_\phi h}{N_x}\right)_{\text{bending}} = - v_{\phi x} \left[\frac{\epsilon(h/a)}{v_{x\phi}(1-v^2)} W + \Lambda \right] (2z/h) \quad (5.6d)$$

in which the approximation that

$$\frac{1}{1 - 2\delta(\frac{z}{h})} \approx 1 + 2\delta(\frac{z}{h}) \quad (5.6e)$$

has been used. A shell subjected to the symmetric type of load-support system described here will usually develop its largest stresses either at midbay or at the frame. Therefore, the computations in this work will be at these stations. Hence, it is convenient to list the nondimensional parameters

$$W_m = -8\left(\frac{a}{L}\right)^2 \frac{E_x}{E_\phi^*} \left[\left(\frac{\gamma \Delta - \Delta_0}{h} \right) - \left(\frac{\gamma \Delta - \Delta_1}{h} \right) \Lambda^{**} \right] \quad (5.7a)$$

$$\Lambda_m = \frac{8\left(\frac{h}{a}\right)^2 \left(\frac{a}{L}\right)^4 \theta^2 E_x}{(1-\nu^2) E_\phi^*} \left[\left(\frac{\gamma \Delta - \Delta_1}{h} \right) (G_4 - 2G_2) \frac{\Delta^{**}}{G_2} \right] \quad (5.7b)$$

$$W_f = -8\left(\frac{a}{L}\right)^2 \frac{E_x}{E_\phi^*} \left[\left(\frac{\gamma \Delta - \Delta_0}{h} \right) - \left(\frac{\gamma \Delta - \Delta_1}{h} \right) \frac{\Delta^{**}}{G_2} \right] \quad (5.7c)$$

$$\Lambda_f = \frac{8\left(\frac{h}{a}\right)^2 \left(\frac{a}{L}\right)^4 \theta^2 E_x}{(1-\nu^2) E_\phi^*} \left[\left(\frac{\gamma \Delta - \Delta_1}{h} \right) (G_3 - 2G_2) \frac{\Delta^{**}}{G_2} \right] \quad (5.7d)$$

where the subscripts m and f imply that the function is calculated at the midbay and frame shell stations, respectively. The stresses can be calculated by substituting Eqs. (5.7) into (5.3) [or (5.6), if the membrane and bending stresses are desired].

The beam-column term γ , in the absence of transverse shear and initial deflections, has been shown to have little effect on the stresses in the primary region of interest [see Ref. 7]. However, the combined

effects of beam-column and initial deflection terms ($\frac{\gamma}{\gamma} \Delta$), or of beam-column and transverse shear terms ($\gamma \xi, \theta$), can be substantial. This can be seen from an examination of Eqs. (5.57) and (5.6). For example, the bending stresses become extremely small in the neighborhood of $\Delta = \Delta_1$ (they vanish when Flugge terms are neglected). When transverse shear deformation is considered the bending stresses may be considerably affected, depending upon the magnitude of ξ .

6. DESIGN FORMULAE

The shell stresses and deflections may now be utilized to develop convenient formulae for several quantities which may be of interest to the designers.

A. Circumferential Normal Stress in Ring

Combining Eqs. (A.26), (3.2), (3.19) and (5.7c) yield the following expression for the circumferential normal stress in a ring:

$$\begin{aligned}\sigma_s &= - (E_{\phi f}/E_x) (N_x/h) [w_f/(\bar{R} - Z)] \\ &= \left(-\frac{N_x}{h}\right) \left(\frac{E_{\phi f}}{E_{\phi}^*}\right) \frac{32 \left(\frac{a}{L}\right)^2}{(\bar{R}-Z)} \left[\left(\frac{\frac{Z}{2} \Delta - \Delta_0}{h}\right) - \left(\frac{\frac{Z}{2} \Delta - \Delta_1}{h}\right) \Lambda^{**} \right]\end{aligned}\quad (6.1)$$

B. Equivalent Line Load on Ring

If a line load \bar{Q}_f acting at the ring datum circle is made statically equivalent to the total inward radial load acting on a ring segment, then radial equilibrium gives

$$\bar{Q}_f = - F_s/\bar{R} \quad (6.2)$$

Then Eqs. (6.2), (3.3), (3.4) and (6.1) combine to yield

$$\bar{Q}_f = \left(-\frac{N_x}{h}\right) \left(\frac{E_{\phi f}}{E_{\phi}^*}\right) \left(\frac{A_f c'}{\bar{R}^2}\right) 32 \left(\frac{a}{L}\right)^2 \left[\left(\frac{\frac{Z}{2} \Delta - \Delta_0}{h}\right) - \left(\frac{\frac{Z}{2} \Delta - \Delta_1}{h}\right) \Lambda^{**} \right] \quad (6.3)$$

where \bar{Q}_f is chosen positive in the inward radial direction.

C. Interaction Pressure

The interaction pressure may be calculated from Eqs. (3.20) and (4.15). Hence,

$$p_c = p(1+\delta)^2 (\alpha_c/\beta_c^*) \left[\frac{4a}{L^2} \left(\frac{1-\beta_c}{\beta_c} \right) \frac{\Delta_1^*}{B} \frac{G_1}{G_2} \right] [(\gamma/\bar{\gamma})\Delta - \Delta_2] \quad (6.4)$$

where

$$\begin{aligned} \Delta_2 = \Delta_0 - L^2 \beta_c B [\delta^* - (v_{\phi}^*/2)(1+\delta)] / 4a(1+\delta)(1-\beta_c)G_1 \\ - \lambda^* L^2 / 4a(1+\delta)^3 [1 + B\beta_c/(1-\beta_c)G_1] \end{aligned} \quad (6.5)$$

Thus, for a large enough outward initial deflection (Δ_2), the interaction pressure vanishes and the frame would be ineffective.

D. Equivalent Line Load on Effective Ring

The line load acting on the section of shell in contact with the frame is defined to act at \bar{R} and to be statically equivalent to the radial loads acting on this shell section.

$$\bar{Q}_h = (ab_c/\bar{R}) \{ p\delta^* - p_c [2\delta^* - (1+\delta)] - (2Q_f/b_c) \} \quad (6.6)$$

where p_c and Q_f are obtained from Eqs. (6.4) and (4.15), respectively.

If the ring and the section of shell attached to it are considered together as an "effective ring", the line load acting at \bar{R} which is statically equivalent to the applied radial loads is obtained from

$$\bar{Q}_c = \bar{Q}_f + \bar{Q}_h \quad (6.7)$$

E. Axial Location of Vanishing Curvature Change

It may be of interest to the designer to know positions along shell generators at which the bending stresses are negligible. An investigation of Eqs. (5.6c) and (5.6b) reveals that the bending stresses become higher order when the change in curvature vanishes, i.e., when

$$\Lambda = 0 \quad (6.8a)$$

or

$$\omega_{,x} = 0 \quad (6.8b)$$

Equation (6.8b) and Eq. (4.14) then combine to give the equation to determine the point x' at which the change in curvature vanishes. Hence,

$$\begin{aligned} & -(1/48\eta_1\eta_2)\{[\psi(G_4/G_2) + 1]/2 + \xi[(G_4/G_2) + \psi]\}g_2(x') \\ & + [(G_4/2G_2) - \xi]g_4(x')\} = 0 \end{aligned} \quad (6.9)$$

x' must, of course, be obtained by a numerical procedure. It is noted that when beam-column effects are considered, x' varies somewhat with γ . Therefore the location at which bending is minimized (in the above sense) varies slightly with applied pressure.

F. Effective Width

If, as in some ring stability analyses, the entire structure were thought of as primarily rings with modified flanges (i.e., the shell skin is treated as an additional flange on the ring), then it is of interest to establish that axial length of shell which may be used as an effective ring flange width. The criterion used to determine this "effective-width" is (see Ref. 5)

$$L_e N'_\varphi \left(\frac{L}{2}\right) = \int_{-L/2}^{L/2} N'_\varphi(x) dx = L N'_{\varphi \text{ average}} \quad (6.10a)$$

where

$$N'_\varphi(x) = h \sigma'_{\varphi M}(x) \quad (6.10b)$$

L_e is the effective width. N'_φ is the resultant of the modified circumferential membrane stress $\sigma'_{\varphi M}(x)$ which, in turn, is that portion of the circumferential membrane stress which is due to axial bending. $\sigma'_{\varphi M}(x)$ is obtained by omitting terms which did not arise from axial bending considerations from the stress given in Eq. (5.6b). Thus, from the circumferential membrane stress one must subtract the hoop stress of an unsupported cylinder under hydrostatic pressure p ; this leaves $\sigma'_{\varphi M}(x)$ as that part of the shell membrane stress which is caused by the ring (which causes the axial bending). Hence, from Eqs. (5.66), (5.3c) and (4.13)

$$\frac{\sigma'_{\varphi M}(x)h}{N_x} = \left(\frac{h}{a}\right) \left(\frac{v_{\varphi x}}{v_{x\varphi}}\right) \left[W(x) + \frac{8E_x \gamma \Delta_0}{\theta^2 N_x}\right] - \frac{\delta}{3} \Lambda(x) \quad (6.11)$$

Considerations of overall equilibrium of a shell loaded only by the interaction pressures leads to

$$L_e N_{\phi_{\text{average}}} = p_c b_c (1 - \delta - 2\delta^*) \quad (6.12)$$

Therefore,

$$L_e = (p_c b_c h / N_x) (1 - \delta - 2\delta^*) / [(\nu_{\phi x} h / \nu_{x\phi} a) (W_f + 8E_x \gamma \Delta_o / N_x \theta^2) - \delta \Lambda_f / 3] \quad (6.13a)$$

When transverse shear, initial deflection and Flugge effects are neglected ($\xi = \alpha = \delta = \Delta = 0$), this relation reduces to (Ref. 7)

$$L_e = LG_1 + b_c \quad (6.13b)$$

G. Axisymmetric Buckling Loads

Axisymmetric buckling of a long, unstiffened, orthotropic, circular cylindrical shell would occur either at

$$\psi = \psi_{cr} = 1 \quad (6.14a)$$

or

$$B = B_{cr} = 0 \quad (6.14b)$$

depending on which of the above conditions occurs at the lowest γ (see Appendix C). When the transverse shear parameter ξ is relatively small

(G_{xz} large) the criterion for buckling of an unsupported, infinite length shell is given by Eq. (6.14a). From this, the axisymmetric buckling load is

$$p^* = \left(\sqrt{1 + 4\xi\alpha} - \xi - \alpha \right) \frac{8 \sqrt{hE^* D^*}}{a^2 (1+\delta)^2} \quad (\text{when } 1 - 4\gamma\xi > 0) \quad (6.15)$$

The ring-reinforced shell, due to its greater rigidity, possesses an axisymmetric critical load p_{cr} in excess of that of an unstiffened shell, i.e.,

$$p_{cr} > p^* \quad \text{or} \quad \gamma_{cr} > \gamma \quad \text{or} \quad \psi_{cr} > 1 \quad (6.16)$$

At the buckling load, the deflection becomes infinitely large. Examination of Eqs. (4.13) and (4.10b) shows that this occurs when

$$8\beta_c^* + G_1(1 - \beta_c)[\beta_c^* + (1 + \delta - 2\delta^*)\alpha_c]/\beta_c = 0 \quad (6.17)$$

However, since $\psi_{cr} > 1$, G_1 in its present form [see Eqs. (4.11d), (4.11c) and (4.7)] is a function of imaginary quantities. In order to avoid this, the buckling criterion is rewritten in the form

$$8\beta_c^* + G_5(1 - \beta_c)[\beta_c^* + (1 + \delta - 2\delta^*)\alpha_c]/\beta_c = 0 \quad (6.18a)$$

where

$$G_5 = \left(\frac{4}{\theta}\right) \frac{\cos^2(\eta_1' \theta) - \cos^2(\eta_2 \theta)}{\left[\frac{B_1}{\eta_1} \sin(\eta_1' \theta) \cos(\eta_1' \theta) + \frac{B_2}{\eta_2} \cos(\eta_2 \theta) \sin(\eta_2 \theta) \right] [1 - 2\xi(2\xi - c)]}$$

(6.18b)

is obtained by setting

$$\eta_1' = -i\eta_1 = \psi = 1/(2/B)$$

(6.18c)

in the equation for G_1 .

If, as occurs often in practice,

$$\beta_c \ll \alpha_c \ll 1$$

(6.19a)

The buckling load can be approximated from a numerical solution for ψ_{cr} of

$$\alpha_c(2\delta^* + 1) + G_5 = 0$$

(6.19b)

If more accuracy is desired, the solution of Eq. (6.19b) may be used as a first approximation in an iterative solution of Eq. (6.18a).

For a rigid frame (shell has clamped ends) $\alpha_c \rightarrow \infty$. Therefore, in order to fulfill the buckling criterion (6.18a)

$$G_5 \rightarrow -\infty$$

(6.20a)

This requires that [see Eq. (6.18b)]

$$\frac{B_1}{\eta_1} \sin(\eta_1' \theta) \cos(\eta_1' \theta) + \frac{B_2}{\eta_2} \cos(\eta_2 \theta) \sin(\eta_2 \theta) = 0 \quad (6.20b)$$

It is noted here that the results presented in this section are valid for both internal and external rings.

7. YIELD CRITERIA

The collapse mechanism of filament wound composite shells is not as yet fully understood. Experiments indicate that collapse occurs near the frame before the buckling pressure is reached [Ref. 1]. Although the severe delamination noticed in ruptured shells indicates an ultimate shear failure, the prevailing opinion seems to be that collapse occurs after a complicated sequence of the combined effects of yielding, local instabilities and crack propagation.

It is not the purpose of this work to develop a mathematical means of describing the collapse mechanism, but rather to describe the stress state while the shell material behaves as an elastic continuum. It would, therefore, be advantageous to have some idea of the range of pressure for which the linear elastic laws are applicable.

In Ref. 11, R. Hill developed a three-dimensional yield criterion to be used on orthotropic materials. He introduced a "plastic potential" function of the stresses which, for an orthotropic material in a state of modified plane stress, with transverse shear, can be written in the form

$$f = \left(\frac{\sigma_\phi}{Y_\phi}\right)^2 + \left(\frac{\sigma_x}{Y_x}\right)^2 - \sigma_x \sigma_\phi \left(\frac{1}{Y_\phi^2} + \frac{1}{Y_x^2} - \frac{1}{Y_z^2}\right) + \frac{\tau_{zx}^2}{Y_{zx}^2} \quad (7.1)$$

where f is the "plastic potential" function, Y_x , Y_ϕ , Y_z and Y_{xz} are the respective axial, circumferential, radial and transverse shear yield stresses. In Ref. 7, in which a composite shell theory was developed

without introducing effects of transverse shear deformation, the corresponding form of Eq. (7.1), i.e., $\tau_{zx} = 0$, was employed.

The yield criterion is defined to be

$$f = 1 \quad (7.2)$$

Equations (7.2), (7.1) and (2.5) combine to give a formula for the pressure necessary for yielding to occur at a particular position of the shell. This "yield-pressure" may be calculated from

$$\begin{aligned} \frac{p_y(x, z)}{Y_z} = & \frac{2 \left(\frac{h}{a} \right)}{(1+\delta)^2} \left\{ \left(\frac{\sigma_\phi h}{N_x} - \frac{\sigma_x h}{N_x} \right) \left[\left(\frac{Y_z}{Y_\phi} \right)^2 \left(\frac{\sigma_\phi h}{N_x} \right) - \left(\frac{Y_z}{Y_x} \right)^2 \left(\frac{\sigma_x h}{N_x} \right) \right] \right. \\ & \left. + \left(\frac{\sigma_x h}{N_x} \right) \left(\frac{\sigma_\phi h}{N_x} \right) + \left(\frac{Y_z}{Y_{xz}} \right)^2 \left(\frac{\tau_{yz} h}{N_x} \right)^2 \right\}^{-1/2} \quad (7.3) \end{aligned}$$

When beam-column effects are considered, the right-hand side of Eq. (7.3) is dependent on p_y through the parameter γ . In such a case the equation is transcendental in p_y . A good first approximation for p_y may be obtained by taking $\gamma = 0$ in the right-hand side of Eq. (7.3); then, if more accuracy is desired, the yield pressure thus obtained could be utilized to initiate an iterative numerical procedure for a more accurate solution.

Fiberglass shells are generally constructed so that the radial direction is normal to every filament. The radial yield stress (Y_z) of such shells is the relatively small yield stress of the resin. Thus, a good approximation to the yield pressure is given by

$$\frac{P_y(x,z)}{\bar{\sigma} Y_z} = \frac{2(\frac{h}{a})}{(1+\delta)^2} \left[\left(\frac{\sigma_x h}{N_x} \right) \left(\frac{\sigma_\phi h}{N_x} \right) + \left(\frac{Y_z}{Y_{xz}} \right)^2 \left(\frac{\tau_{yz} h}{N_x} \right)^2 \right]^{-1/2} \quad (7.4a)$$

since

$$(Y_z/Y_x)^2 \ll 1 \quad (7.4b)$$

and

$$(Y_z/Y_\phi)^2 \ll 1 \quad (7.4c)$$

The most severe stress situations usually occur either at midbay on the outer shell surface, $(x,z) = (0, -h/2)$, or at the frame on the inner shell surface, $(x,z) = (\pm L/2, h/2)$. The yield pressures corresponding to these positions may be calculated by using Eqs. (5.7), (5.4) and (5.3) in Eq. (7.4a) or in Eq. (7.3).

An estimate of the pressure $P_{y_0}(x)$ at which yielding has penetrated through half the shell thickness at midbay [see, for example, Ref. 5], could be obtained by neglecting the bending stresses, i.e., by using Eqs. (5.4), (5.6a), (5.6c) and (5.7) in Eq. (7.3) or (7.4).

The manipulations described above were carried out in Ref. 7, to result in the following yield pressures when transverse shear, Flügge, and initial deflection effects are neglected:

$$P_Y(\pm \frac{1}{2}, \frac{h}{2}) = \frac{h}{a} [\Theta_1 + \bar{\Lambda}^2 (\Theta_2 E_1^2 G_3^2 + \Theta_3 E_1 G_3 + \frac{1}{Y_\varphi^2}) + \frac{\bar{\Lambda}}{2} (\Theta_4 E_1 G_3 + \Theta_5)]^{-1/2} \quad (7.5a)$$

$$P_Y(0, -\frac{h}{2}) = \frac{h}{a} \{\Theta_1 + \bar{\Lambda}^2 [(\frac{G_2}{Y_\varphi})^2 - \Theta_3 E_1 G_2 G_4 + \Theta_2 E_1^2 G_4^2] - \frac{\bar{\Lambda}}{2} (G_2 \Theta_5 + \Theta_4 E_1 G_4)\}^{-1/2} \quad (7.5b)$$

$$P_{Y_0}(0) = (\frac{h}{a}) [-\Theta_1 + G_2 \bar{\Lambda} (G_2 \bar{\Lambda} + \frac{1}{2} \Theta_5)]^{-1/2} \quad (7.5c)$$

in which

$$\bar{\Lambda} = \frac{(1 - \frac{v_{\phi x}}{2})}{\alpha_c + \beta_c + (1 - \beta_c) G_1} [\alpha_c - \frac{\beta_c \delta^* A_f}{b_c R_c (1 - \frac{v_{\phi x}}{2})}] \quad (7.5d)$$

$$\Theta_1 = \frac{1}{2} (\frac{1}{Y_\varphi^2} - \frac{2}{Y_x^2} + \frac{1}{Y_z^2}) \quad (7.5e)$$

$$\Theta_2 = \frac{1 - v_{\phi x}}{Y_x^2} - \frac{v_{\phi x} (1 - v_{\phi x})}{Y_\varphi^2} + \frac{v_{\phi x}}{Y_z^2} \quad (7.5f)$$

$$\Theta_3 = -\frac{1}{Y_x^2} - \frac{1 - 2v_{\phi x}}{Y_\varphi^2} + \frac{1}{Y_z^2} \quad (7.5g)$$

$$\Theta_4 = \frac{2 - 3v_{\phi x}}{Y_\varphi^2} + \frac{v_{\phi x}}{Y_x^2} - \frac{2 + v_{\phi x}}{Y_z^2} \quad (7.5h)$$

$$\Theta_5 = \frac{3}{Y_\varphi^2} - \frac{1}{Y_x^2} + \frac{1}{Y_z^2} \quad (7.5i)$$

$$E_1 = \sqrt{\frac{3E_x}{(1 - v^2)E_\varphi}} \quad (7.5j)$$

Note: for approximation (7.4)

$$\epsilon_5 = \epsilon_3 = 2\epsilon_1 = \frac{1}{Y_z} \quad (7.6a)$$

$$\epsilon_2 = \frac{\nu_{\phi x}}{Y_z} \quad (7.6b)$$

$$\epsilon_4 = \frac{2 + \nu_{\phi x}}{Y_z} \quad (7.6c)$$

The simplest failure criterion is the assumption that the material fails when the maximum stress reaches the uniaxial yield stress of the material. Reference 7 also applied this criterion and arrived at the following results:

$$p_{Y_1} \left(\pm \frac{L}{2}, \frac{h}{2} \right) = \frac{Y_x \left(\frac{h}{a} \right)}{\frac{1}{2} - \bar{\Lambda} E_1 G_3} \quad (7.7a)$$

$$p_{Y_1} \left(0, -\frac{h}{2} \right) = \frac{Y_{\phi} \left(\frac{h}{a} \right)}{1 - \bar{\Lambda} (G_2 - \nu_{\phi x} E_1 G_4)} \quad (7.7b)$$

8. NUMERICAL EXAMPLE AND DISCUSSION OF RESULTS

Numerical computations were performed on the IBM 7040 computer located at the Polytechnic Institute of Brooklyn. These calculations were intended to examine the separate and combined effects of large rotations (beam-column effect), thick shell terms consistent with Flugge accuracy, transverse shear deformation and initial deflections. The particular glass-reinforced-plastic, ring-stiffened, circular, cylindrical shell of interest was one previously investigated by the David Taylor Model Basin [Ref. 15]. The properties of this structure are as follows:

Elastic Constants [see Eqs. (A.21), (3.2), and (3.9)]

$$\begin{aligned}
 E_x &= 4.74 \times 10^6 \text{ psi} & E_\varphi &= 6.14 \times 10^6 \text{ psi} & \kappa G_{xz} &= 0.70 \times 10^6 \text{ psi} \\
 \nu_{x\varphi} &= 0.136 & \nu_{\varphi x} &= 0.176 \\
 E_{sf} &= 7.20 \times 10^6 \text{ psi} & (E_x \nu_{\varphi x} &= E_\varphi \nu_{x\varphi}) & & (8.1)
 \end{aligned}$$

The shear modulus was not available and was taken to correspond to similar structures listed in Ref. 11.

Geometry (see Fig. 1)

$$a = 3.194''$$

(continued on next page)

$$h = 0.388''$$

$$L = 1.273''$$

$$b_c = 0.271''$$

$$d = 0.542''$$

All calculations for stresses, deflections, contact pressure, initial yield pressure and stress resultants were performed only for the case of the internal frame of rectangular cross section.

Using this ring-shell structure as a standard, it was decided to first neglect Flugge terms ($\delta = \alpha = 0$), transverse shear deformation ($\epsilon = 0$) and initial deflections ($\Delta = 0$). The following three types of sample calculations were performed:

1) Shell structure as above; but, in addition, a shell of one-half the original thickness was also considered (i.e., $h = 0.194''$). Ring theory, Eq. (3.13), was used to describe the ring deformation.

2) Shell structures as in (1) but for isotropic structural material with $E = \sqrt{E_x E_\phi} = 5.395 \times 10^6$ psi and $\nu = \sqrt{\nu_{\phi x} \nu_{x\phi}} = 0.1548$. An examination of either the stress equations given in explicit form in Ref. 7 or Eqs. (5.3) of the present report led to this selection for an equivalent isotropic material. Such structures could be analyzed with the use of Ref. 5.

3) Shell as in (2) but with a less stiff frame of modulus $E_f = E = 5.395 \times 10^6$ psi equal to the shell modulus.

The results of the above calculations are presented in Tables 1 and 2 and Figs. 3 through 10. The calculations in (2) and (3) were prompted by the similarity which exists between the isotropic equations found, for example, in Ref. (5) (using $E = \sqrt{E_x E_y}$) and the orthotropic equations [see Ref. 7]. In the few cases considered, this procedure was justified since, for both the thick ($h = 0.388''$) and the thin ($h = 0.194''$) shells, the values of the stresses obtained for the "equivalent isotropic" and the orthotropic cases agree to within 10 percent [see Figs. 3 to 6].

The stiff ring [$E_r/E = 1.335$ in Figs. 3 to 6] caused smaller circumferential stresses but higher axial stresses. The bending stresses were higher for the stiff ring as expected [see Figs. 7 - 10], and the corresponding yield pressures could be slightly lower.

It is evident from Figs. 3 through 10 that in the loading region $0 \leq \gamma \leq 0.4$, the nonlinear beam column effect is small. However, if a line is drawn at the origin tangent to the curves of Figs. 3 through (10) (yielding the linear solution which neglects the beam-column effect), it can be seen that some nonlinearities first appear at $\gamma = 0.25$ [e.g., see Fig. 7]. If γ were taken larger than 0.4, the nonlinearities would no longer be minor. Of course, for the cases considered, when $\gamma > 0.4$, $p > 37,000$ psi (for $h = 0.388$ in.) or $p > 10,000$ psi (for $h = 0.194$ in.) and these pressures are well beyond the yield pressures that were obtained.

The yield pressures presented in Table 2 are those obtained from Eqs. (7.5), (7.6) and (7.7). When the yield pressures were calculated from the approximation described in Eqs. (7.4) and (7.6), they differed from those determined by Eq. (7.5) by less than two percent. Thus, the

low yield pressures obtained are caused by the small radial yield stress. Hence, if the resin yield stress could be increased, there would be a substantial strengthening effect in that significant increases in initial yield pressure could be realized.

The remaining numerical calculations [Figs. 11 through 14] are directed at investigating the effects of transverse shear deformation, initial deflections and thick shell (Flügge) terms. The structure considered is basically that described in Eqs. (8.1) and (8.2). The ring deflection is described by Eq. (3.11).

In the stress vs initial deformation curves [Fig. 11, 13 and 17] the bending stresses can be obtained by measuring the vertical distance between the outer and inner surface stresses, whereas the membrane stresses are equal to half the sum of the outer and inner surface stresses.

When initial deflection and the beam-column effects are negligible, the membrane stresses exhibit very little change with increased transverse shear deformation effects [see Figs. 15 and 16]. However, the axial bending stresses increase at the frame, and decrease at midbay. The lowest (critical) yield pressure decreases slightly (See Table 3). Although in general the beam-column effect becomes more significant when transverse shear deformations are considered (see Table 3), this effect remains negligible for pressures below the initial yield pressure.

The influence of initial deformations stems from beam-column effects. Because of the very small deflections for $\Delta = 0$, referred to earlier (see Table 1), the beam-column terms were insignificant. However, with initial deflections as large as $\Delta = \pm 0.2h$ such terms become important. Additional deflections (w) contribute very little to beam-column effects.

Thus, the results shown in Figs. 11 through 18 have been obtained by using

$$(\gamma/\bar{\gamma})\Delta = \Delta \quad \gamma = 0 \quad (8.3)$$

in Eqs. (5.7). Numerical results for $\gamma \neq 0$ have been obtained and justify the above procedure. For example, at $\gamma = 0.3$ the above procedure gives the stresses to within six percent of the more accurate value. Hence, instead of plotting numerous identical sets of curves for various values of γ , it is sufficient to present the single set of results obtained by using Eqs. (8.3).

In the absence of transverse shear deformations ($\xi = 0$), the bending stresses decrease with increasing outward initial deflection until, at $\Delta = \Delta_1 = -0.072$ in. for the shell considered ($h = 0.388$ in.), the bending stresses become negligible (Fig. 11) and the shell (with $\Delta = \Delta_1$) behaves almost as a membrane. This effect, coupled with the sharp decrease in hoop stress that accompanies large outward (negative) initial deformations causes the yield pressure to increase as Δ becomes more negative (Fig. 12). For $\Delta < \Delta_1$ yielding can begin on the outer surface of the shell at the frame, whereas for $\Delta > \Delta_1$ yielding begins at the inner shell surface of the frame. The actual initial deflection at which yielding occurs throughout the shell wall at the frame varies slightly from the above value when Flugge accuracy is maintained (compare Figs. 14 and 12).

The most important Flugge type correction term is that which increases the axial stress resultant N_x [see Eq. (2.5)]. Further comparison of Figs. 11 and 13 reveals that the stresses (nondimensionalized with respect to N_x/h) are only slightly influenced by Flugge type terms. The actual stresses,

however, are proportional to N_x and change by about 10 percent (for $h = 0.388''$) due to the change in N_x . This shows up as a 10 percent decrease in yield pressure when Flugge terms are included (see Figs. 12 and 14).

The effect of transverse shear deformation is to increase the bending stresses at the frame and decrease those at midbay (Fig. 15). Also, the value of the initial yield pressure (e.g., at the shell inner surface near the frame) decreases when such effects are included (Fig. 16). Comparison of Figs. 11 and 17 reveals that the changes in bending stresses described above become more pronounced with increasing initial deflections. Accordingly, the initial yield pressure decreases with initial inward deflections (Fig. 18).

Thus, from the results obtained the following conclusions may be presented:

1. For the shell material considered here, an equivalent isotropic analysis gives stresses accurate to within ten percent.
2. Stiffening the ring may increase the axial bending stresses enough to weaken the structure by causing early yield. This was observed experimentally in Ref. 1.
3. The relatively short, thick shell deflects very little before yielding and is not susceptible to beam-column effects. Initial deflections, however, may be large enough to cause significant beam-column effects. Short's suggestion (Ref. 9) that the beam-column effect be utilized to strengthen the shell by building in an outward initial deflection that minimizes the bending stresses may be used on this type of shell. All that need be done is to wind the shell on a barrel shaped mandrel.

4. Yield pressures which are well below experimental collapse pressures indicate that yielding begins well in advance of collapse. This may be remedied by increasing the yield stress in the radial direction.

5. If the shell is permitted an additional degree of freedom by allowing transverse shear deformation, the frame bending stresses increase and the initial yield pressure decreases. The transverse shear deformation theory cannot, however, be considered as necessarily more accurate; this is demonstrated in Ref. 2.

6. The only Flugge type term that has a significant effect is that due to using the outer shell diameter when calculating the axial pressure force acting on the shell.

7. For the shell structures examined in the present work, the yield condition was reached before γ , ξ , α or δ exhibited any substantial influence on stress curves. Thus, it was found that a perturbation technique can be employed to give fast and accurate results (see appendix D).

8. In order to obtain reasonable estimates of the stresses in the constituent materials it is necessary to modify the stresses obtained for the equivalent homogeneous shell. This modification can be achieved by multiplying the stresses given by Eqs. (5.3) by appropriate stress concentration factors (see Appendix E).

REFERENCES

1. Hom, K. and Couch, W.P.: Investigation of Filament Reinforced Plastics for Deep Submergence Application. David Taylor Model Basin Report 1824, Nov. 1966.
2. Misovec, A.P. and Kempner, Joseph: Approximate Elasticity Solution for Orthotropic Cylinder Under Hydrostatic Pressure and Band Loads. PIBAL Rep. No. 68-11, May 1968.
3. Von Sanden, K. and Gunther, K.: The Strength of Cylindrical Shells, Stiffened by Frames and Bulkheads, under Uniform External Pressure on All Sides, Werft and Reederie (1920), Vol. 9, pp. 189-198; Vol. 10, pp. 216-221.
4. Viterbo, F.: Sul Problema Della Robustezza di Cilindri Cavi Rinforzati Transversalmente Sottoposti da Ogni Parte a Pressione Esterna, L'Ingegnere, Vol. IV (July 1930), pp. 446-456, (Aug. 1930), pp. 531-540.
5. Pulos, J. and Salerno, V.: Axisymmetric Elastic Deformations and Stresses in a Ring-Stiffened, Perfectly Circular Cylindrical Shell under External Hydrostatic Pressure, David Taylor Model Basin Report 1497, Sept. 1961.
6. Kempner, J.: Unified Thin-Shell Theory. A Symposium on the Mechanics of Plates and Shells for Industry Research Associates, PIBAL Rep. No. 566, pp. 2-7, March 9-11, 1960.
7. Herzner, F.C.: Ring-Reinforced Orthotropic, Circular Cylindrical Shell under Hydrostatic Pressure. M.S. Thesis, Polytechnic Institute of Brooklyn, June 1965.
8. Lunchick, M.E. and Short, R.D.: Behavior of Cylinders with Initial Shell Deflection. David Taylor Model Basin Report 1150, July 1957.
9. Short, R.D.: Membrane Design for Stiffened Cylindrical Shells under Uniform Pressure. David Taylor Model Basin Report 1898, March 1965.
10. Krenzke, M.A. and Short, R.D.: Graphical Method for Determining Maximum Stresses in Ring-Stiffened Cylinders under External Hydrostatic Pressure, David Taylor Model Basin Report 1348, Oct. 1959.
11. Hill, R.: A Theory of the Yielding and Plastic Flow of Anisotropic Metals, Proceedings Royal Society A193, pp. 281-286, 1948.
12. Meyers, N.C.; Lee, G.D.; Wright, F.C. and Daines, J.V.: Investigation of Structural Problems with Filament Wound Deep Submersibles, Final Report, H.I. Thompson Fiber Glass Co.; January 1964.

14. Dow, N.F.; Rosen, B.W.; Shu, L.S. and Zweben, C.H.: Design Criteria and Concepts for Fibrous Composite Structures, General Electric Space Sciences Laboratory, July 1967.
15. Hom, K.; Buhl, J.E. and Couch, W.P.: Hydrostatic Pressure Tests of Unstiffened and Ring Stiffened Cylindrical Shells Fabricated of Glass Filament Reinforced Plastics, David Taylor Model Basin Report 1745, Sept. 1963.
16. Shaffer, Bernard W.: Material Properties of Reinforced Plastics, S.P.E. Transactions, Vol. 4, No. 4, Oct. 1964.
17. Shaffer, B.W.: Stress-Strain Relations of Reinforced Plastics Parallel and Normal to their Internal Filaments, AIAA Journal, Vol. 2, No. 2, Oct. 1962.
18. Dow, N.F. and Rosen, B.W.: Evaluations of Filament-Reinforced Composites for Aerospace Structural Applications, NASA CR-207, April 1965.
19. Tsai, S.W.: Structural Behavior of Composite Materials, NASA CR-71, July 1964.

APPENDIX A

BASIC SHELL EQUATIONS

The differential equations describing the axisymmetric deformation of the shell are obtained by utilizing approximate forms of the basic equations of the theory of elasticity.

First the strain components are found in terms of the displacements and rotation. The length of an infinitesimal line ds_0 in the wall of a circular cylindrical shell with a slight axisymmetric initial deflection w_0 may be obtained from (for example, see Ref. 6)

$$ds_0^2 = d\xi_0^2 + (a - z - w_0)^2 d\varphi^2 + d\zeta_0^2$$

where

$$\xi_0 = x - zw_{0,x} \quad \zeta_0 = z + w_0 \quad w_0 = w_0(x) \quad (A.1)$$

x , φ and z are Lagrangian coordinates in the axial, circumferential and inward radial directions, respectively, and are measured from a point on the median surface at the midbay station of the shell (see Fig. 1). These coordinates are fixed to the shell. ξ_0 and ζ_0 are Eulerian coordinates in the axial and inward radial directions, respectively, measured from the median surface at the midbay station of a perfect, undeformed shell; a is the radius of the median surface and w_0 is the initial inward deflection of that surface. A comma followed by a subscripted variable denotes differentiation with respect to that variable.

After axisymmetric deformation the infinitesimal line attains a new length ds_1 where

$$ds_1^2 = d\xi_1^2 + (a - z - w_0 - w)^2 d\varphi^2 + d\zeta_1^2 \quad (A.2)$$

with

$$\xi_1 = x + \bar{u}$$

$$\zeta_1 = z + w_0 + w$$

$$u = u(x, z)$$

$$w = w(x)$$

ξ_1 and ζ_1 are Eulerian coordinates similar to ξ_0 and ζ_0 . u is the axial displacement of a point in the shell wall and w is the inward deflection of the median surface from the initially deformed shape. If normals to the median surface remain straight and unextended throughout the deformation,

$$\bar{u} = u - z(w + w_{0,x}) \quad (A.3a)$$

$$w = w_{,x} - \gamma_{xz} \quad (A.3b)$$

where u is the axial displacement of a point in the median surface, w is the additional rotation of the median surface normal about a circumferential axis

due to loading and γ_{xz} is the corresponding transverse shearing strain. It is noted here that γ_{xz} and ω are not independent of each other.

The strain components are obtained from [see Eqs. (A.1) and (A.2)]

$$ds_1^2 - ds_0^2 = 2\epsilon_x dx^2 + 2\epsilon_\varphi (a - w_0 - z)^2 d\varphi^2 + 2\epsilon_z dz^2 + \gamma_{xz} dx dz \quad (A.4)$$

Hence,

$$\epsilon_x = u_{,x} + \frac{1}{2} w_{,x} (w_{,x} + 2w_{0,x}) - z(w_{,xx} - \gamma_{xz,x})$$

$$\epsilon_\varphi = -w/(a - z - w_0)$$

$$\epsilon_z = (w_{,x} - \gamma_{xz})w_{0,x} \approx 0$$

$$\gamma_{xz} = w_{,x} - \omega - u_{,x}w_{0,x} \approx w_{,x} - \omega \quad (A.5)$$

in which it has been assumed that

$$u_{,x}^2 \ll w_{,x} (w_{,x} + 2w_{0,x}) \ll 1 \quad w \ll a - z - w_0 \quad (A.6)$$

It is noted that a transverse shear term has been retained so that the usual Kirchhoff assumption that lines originally normal to the median surface remain normal is removed. However, with regard to kinematic considerations, it is assumed that such lines remain straight and unextended.

In order to obtain a set of equilibrium equations consistent with the strain-displacement relations [Eqs. (A.5)] the first variation of the total potential can be set equal to zero

$$\delta(U + V) = 0 \quad \text{or} \quad \delta U + \delta V = 0 \quad (\text{A.7})$$

where U is the strain energy and V is the potential due to externally applied loads. Thus,

$$\delta U = 2\pi \int_{-L/2}^{L/2} \int_{-h/2}^{h/2} (\sigma_x \delta \epsilon_x + \sigma_\phi \delta \epsilon_\phi + \sigma_z \delta \epsilon_z + \tau_{xz} \delta \gamma_{xz}) (a - z - w_0) dz dx \quad (\text{A.8})$$

When Eqs. (A.4) and (A.5) are substituted into Eq. (A.8) and integrations by parts are performed, Eq. (A.8) becomes

$$\begin{aligned} \delta U = 2\pi a \int_{-L/2}^{L/2} \{ [-N_{x,x} + (Qw_{0,x})_{,x}] \delta u + [-M_{x,xx} - (N_x w_{,x} + N_x w_{0,x}) - \frac{N_\phi}{a}] \delta w \\ + (-M_{x,x} + Q) \delta \gamma_{xz} \} dx + 2\pi a \{ [(N_x - Qw_{0,x}) \delta u]_{-L/2}^{L/2} \\ + [(M_{x,x} + N_x \bar{w}_{,x}) \delta w]_{-L/2}^{L/2} + [M_x (\delta \gamma_{xz} - \delta w_{,x})]_{-L/2}^{L/2} \} \end{aligned} \quad (\text{A.9})$$

in which the stress resultants are defined by

$$N_x = \int_{-h/2}^{h/2} \sigma_x [1 - (2z/h)\delta - (w_0/a)] dz \quad (\text{A.10a})$$

$$N_\phi = \int_{-h/2}^{h/2} \sigma_\phi dz \quad (\text{A.10b})$$

$$M_x = \int_{-h/2}^{h/2} \sigma_x [1 - (2z/h)\delta - (w_0/a)] z dz \quad (\text{A.10c})$$

$$Q = \int_{-h/2}^{h/2} \tau_{xz} [1 - (2z/h)\delta - (w_0/a)] dz \quad (\text{A.10d})$$

where σ_x is the axial stress, σ_ϕ is the circumferential stress and τ_{xz} is the transverse shear stress with κ as the corresponding shear coefficient. The potential due to external pressure is obtained by considering the volume change. Thus

$$V_p = \int_{VOL} p d(VOL) \quad (A.11)$$

The increment of volume is given by

$$d(VOL) = \pi \left(a + \frac{h}{2} - \bar{w} \right)^2 (d\xi_1)_{z = -h/2} \quad (A.12)$$

where $\bar{w} = w + w_0$ and

$$(d\xi_1)_{z = -h/2} = \left(1 + u_{,x} + \frac{h}{2} \omega_{,x} \right) dx$$

The variation of this potential is

$$\delta V_p = \pi \pi a^2 \int_{-L/2}^{L/2} \delta \left[\left(1 + \frac{h}{2a} - \frac{\bar{w}}{2a} \right)^2 \left(1 + u_{,x} + \frac{h}{2} \omega_{,x} \right) \right] dx \quad (A.13)$$

After integration by parts, Eq. (A.13) yields

$$\delta V_p = \pi \pi a^2 \int_{-L/2}^{L/2} \left\{ \left[-\frac{2}{a} \left(1 + \frac{h}{2a} - \frac{\bar{w}}{a} \right) \left(1 + u_{,x} + \frac{h}{2} \omega_{,x} \right) \right] \delta w \right.$$

(continued on next page)

$$\begin{aligned}
& + 2 \left(1 + \frac{h}{2a} - \frac{\bar{w}}{2a} \right) \frac{x}{a} (\delta u + \frac{h}{2} \delta \omega) dx \\
& + \pi a^2 \left[\left(1 + \frac{h}{2a} - \frac{\bar{w}}{a} \right)^2 (\delta u + \frac{h}{2} \delta \omega) \right]_{-L/2}^{L/2}
\end{aligned} \tag{A.14}$$

Finally, the variation in the potential due to other externally applied loads is given by

$$\begin{aligned}
\delta V_f = & \left[N_x^* \delta u \right]_{-L/2}^{L/2} - \left[N_x^* w_{,x} \delta w \right]_{-L/2}^{L/2} - \left[M_x^* (\gamma_{xz} - w_{,x}) \right]_{-L/2}^{L/2} \\
& - \left[M_{x,x}^* \delta w \right]_{-L/2}^{L/2} + \left[Q_f^* w_{o,x} \delta u \right]_{-L/2}^{L/2}
\end{aligned} \tag{A.15}$$

The potential of externally applied loads is

$$V = V_p + V_f \tag{A.16}$$

Equation (A.7) to (A.16) leads to the differential equations of equilibrium

$$-N_{x,x} + p \left[1 + h/2a - (w+w_o)/a \right] (w+w_o)_{,x} - (Q_{w_{o,x}})_{,x} = 0 \tag{A.17a}$$

$$- [N_x (w+w_o)_{,x}]_{,x} - N_\phi/a - Q_{,x} - p \left[1 + h/2a - (w+w_o)/a \right] (1 + u_{,x} + h/2 \omega_{,x}) = 0 \tag{A.17b}$$

$$M_{x,x} = Q + \frac{ph}{2} \left[1 + h/2a - (w+w_o)/a \right] (w+w_o)_{,x} = 0 \tag{A.17c}$$

with boundary conditions at $x = \pm L/2$

$$N_x - Qw_{o,x} + (pa/2)[1 + h/2a - (w_f + w_{of})/a]^2 = 0 \quad \text{or} \quad \delta u = 0 \quad (\text{A.18a})$$

$$-M_x + (h/2a)(pa^2/2)[1 + h/2a - (w + w_o)/a]^2 = 0 \quad \text{or} \quad \delta w = 0 \quad (\text{A.18b})$$

$$N_x(w + w_o)_{,x} + Q = 0 \quad \text{or} \quad \delta w = 0 \quad (\text{A.18c})$$

Equations (A.16) combine to yield the resulting axisymmetric equilibrium equations for hydrostatic pressure loading of a shell of uniform thickness (in which the assumptions given by inequalities (2.4) have been utilized), viz.,

$$-N_{x,x} + 2p[1 + \delta - (w + w_o)/a](w + w_o)_{,x} = 0 \quad (\text{A.19a})$$

$$[N_x(w + w_o)_{,x}]_{,x} + M_{x,xx} + N_\delta/a + p[1 + \delta + (w + w_o)/a] = 0 \quad (\text{A.19b})$$

$$-M_{x,x} + Q = 0 \quad (\text{A.19c})$$

where $\delta = h/2a$ (set equal to zero when Flugge accuracy is not required, i.e., when the variation of radius of curvature across the thickness is neglected).

For the problem being considered here, the following conditions must also be satisfied at the shell boundaries $x = \pm L/2$:

$$N_x + (pa/2)[1 + \delta - (w + w_o)/a]^2 = 0 \quad (\text{A.20a})$$

$$w = w_s = w_R \quad (\text{A.20b})$$

$$\omega = 0 \quad (\text{A.20c})$$

where w_R is the deflection of the ring at the contact surface and w_s is the deflection of the section of shell in contact with the ring. For the ring-supported shell considered here the axial stress resultant at the frame is due to the external pressure loading [Eq. (A.20a)]; the ring and the shell remain in contact throughout the deformation [Eq. (A.20b)]; and since the ring flanges are not permitted to bend, the rotation vanishes at the boundary [Eq. (A.20c)].

The stress-strain relationships are those for an orthotropic, linearly elastic shell with surfaces of elastic symmetry defined by normals directed along the coordinates x , ϕ and z , respectively. The shell skin is assumed to be in a state of modified plane stress (i.e., with a transverse shear term permitted), thus

$$\sigma_x = \frac{E_x}{1-\nu^2} (\epsilon_x + \nu_{\phi x} \epsilon_\phi) \quad (\text{A.21a})$$

$$\sigma_\phi = \frac{E_\phi}{1-\nu^2} (\epsilon_\phi + \nu_{x\phi} \epsilon_x) \quad (\text{A.21b})$$

$$\tau_{xz} = G_{xz} \gamma_{xz} \quad (\text{A.21c})$$

$$\sigma_z = 0 \quad (\text{A.21d})$$

and from the axisymmetric nature of the structure and loading

$$\tau_{x\varphi} = \tau_{\varphi z} = 0 \quad (\text{A.21e})$$

where

$$\nu_{x\varphi} E_{\varphi} = \nu_{\varphi x} E_x \quad (\text{A.21f})$$

$$\nu_{x\varphi} \nu_{\varphi x} = \nu^2 \quad (\text{A.21g})$$

in which E_x and E_{φ} are the axial and circumferential elastic moduli, respectively, G_{xz} is the transverse shear modulus, $\nu_{x\varphi}$ and $\nu_{\varphi x}$ are the Poisson ratios.

In order to formulate the problem in terms of the stress resultants, rather than the stresses, Eqs. (A.10) and (A.21) are combined. Thus

$$N_x = [a_x - A_x(w_o/a)]\epsilon_{x_o} + a_{x\varphi}\epsilon_{\varphi_o} - [b_x - B_x(w_o/a)]\omega_{,x} \quad (\text{A.22a})$$

$$N_{\varphi} = \{[1 - (w_o/a)]A_{\varphi} - [1 - 2(w_o/a)]B_{\varphi} + C_{\varphi}\}\epsilon_{\varphi_o} + a_{x\varphi}\epsilon_{x_o} - b_{\varphi x}\omega_{,x} \quad (\text{A.22b})$$

$$M_x = [b_x - B_x (w_0/a)] \epsilon_{x_0} + t_{\varphi x} \epsilon_{\varphi_0} - [dx - C_x (w_0/a)] w_{,x} \quad (A.22c)$$

$$Q = c_{xz} (w_{,x} - w) - \frac{w}{a} (w_{,x} - w) \quad (A.22d)$$

in which

$$\epsilon_{x_0} = u_{,x} + (w_{,x}/2) (w_{,x} + 2w_{0,x}) \quad (A.23a)$$

$$\epsilon_{\varphi_0} = -\frac{w}{a} \quad (A.23b)$$

and

$$\begin{aligned} a_x &= \int_{-h/2}^{h/2} \frac{E_x}{1-\nu^2} \left(1 - \frac{z}{a}\right) dz, & A_x &= \int_{-h/2}^{h/2} \frac{E_x}{1-\nu^2} dz \\ b_{\varphi x} &= \int_{-h/2}^{h/2} \frac{E_{\varphi x \varphi}}{1-\nu^2} z dz, & a_{x\varphi} &= \int_{-h/2}^{h/2} \frac{E_x \nu_{\varphi x}}{1-\nu^2} dz \\ b_x &= \int_{-h/2}^{h/2} \frac{E_x}{1-\nu^2} \left(1 - \frac{z}{a}\right) z dz, & B_x &= \int_{-h/2}^{h/2} \frac{E_x}{1-\nu^2} z dz \\ A_{\varphi} &= \int_{-h/2}^{h/2} \frac{E_{\varphi}}{1-\nu^2} dz, & B_{\varphi} &= \frac{1}{a} \int_{-h/2}^{h/2} \frac{E_{\varphi}}{1-\nu^2} z dz \\ c_{\varphi} &= \frac{1}{a} \int_{-h/2}^{h/2} \frac{E_{\varphi}}{1-\nu^2} z^2 dz, & C_x &= \int_{-h/2}^{h/2} \frac{E_x z^2}{1-\nu^2} dz \\ d_x &= \int_{-h/2}^{h/2} \left(1 - \frac{z}{a}\right) \frac{E_x}{1-\nu^2} z^2 dz, & c_{xz} &= \kappa \int_{-h/a}^{h/2} G_{xz} \left(1 - \frac{z}{a}\right) dz \end{aligned} \quad (A.24)$$

The basic Eqs. (A.5), (A.19) and (A.22) subject to boundary conditions given by Eq. (A.20) describe the deformation of the shell. These consist of ten equations in the unknowns N_x , Q , M_x , N_φ , w , u , ω , ϵ_x , ϵ_φ and γ_{xz} .

Integration of Eq. (A.19a) and application of the boundary condition Eq. (A.20a) reveals that N_x is very nearly constant. In fact, the assumption that

$$(w + w_0)/a < 1 + \delta \quad (A.25)$$

leads to

$$N_x = - (pa/2)(1 + \delta)^2 \quad (A.26)$$

If Eq. (A.22a) is used to eliminate ϵ_{x_0} from Eq. (A.22b-d) and if Eq. (A.23b) is introduced, the resulting equations reduce to the linear relations

$$M_x = z_1 N_x - \frac{2a}{3} \delta^3 E_{\varphi x}^* w - D_{x,x}^* \omega \quad (A.27a)$$

$$N_\varphi = \nu_{\varphi x}^* N_x - 2\delta E_{\varphi}^* w - \frac{2a^2}{3} \delta^3 E_{\varphi x}^* \omega_{,x} \quad (A.27b)$$

$$Q = hG_{xz} [1 - (w/a)] (w_{,x} - \omega)$$

$$= hG_{xz} [1 - (\frac{w_0}{a})] \gamma_{xz} \quad (A.27c)$$

where

$$z_1 = [b_x - B_x(w_0/a)]/[a_x - A_x(w_0/a)]$$

$$\frac{2a}{3} \delta^3 E_{\varphi x}^* = b_{\varphi x} - a_x \varphi z_1$$

$$D_x^* = d_x - c_x \frac{w_0}{a} - [b_x - B_x(w_0/a)] z_1$$

$$v_{\varphi x}^* = \frac{a_x \varphi}{a_x - A_x \frac{w_0}{a}}$$

$$hE_{\varphi}^* = -a_x v_{\varphi x}^* + [1 - (w_0/a)] A_{\varphi} - [1 - 2(w_0/a)] B_{\varphi} + c_{\varphi}$$

$$hG_{xz}^* = c_{xz} \quad (A.28)$$

In view of the fact that N_x is a known constant given by Eq. (A-26), the three remaining stress resultants are seen to be linear functions of w and ω .

In order to avoid variable coefficients in the final differential equations the shell material must be assumed to be homogeneous in the axial direction; in addition the w_0 terms must be neglected in Eqs. (A.28). Thus, w_0 must be small enough for the following assumptions to apply:

$$w_0/a \ll 1/2$$

$$\frac{w_0}{a} \ll (d_x - z_1 b_x)/(c_x - z_1 B_x) = O(1)$$

(continued on next page)

$$\frac{w_0}{a} \ll \frac{a_x}{A_x} = 0(1)$$

$$\frac{w_0}{a} \ll \frac{b_x}{B_x} = 0(1) \quad (\text{A.29})$$

If the shell material is also homogeneous through the thickness, the condition $w_0/a \ll 1/2$ prevails and, hence Eqs. (A.28) reduce to

$$z_1 = - (a/3)\delta^2$$

$$E_{\varphi x}^* = \nu_{\varphi x} E_x / (1 - \nu^2)$$

$$D_x^* = D_x [1 - (\delta^3/3)]$$

$$E_{\varphi}^* = E_{\varphi} [1 + (\delta^3/3)/(1 - \nu^2)]$$

$$\nu_{\varphi x}^* = \nu_{\varphi x}$$

$$G_{xz}^* = \kappa G_{xz}$$

(A.28a)

where

$$D_x = (1/12) E_x h^3 / (1 - \nu^2)$$

When Eqs. (A.27), (A.28a) and (A.29) are substituted into Eqs. (A.19b) and (A.19c) the shell problem reduces to the solution of the following pair of linear, second order differential equations with constant coefficients:

$$L_{11}w + L_{12}w_{,x} = L_{13}w_0 + L_{14} \quad (\text{A.30a})$$

$$L_{21}w + L_{22}w_{,x} = L_{23}w_0 \quad (\text{A.30b})$$

where L_{ij} are commutative differential operators defined by

$$L_{11} = (-N_x + \frac{2a}{3} \delta^3 E_{\varphi x}^* - \frac{ph}{4}) \frac{d^2}{dx^2} + \frac{2}{a} \delta E_{\varphi}^* \approx (-N_x + \frac{2a}{3} \delta^3 E_{\varphi x}^*) \frac{d^2}{dx^2} + \frac{2}{a} \delta E_{\varphi}^*$$

$$L_{12} = D_x^* \frac{d^2}{dx^2} + \frac{2a}{3} \delta^3 E_{\varphi x}^*$$

$$L_{21} = (\frac{2a}{3} \delta^3 E_{\varphi x}^* + hG_{xz}^* + \frac{ph}{2}) \frac{d^2}{dx^2} \approx (\frac{2a}{3} \delta^3 E_{\varphi x}^* + hG_{xz}^*) \frac{d^2}{dx^2}$$

$$L_{22} = D_x^* \frac{d^2}{dx^2} - hG_{xz}^*$$

$$L_{13} = (N_x + \frac{ph}{4}) \frac{d^2}{dx^2} \approx N_x \frac{d^2}{dx^2}$$

$$L_{14} = \frac{v_0}{a} N_x + p(1 + \delta)$$

$$L_{23} = \frac{ph}{2} \frac{d^2}{dx^2} \approx 0$$

The approximations indicated above are associated with terms which are due to coupled beam-column and Flugge effects. For the shell considered here these terms are extremely small and hence are neglected.

Elimination of ω from Eqs. (A.30) yields the following fourth order equation in the deflection w :

$$w_{,xxxx} + 4(\theta/L)^2 (A/B) w_{,xx} + 4(\theta/L)^4 w/B = (4\gamma\xi/B) w_{o,xxxx} - [4\gamma(\theta/L)^2/B] w_{o,xx} + 8(\theta/L)^2 \bar{\gamma} [1 - (\nu_{\varphi x}^{**}/2)(1+\delta)]/aB(1+\delta) \quad (A.31)$$

where

$$A = \gamma - \xi + \alpha$$

$$B = 1 - 4\gamma\xi$$

$$(\theta/L)^4 = hE_{\varphi}^{**}/4a^2 D_x^{**}$$

$$\gamma = \bar{\gamma} = -N_x/4D_x^{**}/(\theta/L)^2$$

$$\xi = (\theta/L)^2 D_x^{**}/hG_{xz}^{**}$$

$$\alpha = a\delta^3 E_{\varphi x}^{**}/3D_x^{**}(\theta/L)^2 \quad (A.32)$$

Subtraction of Eq. (A.30b) from Eq. (A.30a) yields a convenient expression for the change in curvature

$$\omega_{,x} = \{Bw_{,xx} - 4\xi(\theta/L)^2 w + 8\bar{\gamma}\xi[1 - (\nu_{\varphi x}^{**}/2)(1+\delta)]/a(1+\delta) - 4\gamma\xi w_{o,xx}\}/(1+2\alpha\xi) \quad (A.33)$$

Eqs. (A.19c), (A.27a) and (A.33) combined to give the following relation for the transverse shear stress resultant:

$$Q = -D_x^* \{ w_{,xxx} - 2(\theta/L)^2 (2\xi - \alpha) w_{,x} - 4\gamma \xi w_{0,xxx} \} / (1 + 2\alpha\xi) \quad (A.34)$$

Finally, Eqs. (A.34) and (A.27c) combine [using conditions (A.29)] to give the rotation as a function of w

$$\omega = \{ [1 + 4\xi(\alpha - \xi)] w_{,x} + \xi(L/\theta)^2 (Bw - 4\gamma\xi w_0)_{,xxx} \} / (1 + 2\alpha\xi) \quad (A.35)$$

The governing differential equations of the shell consist of any two of Eq. (A.31), (A.33) and (A.35).

In Eqs. (A.32) the nondimensional parameter γ is a measure of the nonlinear "beam-column" effects (see Ref. 5). Although $\bar{\gamma}$ and γ are numerically equal, γ terms result from nonlinear effects while $\bar{\gamma}$ terms result from the linear effects of the pressure. Thus if the beam-column effect is neglected $\gamma = 0$ while $\bar{\gamma} \neq 0$.

The nondimensional parameter ξ is a measure of the transverse shear effect. If no transverse shear is permitted $G_{xz}^* \rightarrow \infty$ and $\xi \rightarrow 0$. Furthermore, the nondimensional parameters α and δ vanish when Flugge type accuracy is not desired.

It is noted that special cases exist when A or B vanish. When $\xi = 0$, $\gamma = 0$, $A = 0$ and $B = 1$, Eq. (A.31) reduces to the equation corresponding to the omission of both transverse shear and beam-column effects. When

the transverse shear and beam-column effects combine to cause $\delta = 0$, the entire nature of the differential equation changes. When the higher order effects are omitted, i.e., when $\gamma = \xi = \delta = \alpha = \Delta = 0$, except the δ term in the denominator, Eq. (A.31) corresponds to that obtained in Ref. 1, in which Hom provided for the only significant Flugge type term, which corresponds to $\delta \neq 0$ in the expression for the axial stress resultant [see Eq. (A.26)].

When transverse shear deformations are neglected ($\xi = 0$) only one equation is necessary to describe the shell deformation. In this case Eqs. (A.33) and (A.35) are satisfied by the condition that $w = w_{,x}$; and Eq. (A.31) reduces to

$$w_{,xxxx} + 4(\theta/L)^2(\gamma + \alpha)w_{,xx} + 4(\theta/L)^4w = -4\gamma(\theta/L)^2w_{0,xx} + 8(\theta/L)^2\gamma[1 - (\nu_{\phi x}^*/2)(1 + \xi)]/a(1 + \delta) \quad (A.31a)$$

If Flugge thickness terms are also neglected ($\alpha = \delta = 0$) and if no initial deflections are considered ($w_0 \equiv 0$), Eq. (A.31a) reduces to

$$w_{,xxxx} + 4\gamma(\theta/L)^2w_{,xx} + 4(\theta/L)^4w = 8(\theta/L)^2\gamma(1 - \nu_{\phi x}^*/2)/a \quad (A.31b)$$

Equation (A.31b) corresponds to that obtained in Ref. 7, in which similar formulae as those presented here were developed and, in addition, the results were expressed explicitly in terms of the load and the basic shell material and geometrical input quantities.

APPENDIX B (Ref. 7)

EVALUATION OF c'

The geometric ring parameter c' is defined as [see Eq. (3.4)]

$$c' = \frac{\bar{R}}{A_f} \int_{-h_o}^{h_i} \frac{b'(Z)}{\bar{R} - Z} dZ = \frac{\bar{R}}{A_f} \int_{R_i}^{R_o} \frac{b'(\zeta)}{\zeta} d\zeta \quad (B1)$$

where $\zeta = \bar{R} - Z$. From the definition (B1), it can be seen that c' is dependent only upon the geometry of the ring cross section and is therefore independent of the choice of origin of Z .

Performing the integration indicated in (B1) for a general "I" section yields

$$c' = \frac{\bar{R}}{A_f} \left\{ (b_i - h_w) \log\left(1 + \frac{t_i}{R_i}\right) - (b_o - h_w) \log\left(1 - \frac{t_o}{R_o}\right) - h_w \log\left(1 - \frac{d}{R_o}\right) \right\} \quad \text{GENERAL "I"} \quad (B2)$$

where, $d = R_o - R_i$ is the total height of the ring cross section.

A. Origin of Z at Mid-Height of Ring:

For this choice of the origin of Z

$$h_o = h_i = \frac{d}{2} \quad \text{and} \quad R_i = \bar{R} - \frac{d}{2} \quad ; \quad R_o = \bar{R} + \frac{d}{2}$$

Therefore, Eq. (B2) becomes

$$c' = \frac{\bar{R}}{A_f} \left\{ (b_i - h_w) \log \left[1 + \frac{t_i/\bar{R}}{1-d/2\bar{R}} \right] - (b_o - h_w) \log \left[1 - \frac{t_o/\bar{R}}{1+d/2\bar{R}} \right] - h_w \log \left[\frac{1-d/2\bar{R}}{1+d/2\bar{R}} \right] \right\}$$

GENERAL "I" (83)

However, recalling that

$$\log(1+x) = \sum_{n=1}^{\infty} (-1)^{n-1} \frac{x^n}{n} \quad \text{for } -1 < x < 1$$

$$\log(1-x) = - \sum_{n=1}^{\infty} \frac{x^n}{n} \quad \text{for } -1 < x < 1$$

and that

$$\frac{1}{1+x} = \sum_{n=0}^{\infty} (-x)^n \quad \text{for } -1 < x < 1$$

permits Eq. (83) to be rewritten as

$$\begin{aligned} c' \approx \frac{\bar{R}}{A_f} \left\{ (b_i - h_w) \frac{t_i}{\bar{R}} \left[1 + \frac{1}{2} \left(1 + \frac{1}{2} \frac{d}{\bar{R}} \frac{d}{\bar{R}} - \frac{1}{2} \frac{t_i}{\bar{R}} \left(1 + \frac{d}{\bar{R}} + \frac{2}{3} \frac{t_i}{\bar{R}} \right) \right) \right] \right. \\ \left. + (b_o - h_w) \frac{t_o}{\bar{R}} \left[1 - \frac{1}{2} \left(1 - \frac{1}{2} \frac{d}{\bar{R}} \frac{d}{\bar{R}} + \frac{1}{2} \frac{t_o}{\bar{R}} \left(1 - \frac{d}{\bar{R}} + \frac{2}{3} \frac{t_o}{\bar{R}} \right) \right) \right] \right. \\ \left. + h_w \frac{d}{\bar{R}} \left[1 + \frac{1}{12} \left(\frac{d}{\bar{R}} \right)^2 \right] \right\} \end{aligned}$$

GENERAL "I" (84)

in which all terms of third or higher order have been neglected due to the fact that t and d are small compared to \bar{R} , i.e.,

$$1 - \left(\frac{t}{R}\right)^3 \approx 1 - \left(\frac{d}{R}\right)^3 \approx 1$$

where here, and in subsequent expansions, \bar{R} is considered to be very much greater than d .

1. Rectangular Section

For a rectangular ring cross section of height d and width h_w ,

$$A_f = dh_w \quad \text{and} \quad t_i = t_o = t$$

Therefore, Eq. (B4) becomes ($\bar{R} \gg d$)

$$c'_{\text{rect}} = 1 + \frac{1}{12} \left(\frac{d}{R}\right)^2 \approx 1 \quad \text{RECTANGULAR} \quad (B5)$$

2. Equal Flange 'I' Section

For an equal flange 'I' ring cross section,

$$b_o = b_i \equiv b \quad ; \quad t_o = t_i \equiv t$$

Therefore, Eq. (B4) becomes

$$c'_I = \frac{\bar{R}}{A_f} \left\{ (b - h_w) \frac{t}{R} \left[2 + \frac{1}{2} \left(\frac{d}{R}\right)^2 - \frac{td}{R^2} + \frac{2}{3} \left(\frac{t}{R}\right)^2 \right] + h_w \left(\frac{d}{R}\right) \left[1 + \frac{1}{12} \left(\frac{d}{R}\right)^2 \right] \right\}$$

EQUAL 'I' (B6)

where,

$$A_f = 2t(b-h_w) + dh_w$$

If the second order terms in t and d of (B6) are dropped as being small ($\bar{R} \gg d$)

$$c_I' \approx 1$$

3. Idealized "I" Section

For an idealized "I" section

$$h_w = 0 \quad ; \quad A_f = 2bt \neq 0 \quad ; \quad t_o = t_i \equiv t \rightarrow 0$$

Therefore, Eq. (B6) becomes ($\bar{R} \gg d$)

$$c_I' = 1 + \frac{1}{4} \left(\frac{d}{\bar{R}}\right)^2 \approx 1$$

IDEAL "I"

(B7)

B. Origin of Z at Centroid of Ring Cross Section:

Since Eq. (B4) contains terms which can be related to the first moment of area, it is logical to choose \bar{R} to be the radius to the centroid of the ring cross section.

The definition of c' can be rewritten as [see Eq. (B1)]

$$c' = \frac{\bar{R}}{A_f} \int \frac{dA_f}{\bar{R}-Z} = \frac{1}{A_f} \int \frac{dA_f}{1-Z/\bar{R}} \quad (B1a)$$

or,

$$c' = 1 + \frac{A_f}{R} \int Z dA_f + \frac{A_f}{R^2} \int \frac{Z^2 dA_f}{1-Z/R} \quad (B1b)$$

However, since the origin of Z is taken to be the centroid of the cross-sectional area,

$$\int Z dA_f \equiv 0$$

Therefore,

$$c' = 1 + \left(\frac{\rho}{R}\right)^2 c \quad (B8)$$

where,

$$\rho = \sqrt{I_f/A_f}$$

is the radius of gyration of the cross-sectional area,

$I_f = \int Z^2 dA_f$ is the moment of inertia of the cross-sectional area about $Z = 0$,

and

$$c = \frac{1}{I_f} \int \frac{Z^2 dA_f}{1-Z/R} = \frac{1}{I_f} \int_{-h_0}^{h_i} \frac{Z^2 b(Z) dZ}{1-Z/R} \quad (B9)$$

Expanding $Z^2/(1 - Z/\bar{R})$ in a series ($\bar{R} \gg d$), performing the integration indicated in (89) for a general 'I' section, and neglecting terms of order (Z^5/\bar{R}^5) and higher, yields the following expression for c

$$c \approx 1 + \frac{1}{I_f} \left\{ \frac{b_o}{4\bar{R}} [(h_o - t_o)^4 - h_o^4] + \frac{b_i}{4\bar{R}} [h_i^4 - (h_i - t_i)^4] + \frac{h_w}{4\bar{R}} [(h_i - t_i)^4 - (h_o - t_o)^4] \right\} \quad \text{GENERAL 'I'}$$

(B10)

APPENDIX C. AXISYMMETRIC BUCKLING LOAD OF INFINITE, UNSUPPORTED
ORTHOTROPIC CYLINDER UNDER AXIAL
COMPRESSION

The differential equation governing the deflection of a perfect shell subjected to axial compression is taken from Eq. (2.1); i.e.,

$$w_{,xxxx} + \frac{4\left(\frac{\theta}{L}\right)^2(\gamma-\xi+\alpha)}{1-4\gamma\xi} w_{,xx} + \frac{4\left(\frac{\theta}{L}\right)^4}{1-4\gamma\xi} w = 0 \quad (C1)$$

The nontrivial (axisymmetric buckling) solution is

$$w = D \cos \lambda \frac{x}{L} \quad (C2)$$

where L is the wavelength of the buckling pattern. Substitution gives

$$\lambda^4 - 4\theta^2 a \lambda^2 + 4\theta^4 b = 0 \quad (C3a)$$

$$a = \frac{\gamma-\xi+\alpha}{1-4\gamma\xi} \quad (C3b)$$

$$b = \frac{1}{1-4\gamma\xi} \quad (C3c)$$

Thus

$$\lambda^2 = 2\theta^2(a \pm a^2 - b) \quad (C4)$$

In order for w to remain finite λ must be real. Then the following two possibilities exist:

$$0 < b < a^2 \quad (C5a)$$

or

$$b < 0 \quad (C5b)$$

In the first case substituting Eqs. (C3b) and (C3c) into (C5) yields an expression for the buckling load parameter γ^*

$$\gamma^* = \sqrt{1 + 4\xi\alpha - \xi - \alpha} \quad (C6a)$$

when

$$\gamma^* < \frac{1}{4\xi} \quad (C6b)$$

For sufficiently small α Eq. (C6a) is closely approximated by

$$\gamma^* = 1 - \alpha - \xi(1 - 2\alpha) \quad (C7)$$

In the second case ($b < 0$) the buckling load given by Eq. (C5b) is

$$\gamma_1^* = \frac{1}{4\xi} \quad (C8)$$

Equations (C7) and (C8) intersect (in the γ, ξ plane) when

$$\frac{1}{4\xi} = 1 - \alpha - \xi(1 - 2\alpha) \quad (C9a)$$

$$2\bar{\xi} = \frac{1}{1-2\alpha}, \quad 1 \quad (C9b)$$

Thus, when $\xi \leq 1/2$ the buckling load is given by Eq. (C7); when shear deformation effects are more significant, $\xi \geq 1/2$, the buckling load is given by Eq. (C8). The buckling load γ^* is plotted as a function of ξ for $\alpha = 0.00549$ in Fig. 19, although this figure is applicable as long as $\alpha \ll 1$. For the shell comparable to that described by Eqs. (8.1) and (8.2) (i.e., $\xi = 0.1367$) the buckling load is given by

$$\gamma^* = 0.857 \quad (C10)$$

The corresponding critical pressure is $p^* = 7.078 \times 10^4$ psi

APPENDIX D. PERTURBATION SOLUTION

The results described in section 8 show that the stresses are approximately linear functions of the parameter ψ (see Figs. 3 to 10). This observation suggests that a perturbation solution should give accurate predictions of the stresses and displacements when the parameter ψ is small [see Eqs. (4.5d), (2.1) and (2.2)]. For the initial deflections considered here [see Eq. (4.1)], the governing differential equations [Eqs. (2.1) and (2.2)] are

$$w_{,xxxx} + (4/B)(\theta/L)^4 w = (L/B)(\theta/L)^4 w_p - 4(\theta/L)^2 \frac{\psi}{\sqrt{B}} w_{,xx} \quad (D1a)$$

$$\omega_{,x} = B w_{,xx} - 4\xi(\theta/L)^4 (w - w_p) \quad (D1b)$$

where w_p may be obtained from Eqs. (4.2).

When ψ is small, a solution may be assumed to be of the form

$$w = \sum_{i=0}^{\infty} \bar{w}_i(x) \psi^i, \quad \omega = \sum_{i=0}^{\infty} \bar{\omega}_i(x) \psi^i \quad (D2)$$

Substitution of Eqs. (D2) into (D1) leaves

$$\begin{aligned} & [\bar{w}_{0,xxxx} + (4/B)(\theta/L)^4 \bar{w}_0 - (4/B)(\theta/L)^4 w_p] + \psi [\bar{w}_{1,xxxx} + (4/B)(\theta/L)^4 \bar{w}_1 \\ & + (4/\sqrt{B})(\theta/L)^2 \bar{w}_{0,xx}] + \psi^2 [\dots] + \dots = 0 \end{aligned} \quad (D3a)$$

and

$$[\bar{\omega}_{0,x} - B\bar{\omega}_{0,xx} + 4\xi(\theta/L)^4(\bar{w}_0 - w_p)] + \psi[\bar{\omega}_{1,x} - B\bar{\omega}_{1,xx} + 4\xi(\theta/L)^4\bar{w}_1] + \psi^2[\] + \dots = 0 \quad (D3b)$$

The first approximate solution \bar{w}_0 , $\bar{\omega}_0$ may be obtained by setting $\psi = 0$ in Eqs. (D3). Thus,

$$\bar{w}_{0,xxxx} + (4/B)(\theta/L)^4\bar{w}_0 = (4/B)(\theta/L)^4w_p \quad (D4a)$$

$$\bar{\omega}_{0,x} = B\bar{\omega}_{0,xx} - 4\xi(\theta/L)^4(\bar{w}_0 - w_p) \quad (D4b)$$

The solution for \bar{w}_0 is taken in the form

$$\bar{w}_0 = w_p[1 + c_{10}\bar{g}_1(x) + c_{20}\bar{g}_2(x) + c_{30}\bar{g}_3(x) + c_{40}\bar{g}_4(x)]$$

where

$$\bar{g}_1(x) = \sinh(\theta x/L/B) \cos(\theta x/L/B)$$

$$\bar{g}_2(x) = \sinh(\theta x/L/B) \sin(\theta x/L/B)$$

$$\bar{g}_3(x) = \cosh(\theta x/L/B) \sin(\theta x/L/B)$$

$$\bar{g}_4(x) = \cosh(\theta x/L/B) \cos(\theta x/L/B) \quad (D5)$$

The arbitrary constants c_{10} are determined by using symmetry [see Eq. (4.9)] and by applying Eqs. (2.9b,c) in conjunction with Eqs. (3.18), (3.20), (A.34), (A.35), (4.10), (D4) and (D5). Thus,

$$\begin{aligned} \bar{w}_0 = & [8(\gamma_\Delta - \bar{\gamma}_{\Delta p})/\theta^2] \{ 1 - [(\gamma_\Delta - \bar{\gamma}_{\Delta 1})/(\gamma_\Delta - \bar{\gamma}_{\Delta p})] [\bar{g}_4(x) \\ & + (\bar{g}_2(x)/B) (G_{40}/G_{20})] \Lambda_0^* \} \end{aligned}$$

and

$$\begin{aligned} \bar{w}_{0,x} = & - (32\Lambda^*/L^2) (\gamma_\Delta - \bar{\gamma}_{\Delta 1}) \{ -[(1/2B) + \xi (G_{40}/G_{20})] [\bar{g}_2(x)/B] \\ & + [(1/2B) (G_{40}/G_{20}) - \xi] \bar{g}_4(x) \} \end{aligned} \quad (D6)$$

where

$$G_{10} = (2/\theta) (\bar{g}_{30}^2 + \bar{g}_{10}^2) / [B_1 (\bar{g}_{30} \bar{g}_{20} + \bar{g}_{10} \bar{g}_{40}) + B_2 (\bar{g}_{30} \bar{g}_{40} - \bar{g}_{10} \bar{g}_{20})]$$

$$G_{20} = (B_1 \bar{g}_{10} + B_2 \bar{g}_{30}) / [B_1 (\bar{g}_{30} \bar{g}_{20} + \bar{g}_{10} \bar{g}_{40}) + B_2 (\bar{g}_{30} \bar{g}_{40} - \bar{g}_{10} \bar{g}_{20})]$$

$$G_{40} = (B_1 \bar{g}_{30} - B_2 \bar{g}_{10}) / [B_1 (\bar{g}_{30} \bar{g}_{20} + \bar{g}_{10} \bar{g}_{40}) + B_2 (\bar{g}_{30} \bar{g}_{40} - \bar{g}_{10} \bar{g}_{20})]$$

$$\Lambda_0^* = \beta_c^* B G_{20} / [\beta_c^* + G_{10} (1 - \beta_c) [\beta_c^* + (1 + \delta - 2\delta^*) \alpha_c] / \beta_c]$$

$$\bar{g}_{10} = \bar{g}_1 (L/2)$$

(continued on next page)

$$B_1 = 1 + 2\xi(1 - 2\xi + \alpha)$$

$$B_2 = 1 - 2\xi(1 + 2\xi - \alpha)$$

The corresponding stresses may be obtained by direct substitution of Eqs. (D6) into Eqs. (5.3). This solution could, of course, be obtained from the solution presented in the text by simply setting $\psi = 0$ in Eqs. (4.14) and (4.13).

The first perturbation yields

$$\bar{w}_{1,xxxx} + (4/B)(\theta/L)^4 \bar{w}_1 = - (4/\sqrt{B})(\theta/L)^2 \bar{w}_{0,xx} \quad (D7a)$$

and

$$\bar{\omega}_{1,x} = \bar{w}_{1,xx} - 4\xi(\theta/L)^4 \bar{w}_1 \quad (D7b)$$

with boundary conditions

$$\bar{w}_1(\pm L/2) = 0, \quad \bar{\omega}_1(\pm L/2) = 0 \quad (D8)$$

The solution for \bar{w}_1 can be shown to be

$$\bar{w}_1 = -[8(\gamma_\Delta - \gamma_{\Delta_1})/\theta^2] \{c_2 \bar{g}_2(x) + c_4 \bar{g}_4(x) + (\theta x/L)[c_1 \bar{g}_1(x) + c_3 \bar{g}_3(x)]\} \quad (D9a)$$

where

$$c_{11} = - (1/2) [1 - (G_{40}/G_{20})], \quad (D9b)$$

$$c_{31} = - (1/2) [1 + (G_{40}/G_{20})], \quad (D9c)$$

$$c_{21} = \bar{A} G_{40} + \bar{B} \bar{g}_{40} / [B_1 (\bar{g}_{30} \bar{g}_{20} + \bar{g}_{10} \bar{g}_{40}) + B_2 (\bar{g}_{30} \bar{g}_{40} - \bar{g}_{10} \bar{g}_{20})], \quad (D9d)$$

$$c_{41} = + \bar{A} G_{20} - \bar{B} \bar{g}_{20} / [B_1 (\bar{g}_{30} \bar{g}_{20} + \bar{g}_{10} \bar{g}_{40}) + B_2 (\bar{g}_{30} \bar{g}_{40} - \bar{g}_{10} \bar{g}_{20})], \quad (D9e)$$

$$\bar{A} = (-e/2) (c_{11} \bar{g}_{10} + c_{31} \bar{g}_{30}) \quad (D9f)$$

$$\begin{aligned} \bar{B} = & - [1 - 2\xi(2\xi - \alpha)] \{ c_{11} \bar{g}_{10} + c_{31} \bar{g}_{30} + (e/2) [c_{11} (\bar{g}_{40} - \bar{g}_{20}) + c_{31} (\bar{g}_{20} + \bar{g}_{40})] \} \\ & - 2\xi [-2c_{11} \bar{g}_{30} + 2c_{31} \bar{g}_{10} + (e/2) [-c_{11} (\bar{g}_{20} + \bar{g}_{40}) + c_{31} (\bar{g}_{40} - \bar{g}_{20})]] \} \end{aligned} \quad (D9g)$$

The solution may now be written to include the first perturbation, thus

$$w = \bar{w}_0 + \epsilon \bar{w}_1 \quad \text{and} \quad u = \bar{u}_0 + \epsilon \bar{u}_1 \quad (D10)$$

When γ and ξ are small (as they are in the region of p for which the shells considered in this work behave elastically)

$$B = 1 - 4\gamma \xi \approx 1 \quad [\text{see Eqs. (2.4)}]$$

Then the linearized form of G_{10} , G_{20} and G_{40} become

$$\begin{aligned} G_{10} &\approx F_1 \left[1 - 2\xi \sqrt{\frac{0.91}{3}} F_3 \right] \\ G_{20} &\approx F_2 - 2\xi \sqrt{\frac{0.91}{3}} (F_4 + F_2 F_3) \\ G_{40} &\approx \sqrt{\frac{0.91}{3}} F_4 + 2\xi \left[F_2 - \frac{0.91}{3} F_3 F_4 \right] \end{aligned} \quad (D11)$$

where

$$\begin{aligned} F_1 &= (2/\theta) (\bar{g}_{30}^2 + \bar{g}_{10}^2) / [(\bar{g}_{30}\bar{g}_{20} + \bar{g}_{10}\bar{g}_{40}) + (\bar{g}_{30}\bar{g}_{40} - \bar{g}_{10}\bar{g}_{20})] \\ F_2 &= (\bar{g}_{10} + \bar{g}_{30}) / [(\bar{g}_{30}\bar{g}_{20} + \bar{g}_{10}\bar{g}_{40}) + (\bar{g}_{30}\bar{g}_{40} - \bar{g}_{10}\bar{g}_{20})] \\ \sqrt{\frac{0.91}{3}} F_3 &= [\bar{g}_{40}\bar{g}_{30} - \bar{g}_{10}\bar{g}_{20} - (\bar{g}_{30}\bar{g}_{20} + \bar{g}_{10}\bar{g}_{40})] / [(\bar{g}_{30}\bar{g}_{20} + \bar{g}_{10}\bar{g}_{40}) + (\bar{g}_{30}\bar{g}_{40} - \bar{g}_{10}\bar{g}_{20})] \\ \sqrt{\frac{0.91}{3}} F_4 &= [\bar{g}_{30} - \bar{g}_{10}] / [(\bar{g}_{30}\bar{g}_{20} + \bar{g}_{10}\bar{g}_{40}) + (\bar{g}_{30}\bar{g}_{40} - \bar{g}_{10}\bar{g}_{20})] \end{aligned} \quad (D12)$$

The functions F_i , correspond to the functions F_i listed in Ref. (12) which were displayed graphically as functions of θ for the isotropic case.

The stresses can be obtained by substituting Eqs. (D10) into Eqs. (5.3) and using Eqs. (5.6). In general Eqs. (D11) and (D12) may be used in place of the definitions for G_0 given in Eqs. (D6). When this is done, the charts of F_i vs θ offered in Ref. 13 may be utilized to obtain G_0 . This procedure results in a considerable reduction of computation time and provides accurate stresses and displacements for the most general case provided that ψ is reasonably small.

To obtain the F_i vs θ relations displayed as functions of γ as well as θ in Ref. 6, it is necessary to set $\xi = \delta = \alpha = 0$ in Eqs. (4.12) and to replace G_1 , G_2 , G_3 and G_4 in Eqs. (4.12), with F_1 , F_2 , $\sqrt{0.91/3} F_3$ and $\sqrt{0.91/3} F_4$, respectively. These functions are displayed graphically in Ref 5.

APPENDIX E
STRESSES IN NONHOMOGENEOUS SHELL

It was observed in Ref. 13 that because of the nonhomogeneity of material properties through the thickness of the composite, Hill's yield criteria for a homogeneous orthotropic material could not be expected to provide accurate estimates of the yield pressure. This short coming motivated the work that is discussed in this appendix.

The elastic constants given in Eq. (8.1) were obtained experimentally by measuring the strains in a pressurized cylinder (of 3C:2L winding ratio) and utilizing stress strain relationships in a simple homogeneous shell theory (Ref. 14). Hence, it is reasonable to expect that the homogeneous shell theory utilized in this work will accurately predict the shell deformations [Eqs. (4.13) and (4.14)]. However, the nominal stresses obtained with these constants for an equivalent homogeneous material [Eqs. (5.3)] cannot always be expected to correspond to the actual stresses acting in the nonhomogeneous composite shell, which consists of materials of widely varying elastic properties.

If the deformations predicted by shell theory are accurate, then the individual constituents of the shell material must deform according to Eqs. (4.13) and (4.14). Once these deformations are known, it is necessary to use Eqs. (5.1) to calculate the stresses in the constituent materials.

It is possible, however, to obtain approximate values for the stresses in the nonhomogeneous shell by utilizing the uniaxial stress strain relationships suggested in Ref. 15 and Ref. 16. For example, the effective composite modulus E_2 , say, in a direction normal to the fiber direction could be obtained by assuming the fiber resin system to behave as a spring in series. This results in (see Ref. 15)

$$E_2 = E_e \left(\frac{1 + V_g/V_e}{1 + E_e V_g/E_g V_e} \right) \text{ for } V_g > 68 \text{ percent} \quad (E.1)$$

in which E_e and E_g are the moduli of the resin and fiberglass, respectively, V_e and V_g are the percentages, by volume, of the resin and fiberglass. In Ref. 15 it is shown that a more complicated relation is necessary for composites with $V_g < 68$ percent.

It is noted that the effective modulus given by Eq. (E.1) is based upon the assumption that the spacing between the fibers is uniform in that the volume percentage ratio V_g/V_e is assumed to be equal to the (presumably) uniform ratio of fiber cross section to resin cross section. Shaffer* has pointed out winding irregularities could cause serious fluctuations in this ratio.

The effective composite modulus E_1 in a direction parallel to the fiber direction is given by

$$E_1 = E_g \left(\frac{1 + E_e V_e/E_g V_g}{V_e/V_g + 1} \right) \quad (E.2)$$

* Shaffer, B.W.: Filament Reinforced Plastics Micro-Mechanics-Structural Mechanics: Seminar given at Polytechnic Institute of Brooklyn, Feb. 9, 1968.

In the filament winding direction the stresses in each of the constituents may be obtained by multiplying the stresses in the equivalent homogeneous shell by appropriate ratios of the elastic constants (these ratios are often referred to as stress concentration factors). There is some approximation involved due to neglecting Poisson ratio changes, but the error induced in this manner is expected to be small. If more accuracy is desired, the deformations given by shell theory could be substituted directly into Eqs. (5.1). In the directions normal to the filament winding direction, the stresses are transmitted from one constituent to the other and must be matched across the glass resin interface in order to satisfy equilibrium requirements. In these directions it may be assumed that the stresses in the fiberglass and resin are equal.

Since the stresses in an equivalent homogeneous shell have been calculated (see Table 3), the stresses of the constituents may be approximated as follows:

1. In a fiberglass filament

$$\left(\frac{\sigma_x}{N_x}\right)_g = \frac{E_g(1-\nu_g^2)}{E_x(1-\nu_g^2)} \left(\frac{\sigma_x}{N_x}\right)$$

in a longitudinal layer

$$\left(\frac{\sigma_\phi}{N_x}\right)_g = \left(\frac{1+\nu_g/\nu_e}{1+E_g\nu_g/E_e\nu_e}\right) \frac{E_e}{E_\phi} \left(\frac{\sigma_\phi}{N_x}\right)$$

(continued on next page)

$$\left(\frac{\sigma_x}{N_x}\right)_g = \left(\frac{1+V_g/V_e}{1+E_g V_e/E_g V_e}\right) \frac{E_e}{E_x} \left(\frac{\sigma_x}{N_x}\right)$$

in a circumferentially wound layer

$$\left(\frac{\sigma_\phi}{N_x}\right)_g = \frac{E_g (1-\nu_g^2)}{E_\phi (1-\nu_g^2)} \left(\frac{\sigma_\phi}{N_x}\right) \quad (E.3)$$

2. In the resin

$$\left(\frac{\sigma_x}{N_x}\right)_e = \frac{E_e (1-\nu_e^2)}{E_x (1-\nu_e^2)} \left(\frac{\sigma_x}{N_x}\right)$$

in a longitudinal layer

$$\left(\frac{\sigma_\phi}{N_x}\right)_e = \left(\frac{1+V_g/V_e}{1+E_g V_e/E_g V_e}\right) \frac{E_e}{E_\phi} \left(\frac{\sigma_\phi}{N_x}\right)$$

$$\left(\frac{\sigma_x}{N_x}\right)_e = \left(\frac{1+V_g/V_e}{1+E_g V_e/E_g V_e}\right) \frac{E_e}{E_x} \left(\frac{\sigma_x}{N_x}\right)$$

in a circumferentially wound layer

$$\left(\frac{\sigma_\phi}{N_x}\right)_e = \frac{E_e}{E_\phi} \frac{(1-\nu_e^2)}{(1-\nu_e^2)} \left(\frac{\sigma_\phi}{N_x}\right) \quad (E.4)$$

ν_g and ν_e are the Poisson ratio's of the glass and resin. The g and e subscripts denote the local stresses in the fiberglass and the resin, respectively.

Once the stresses have been obtained from the above relations a maximum stress yield criterion can be used to approximate the magnitude of the pressure at which yielding begins. Thus,

$$\frac{p_{Yg}}{Y_g} = \frac{2(h/a)}{(1+\delta)^2 \left(\frac{\sigma h}{N_x}\right)_g} \quad \text{in the fiberglass}$$

$$\frac{p_{Ye}}{Y_e} = \frac{2(h/a)}{(1+\delta)^2 \left(\frac{\sigma h}{N_x}\right)_e} \quad \text{in the resin} \quad (E.5)$$

where Y_g and Y_e are the yield stresses of the fiberglass and the resin, respectively.

Limited calculations were performed on a shell of dimensions equal to those of the equivalent homogeneous shell [Eqs. (8.1)]. The constituent elastic constants and yield stresses were taken from Ref. (18), while the volume ratio was deduced from Ref. 1.

$$E_g = 10.5 \times 10^6 \text{ psi} \quad , \quad E_e = 0.5 \times 10^6 \text{ psi}$$

$$\nu_g = 0.2 \quad , \quad \nu_e = 0.35$$

$$Y_g \geq 200,000 \text{ psi} \quad , \quad Y_e = 22,000 \text{ psi}$$

$$V_g/V_e = 2.188$$

Substitution of Eqs. (E.6) into (E.5) to (E.3) gives approximate values of the initial yield pressure. It is found that the yielding would initiate in the resin near the shell inner surface, next to the frame, at pressures of

$p_{ye} = 11785$ due to circumferential stress in a longitudinal layer

$p_{ye} = 11157$ due to longitudinal stress in a circumferential layer

These yield pressures are within ten percent of the experimentally determined collapse load of the shell examined in the text. Hence, the shell appears to be weakest at the frame, near the inner shell surface. The stresses in the direction perpendicular to the fiber directions exceed the relatively low yield stress of the resin at extremely low pressures. When this happens the shell might be considered to be delaminating in that the resin is no longer binding the layers together.

Winding irregularities, as noted earlier, may, through effective modulus changes, cause yielding to occur very early in some portions of the shell. Evidently, this early yielding results in little more than slight changes in the composite moduli (e.g., see Ref. 14 and Ref. 19).

TABLE 1
STRESSES, DEFLECTIONS AND LOADS ($\alpha = \delta = \epsilon = 0$)

		h = 0.388 in.			h = 0.194 in.		
	γ	ORTHO-TROPIC	ISOTROPIC		ORTHO-TROPIC	ISOTROPIC	
			$E = 5.395 \times 10^6$ (PSI)			$E = 5.395 \times 10^6$ (PSI)	
			(E_f/E) = 1.335	$(E_f/E) = 1$		(E_f/E) = 1.335	$(E_f/E) = 1$
$P \times 10^{-4}$ (PSI)	0.1 0.2 0.3 0.4	0.931 1.861 2.791 3.722			0.247 0.495 0.742 0.990		
$\sigma_u \times 10^{-5}$ (PSI)	0.1 0.2 0.3 0.4	0.766 1.532 2.298 3.064			0.395 0.790 1.185 1.580		
$w_m \times 10^2$ (IN.)	0.1 0.2 0.3 0.4	2.716 5.435 8.157 10.88	3.013 6.029 9.045 12.06	3.236 6.474 9.714 12.96	1.226 2.466 3.724 5.001	1.324 2.661 4.013 5.382	1.442 2.895 4.360 5.839
$w_f \times 10^2$ (IN.)	0.1 0.2 0.3 0.4	2.652 5.303 7.953 10.60	2.950 5.898 8.846 11.79	3.185 6.370 9.553 12.74	1.034 2.062 3.085 4.102	1.136 2.267 3.394 4.516	1.283 2.561 3.836 5.105
$-Q_o \times 10^{-3}$ (Lb/in)	0.1 0.2 0.3 0.4	1.407 2.815 4.220 5.625	1.569 3.135 4.702 6.267	1.759 3.517 5.275 7.041	0.538 1.072 1.601 2.125	0.594 1.186 1.773 2.357	0.504 1.004 1.501 1.996
$P_c \times 10^{-4}$ (PSI)	0.1 0.2 0.3 0.4	1.268 2.536 3.803 5.070	1.418 2.821 4.230 5.640	1.141 2.282 3.428 4.564	0.494 0.986 1.475 1.962	0.543 1.084 1.623 2.159	0.460 0.918 1.374 1.829
L_e/L_f	0.1 0.2 0.3 0.4	0.9711 0.9704 0.9696 0.9689	0.9775 0.9773 0.9767 0.9760	0.9775 0.9770 0.9765 0.9760	0.8919 0.8870 0.8817 0.8759	0.9133 0.9097 0.9059 0.9017	0.9133 0.9097 0.9059 0.9017

TABLE 2 YIELD PRESSURE

YIELD CRITERION P - PLASTIC POTENTIAL M- MAXIMUM STRESS	YIELD STRESSES $\times 10^{-5}$ PSI			YIELD PRESSURE $\times 10^{-4}$ PSI					
				FRAME INNER SURFACE		MIDBAY OUTER SURFACE		MIDBAY MEDIUM SURFACE	
	Y_x	Y_y	Y_z	h, in.					
				0.388	0.194	0.388	0.194	0.388	0.194
ORTHOTROPIC: $E_x = 4.74 \times 10^6$ PSI, $E_s = 6.14 \times 10^6$ PSI, $E_f = 7.2 \times 10^6$ PSI									
$P(\sigma_z = 0)$	1.0	1.7	0.22	0.3749	0.1702	0.3992	0.1902	0.4325	0.2338
$P(\sigma_z = 0)$	∞	∞	0.22	0.3740	0.1713	0.3979	0.1901	0.4308	0.2329
$P(\sigma_z \neq 0)$	∞	∞	0.22	0.3740	0.1733	0.4332	0.2090	0.4997	0.2503
M	1.0	1.7		1.858	0.6641	2.637	1.444		
ISOTROPIC: $E = E_x = E_s = 5.395 \times 10^6$ PSI, $E_f = 7.2 \times 10^6$ PSI									
$P(\sigma_z = 0)$	1.0	1.0	0.22	0.3753	0.1700	0.4015	0.1921	0.4373	0.2397
$P(\sigma_z = 0)$	1.7	1.7	0.22	0.3754	0.1705	0.4019	0.1922	0.4383	0.2400
$P(\sigma_z = 0)$	∞	∞	0.22	0.3754	0.1707	0.4021	0.1922	0.4389	0.2401
$P(\sigma_z \neq 0)$	∞	∞	0.22	0.3754	0.1707	0.5060	0.2115	0.5054	0.2533
$P(\sigma_z = 0)$	1.0	1.0	1.0	1.695	0.7157	1.771	0.8718	1.855	1.052
$P(\sigma_z = 0)$	1.7	1.7	1.7	2.882	1.217	3.011	1.482	2.153	1.789
M	1.0	1.0		1.808	0.6303	1.610	0.9004		
M	1.7	1.7		3.074	1.071	2.736	1.531		

* Maximum Stress - Axial

*** Maximum Stress - Circumferential

Reproduced From
Best Available Copy

(continued on next page)

TABLE 2 YIELD PRESSURE

YIELD CRITERION P - PLASTIC POTENTIAL M - MAXIMUM STRESS	YIELD STRESSES × 10 ⁻⁵ PSI			YIELD PRESSURE × 10 ⁻⁴ PSI					
				FRAME INNER SURFACE		MIDBAY OUTER SURFACE		MIDBAY MEDIAN SURFACE	
	Y _x	Y _y	Y _z	h, in.					
				0.388	0.194	0.388	0.194	0.388	0.194
ISOTROPIC: E = E _x = E _s = E _f = 5.395 × 10 ⁶ PSI									
P(σ _z = 0)	1.0	1.0	0.22	0.3730	0.1706	0.3946	0.1897	0.4228	0.2304
P(σ _z = 0)	1.7	1.7	0.22	0.3733	0.1708	0.3953	0.1897	0.4242	0.2309
P(σ _z = 0)	1.0	1.0	1.0	1.656	0.7519	1.701	0.8613	1.753	0.9902
P(σ _z = 0)	1.7	1.7	1.7	2.814	1.278	2.891	1.461	2.981	1.683
M	1.0	1.0		*	*	**	**		
M	1.7	1.7		*	*	**	**		
				1.901	0.6825	1.516	0.8423		
				3.232	1.160	2.576	1.432		

*Maximum Stress - Axial

**Maximum Stress - Circumferential

TABLE 3. TRANSVERSE SHEAR DEFORMATION AND BEAM COLUMN EFFECTS

$$(\Delta = 0, \delta^2 = 0.003689, \alpha = 0.005489)$$

$\bar{\gamma} = 0.2$	$\gamma = 0$		$\gamma = 0.2$	
	MIDBAY	FRAME	MIDBAY	FRAME
$\frac{E_x w}{N_x}$	-8.255*** -8.381	-8.076 -7.984	-8.261 -8.870	-8.073 -8.424
$\frac{\sigma_x h}{N_x}$ MEMBRANE	0.9973 0.9990	1.006 1.008	0.9971 0.9979	1.006 1.009
$\frac{\sigma_x h}{N_x}$ BENDING	± 0.125 ± 0.0405	± 0.284 ± 0.395	± 0.133 ± 0.0925	± 0.294 ± 0.455
$\frac{\sigma_x h}{N_x}$ MEMBRANE	1.473 1.493	1.447 1.432	1.474 1.570	1.446 1.502
$\frac{\sigma_x h}{N_x}$ BENDING	± 0.0570 ± 0.0735	± 0.128 ± 0.146	± 0.0560 ± 0.0685	± 0.129 ± 0.161
$\frac{\sigma_x h}{N_x}$ INNER SURFACE	1.535 1.572	1.579 1.583	1.535 1.644	1.580 1.668
$\frac{\sigma_x h}{N_x}$ OUTER SURFACE	1.421 1.425	1.324 1.291	1.423 1.507	1.322 1.346
$\frac{\sigma_x h}{N_x}$ INNER SURFACE	0.8730 0.9591	1.290 1.404	0.8646 0.9060	1.300 1.465
$\frac{\sigma_x h}{N_x}$ OUTER SURFACE	1.123 1.040	0.7220 0.6132	1.131 1.091	0.7128 0.5545
$\frac{T_{xz}}{N_x}$ MEDIAN SURFACE	0 0	0.1261 0.1283	0 0	0.1261 0.1259
$\frac{P_y}{Y_z}$ INNER SURFACE	0.1873 0.1766	0.1517 0.1451	0.1882 0.1776	0.1510 0.1384
$\frac{P_y}{Y_z}$ MEDIAN SURFACE	0.1788 0.1775	0.1771 0.1745	0.1788 0.1732	0.1771 0.1708
$\frac{P_y}{Y_z}$ OUTER SURFACE	0.1714 0.1780	0.2217 0.2435	0.1707 0.1690	0.2233 0.2505

$$^* \xi = 0.1367$$

$$^{***} \xi = 0$$

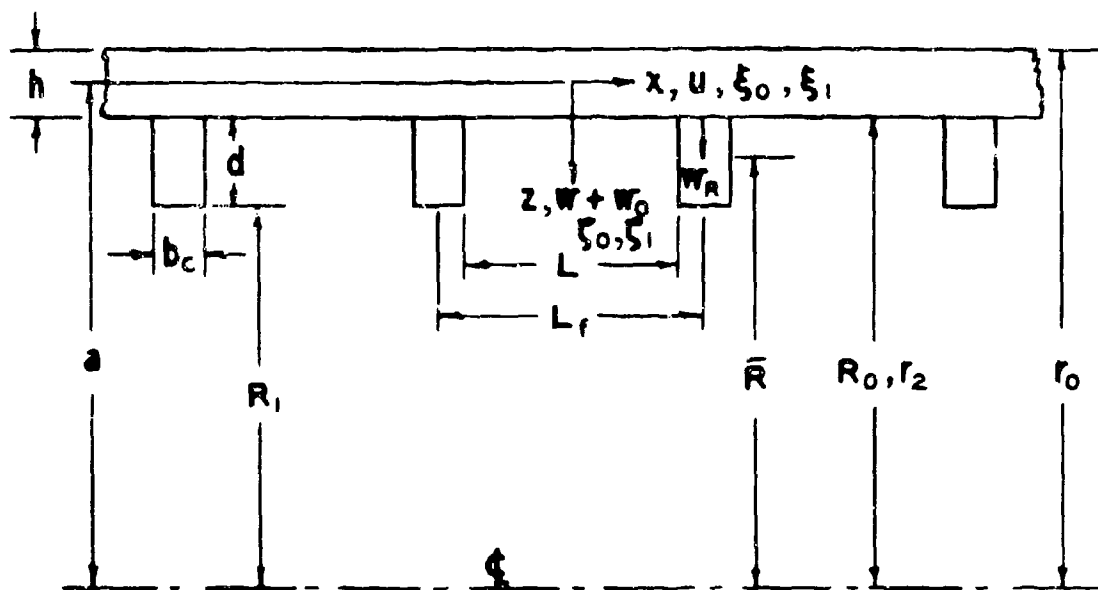
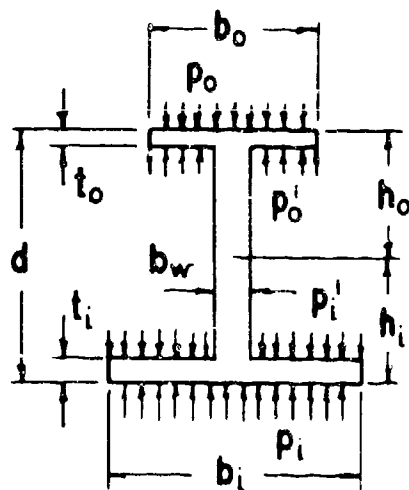
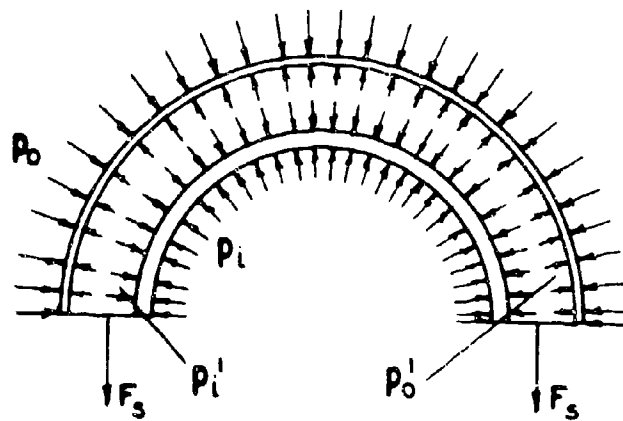


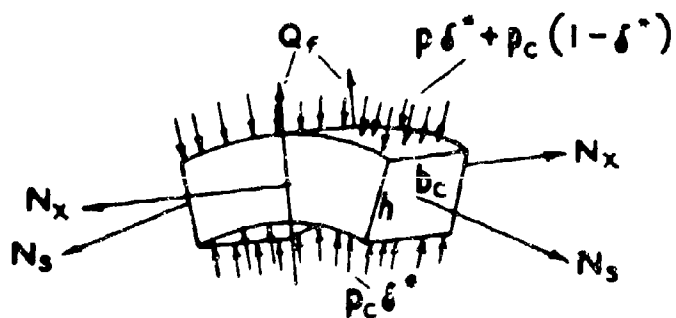
FIG. 1
SCALE SECTION OF STRUCTURE (WITH
RECTANGULAR CROSS SECTION RINGS)



a) CROSS SECTION



b) FREE BODY DIAGRAM



c) FREE BODY DIAGRAM OF SECTION OF SHELL IN CONTACT WITH RING

FIG. 2 REINFORCING RING

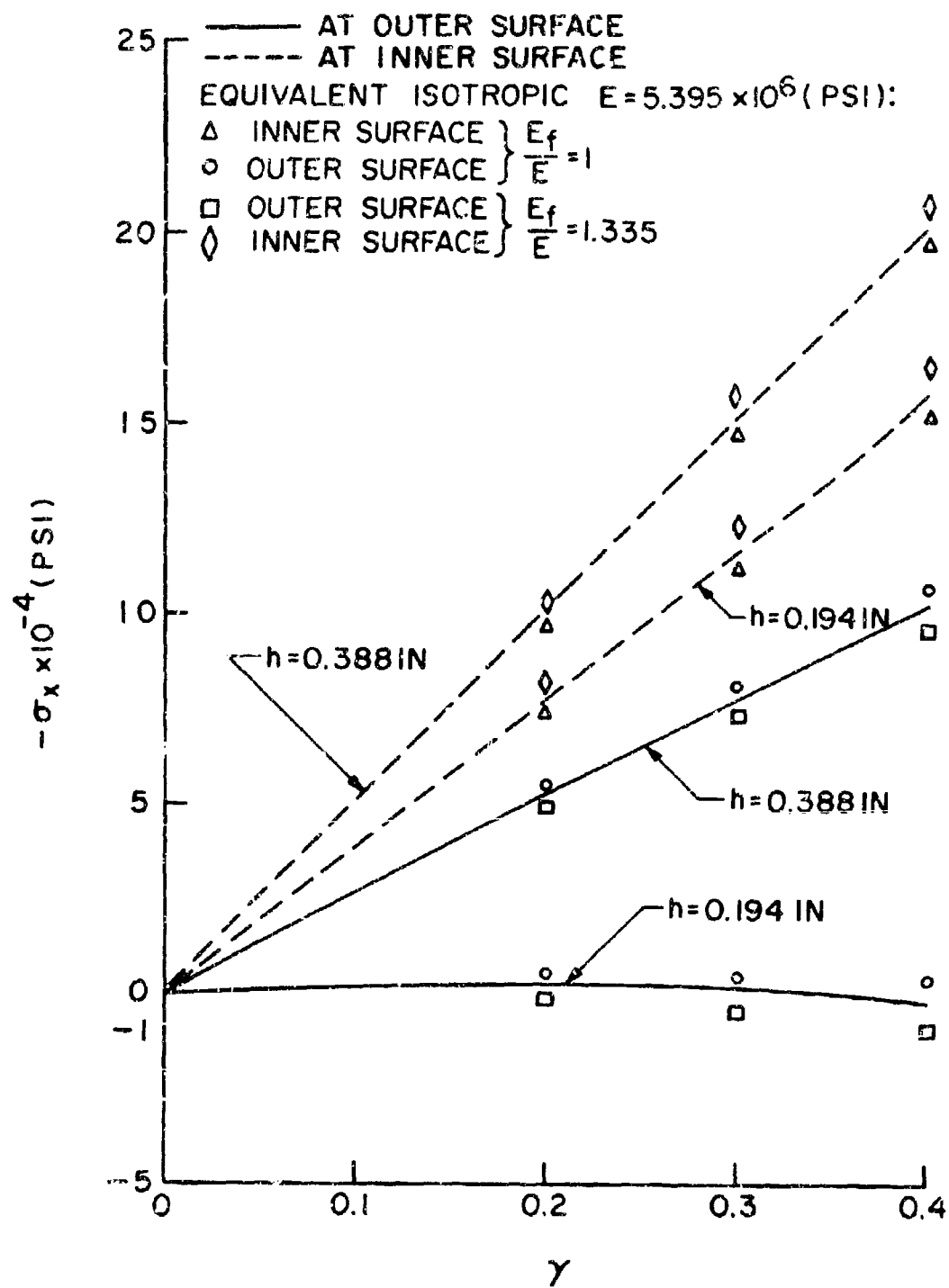


FIG. 3 AXIAL STRESSES AT FRAME

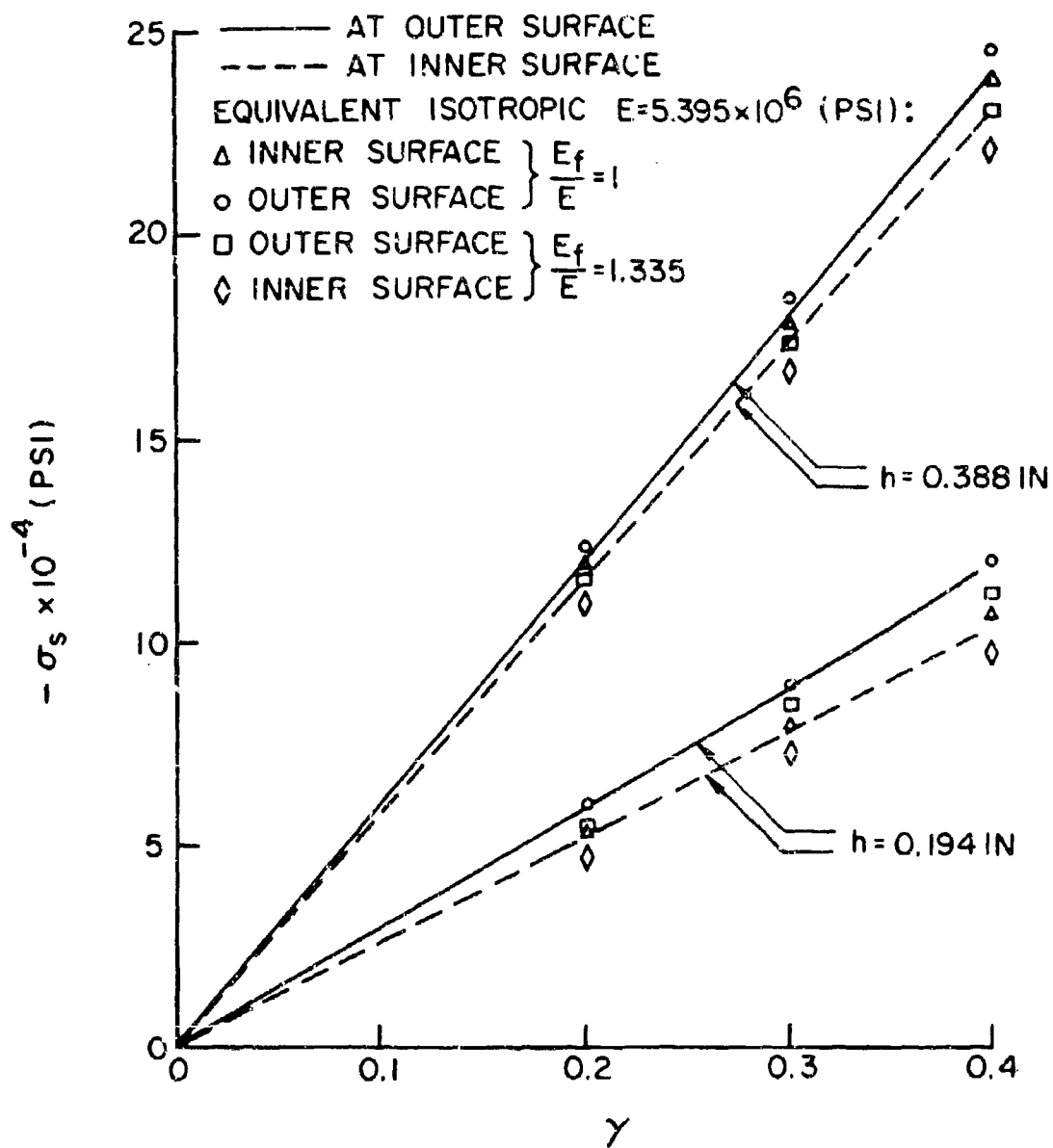


FIG. 4 CIRCUMFERENTIAL STRESSES AT MIDBAY

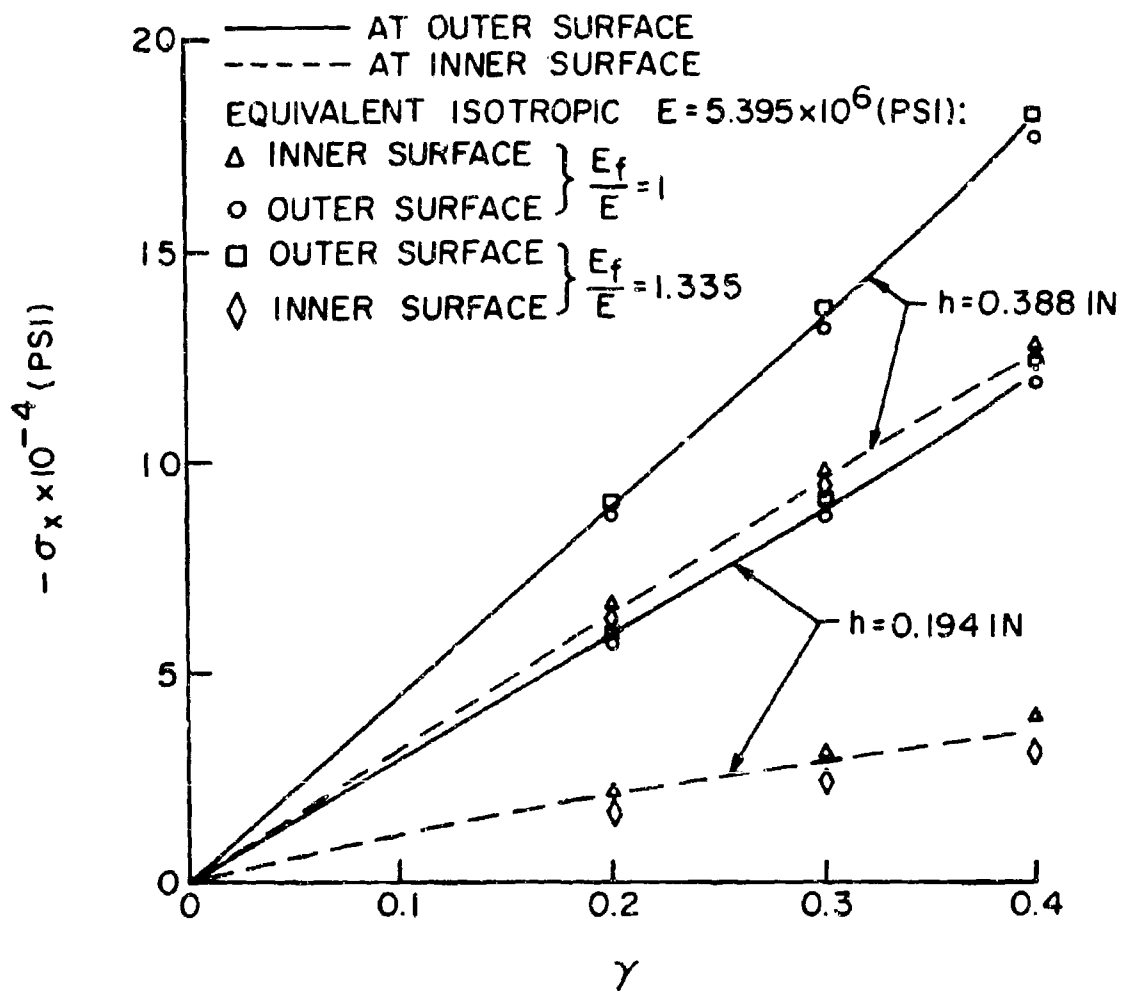


FIG. 5 AXIAL STRESSES AT MIDBAY

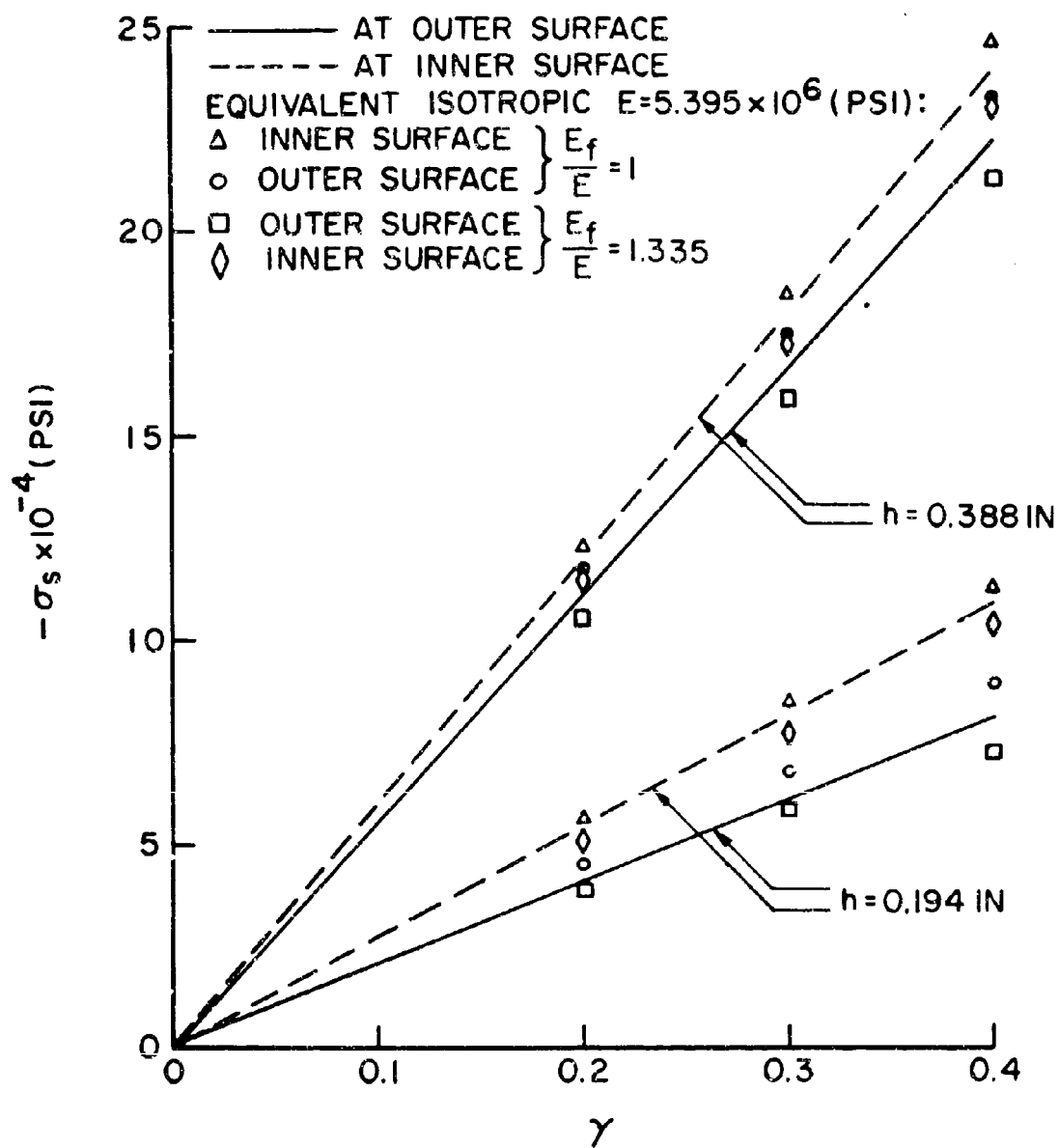


FIG. 6 CIRCUMFERENTIAL STRESSES AT FRAME

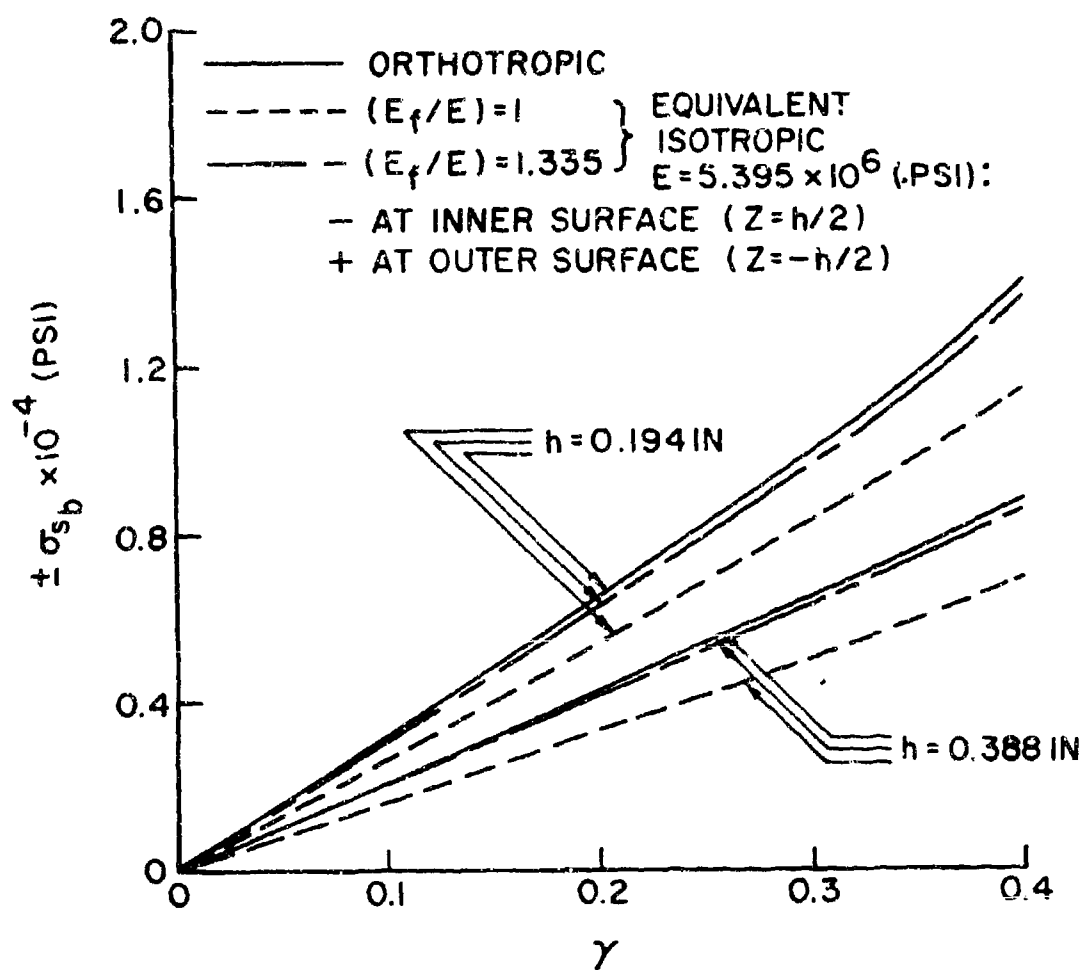


FIG. 7 CIRCUMFERENTIAL BENDING STRESSES AT FRAME

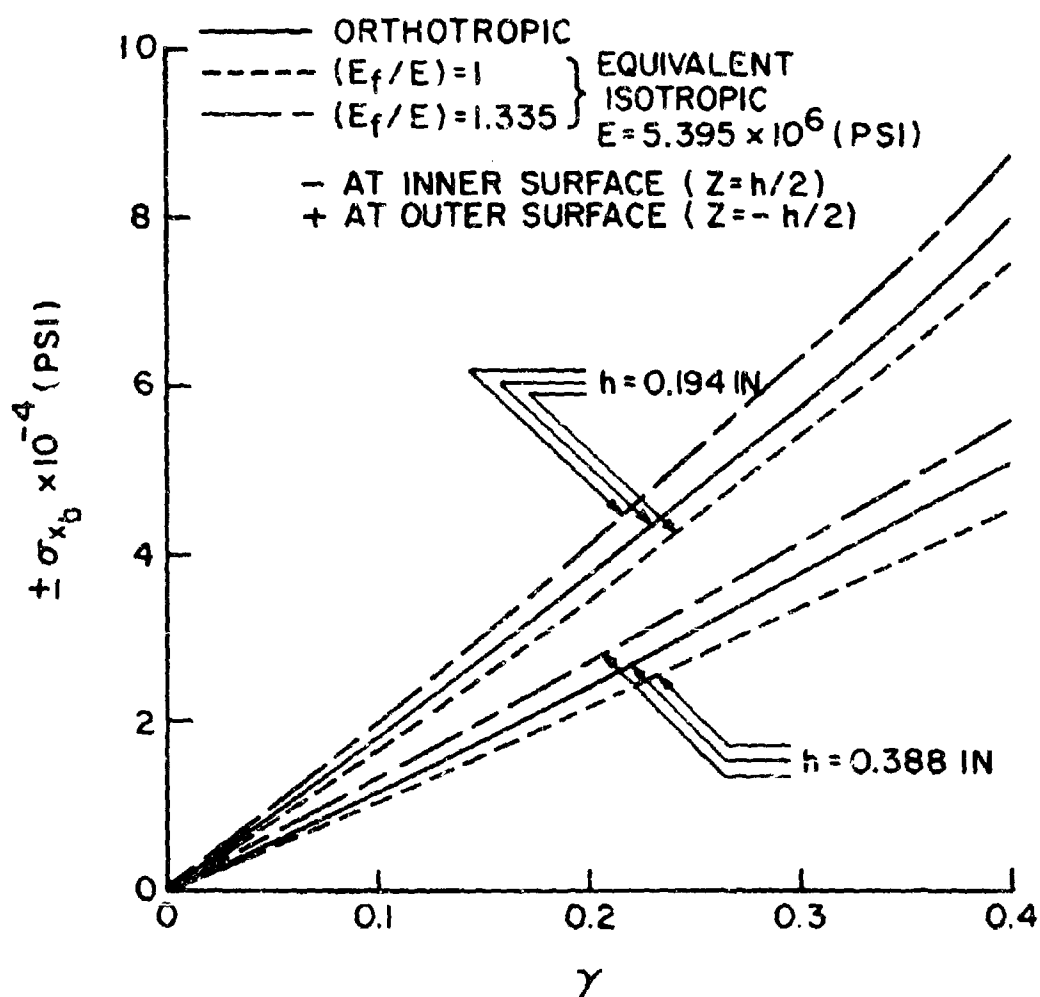


FIG. 8 AXIAL BENDING STRESSES AT FRAME

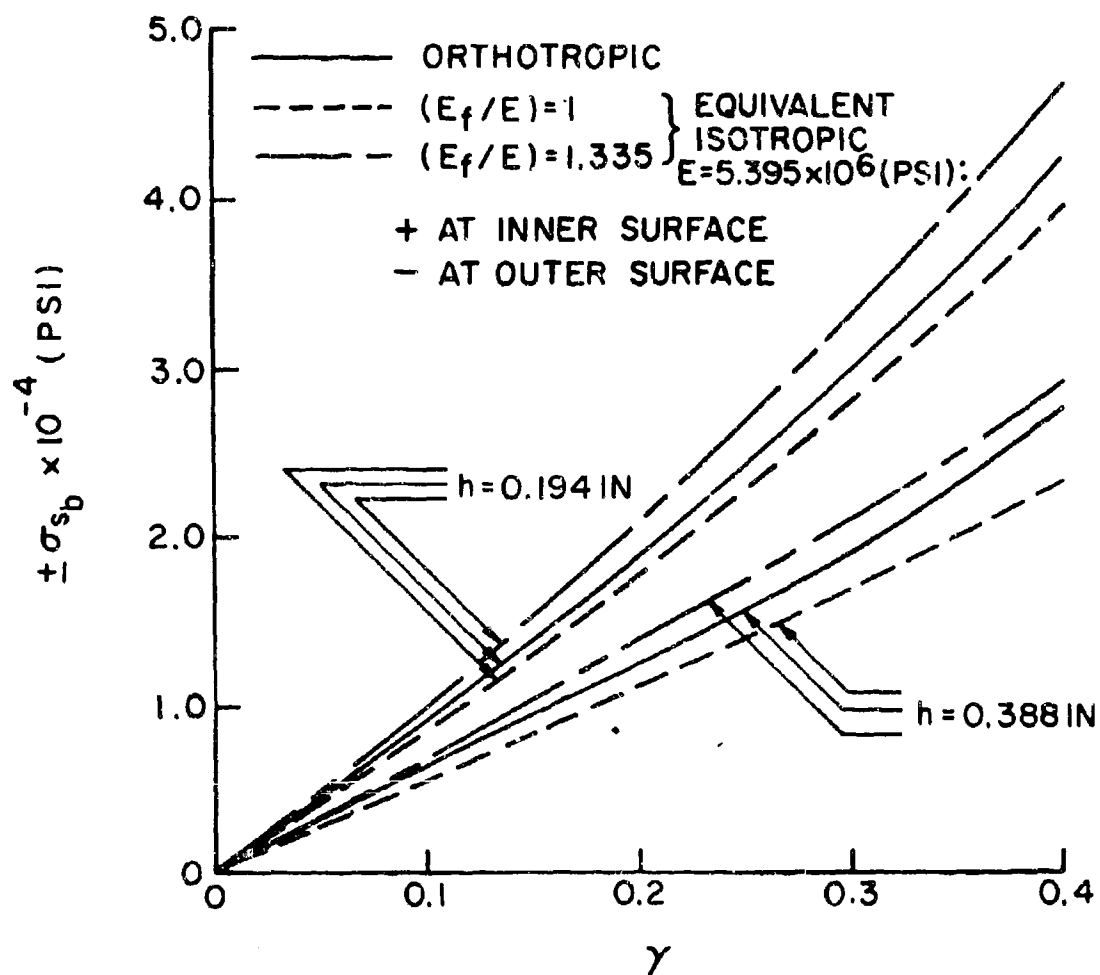


FIG. 9 AXIAL BENDING STRESSES AT MIDBAY

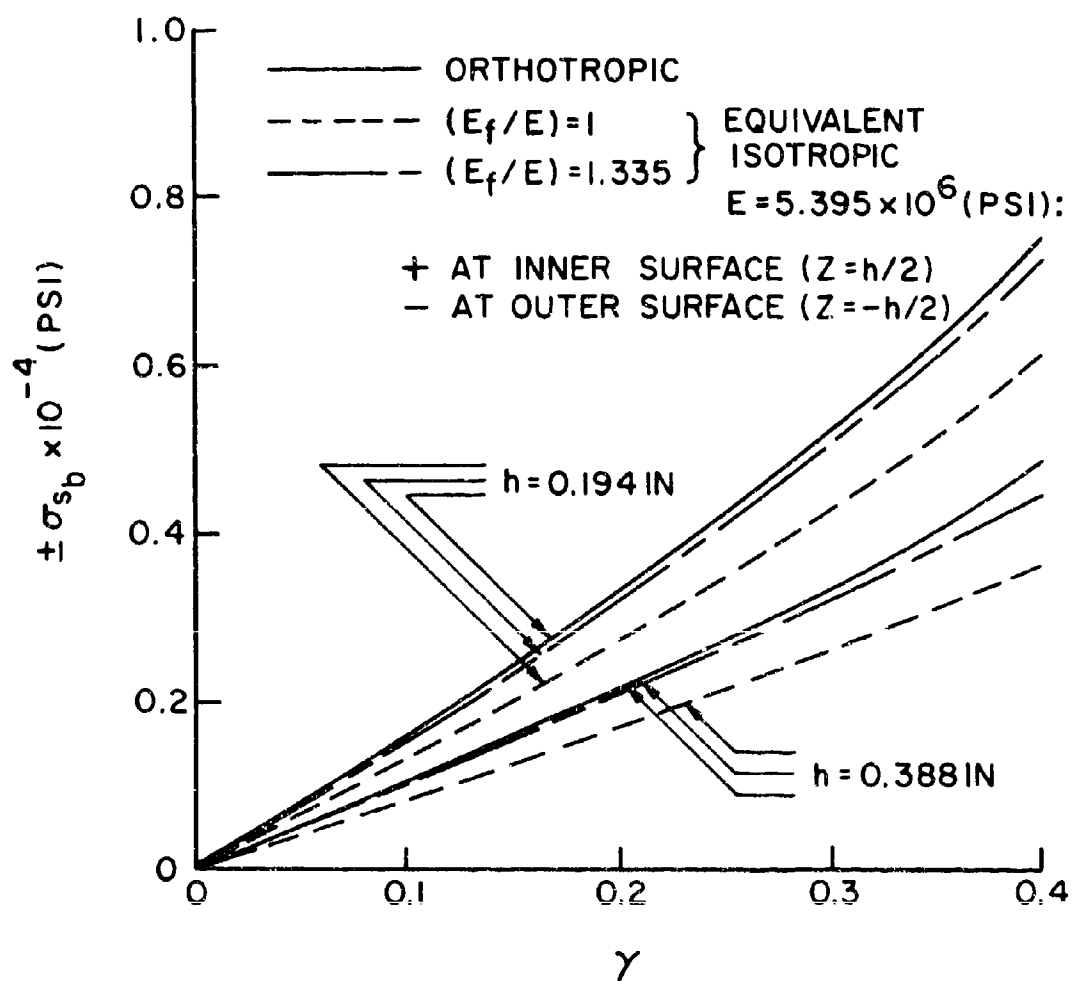


FIG. 10 CIRCUMFERENTIAL BENDING STRESSES AT MIDBAY

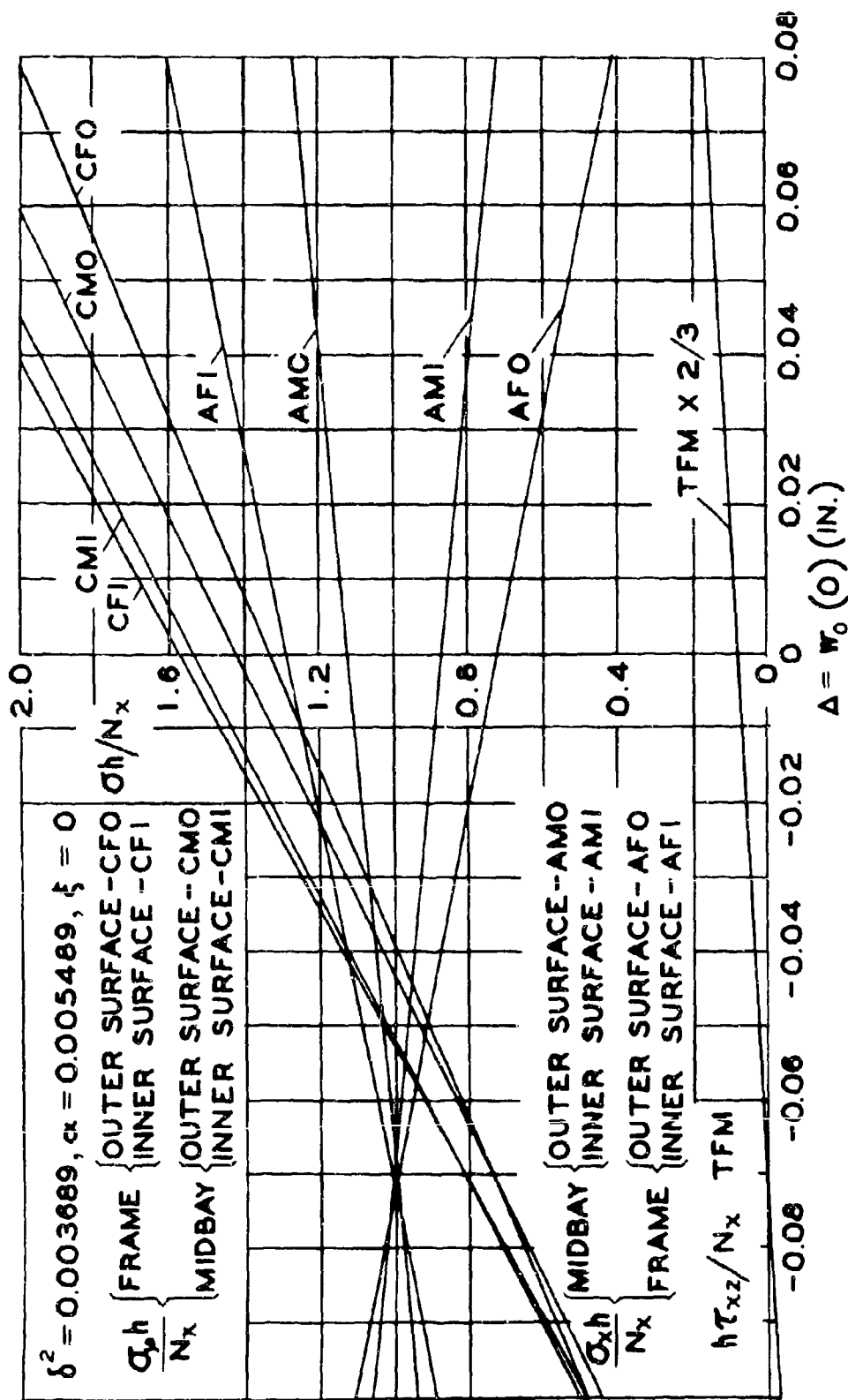


FIG. 11 EFFECT OF INITIAL DEFLECTION ON STRESSES

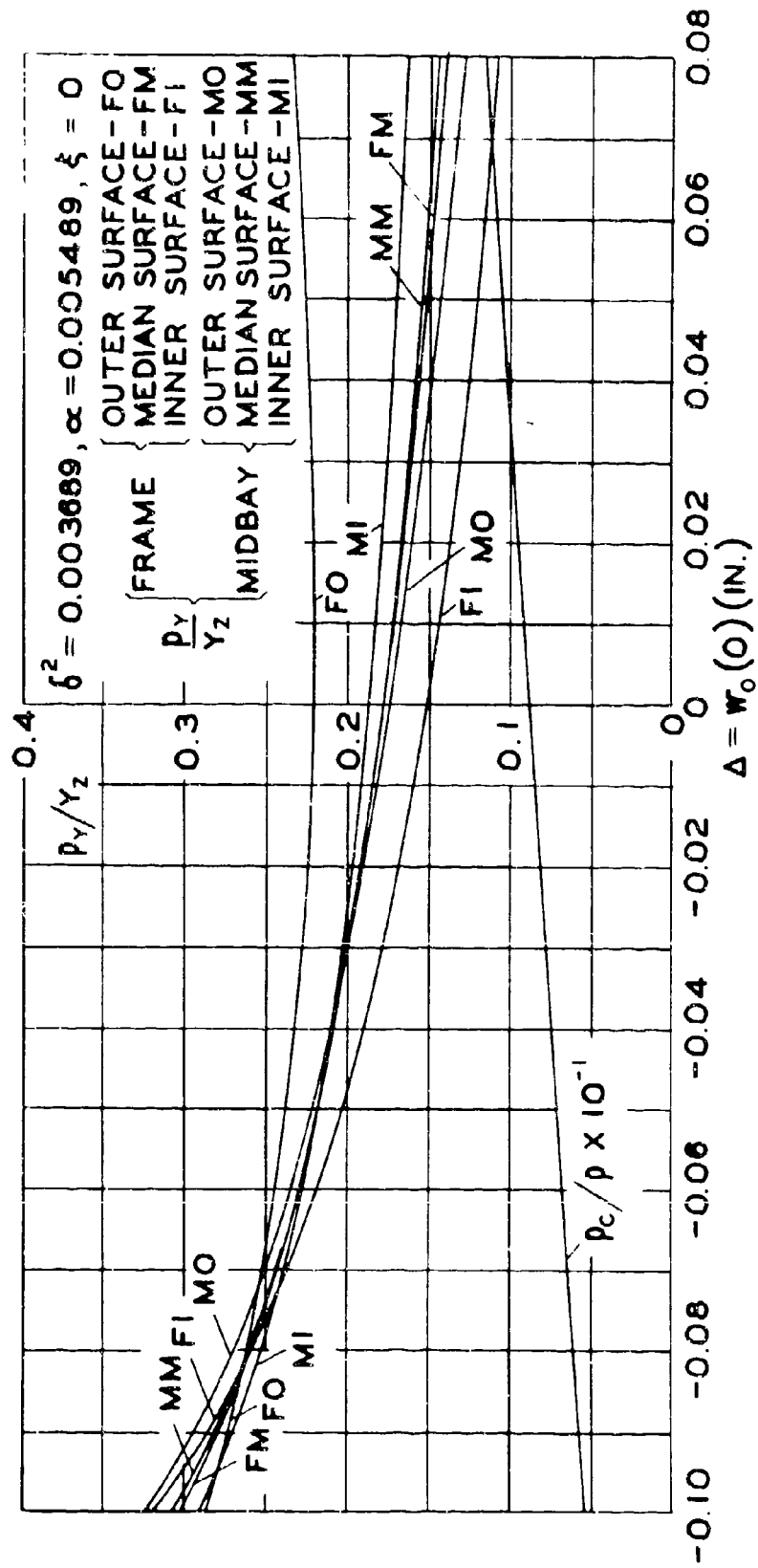


FIG. 12 EFFECT OF INITIAL DEFLECTION ON YIELD PRESSURE

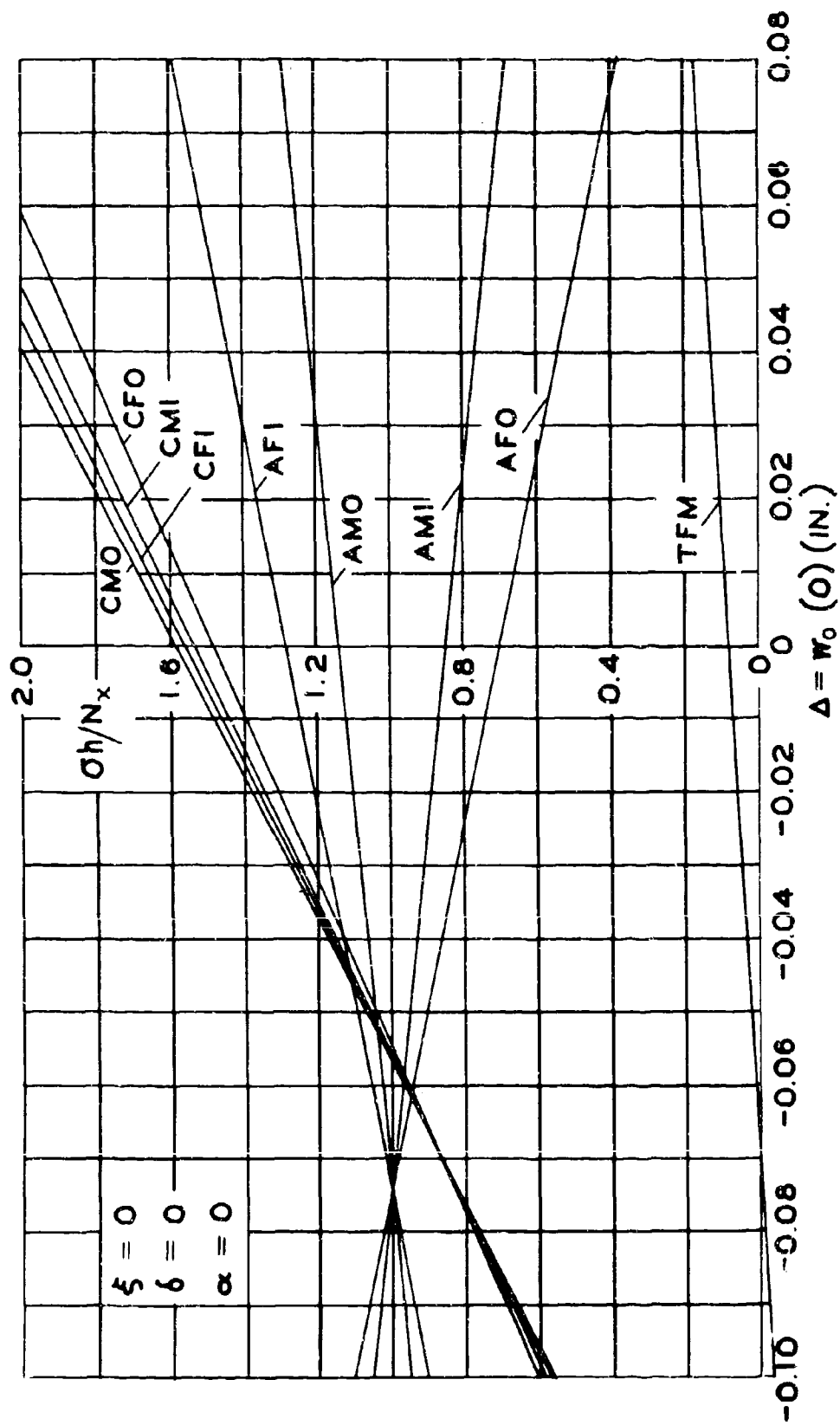


FIG. 13 EFFECT OF INITIAL DEFLECTION ON STRESSES

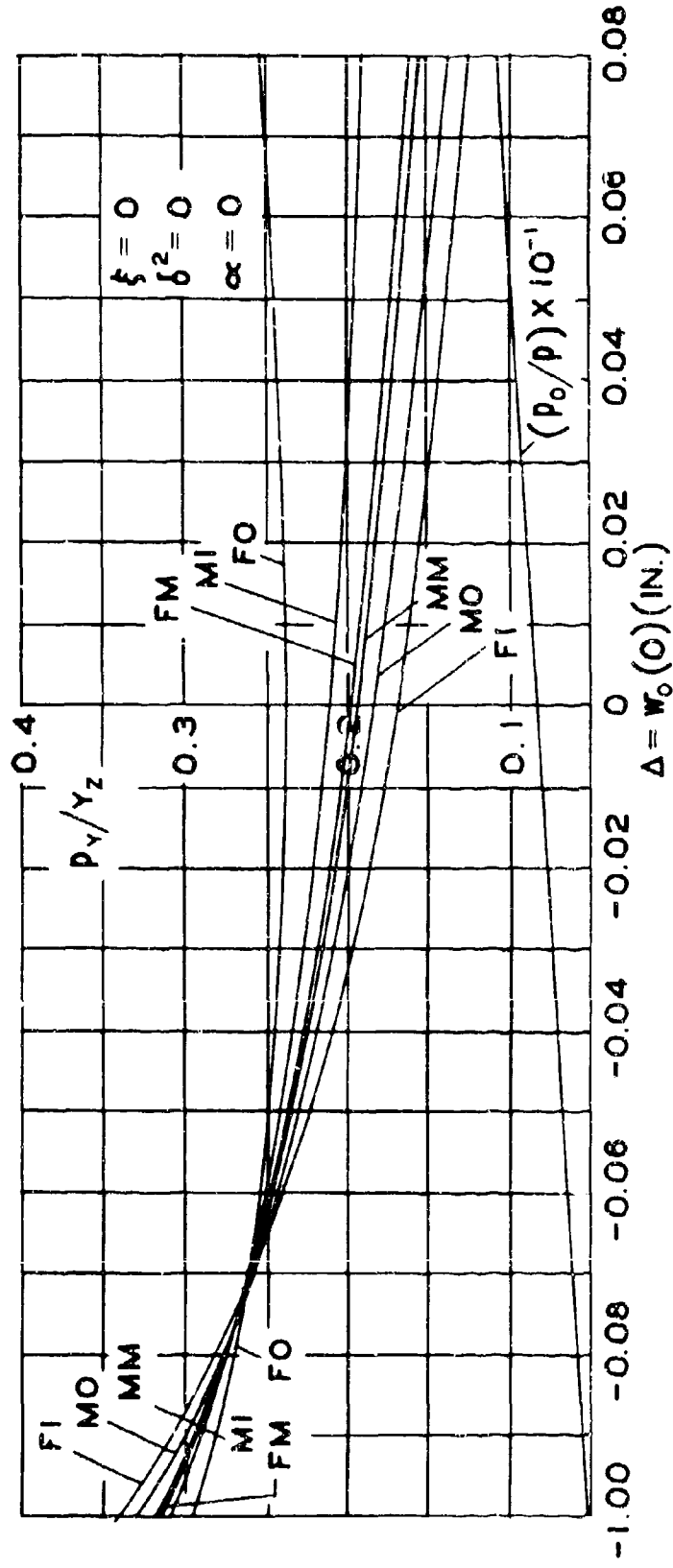


FIG. 14 EFFECT OF INITIAL DEFLECTION ON YIELD PRESSURE

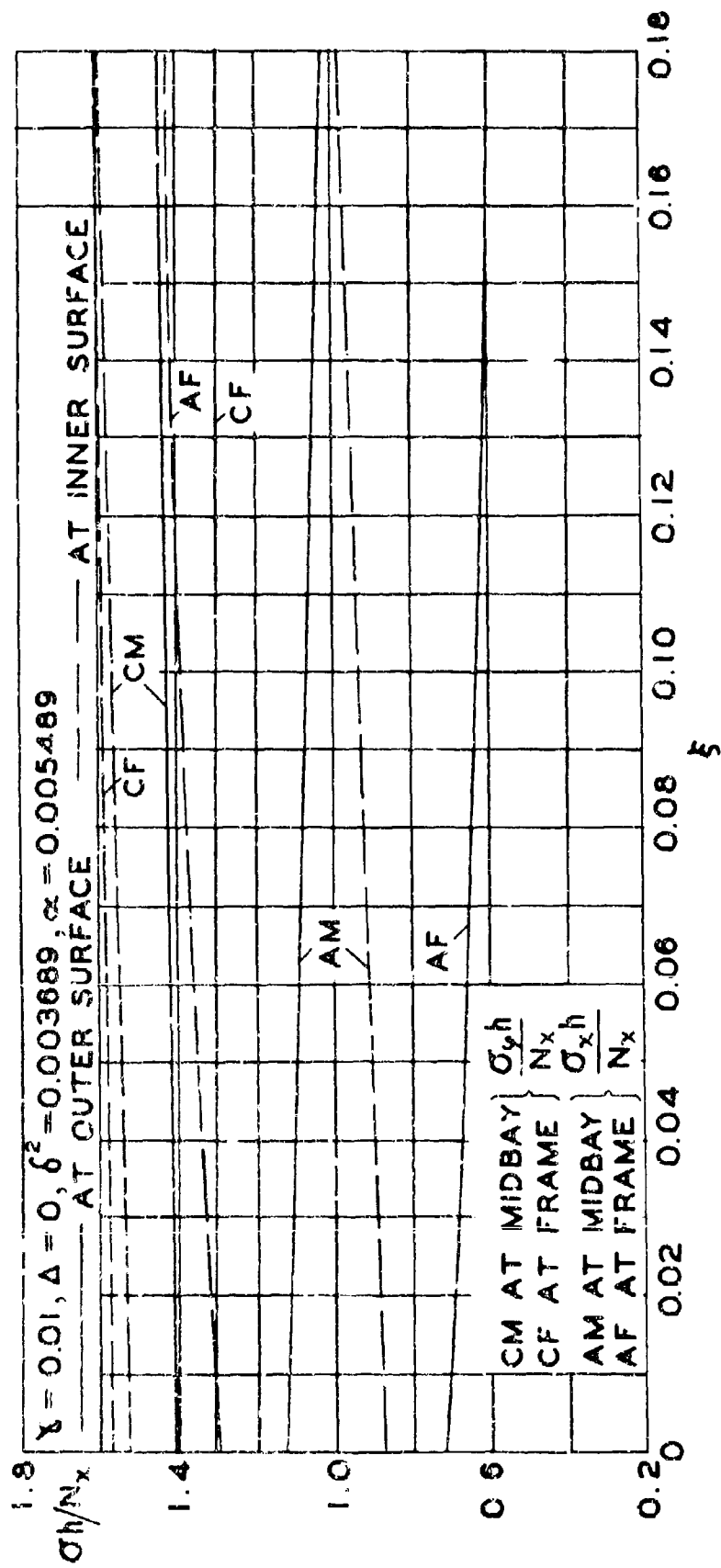


FIG. 15
EFFECTS OF TRANSVERSE SHEAR DEFORMATIONS ON STRESSES

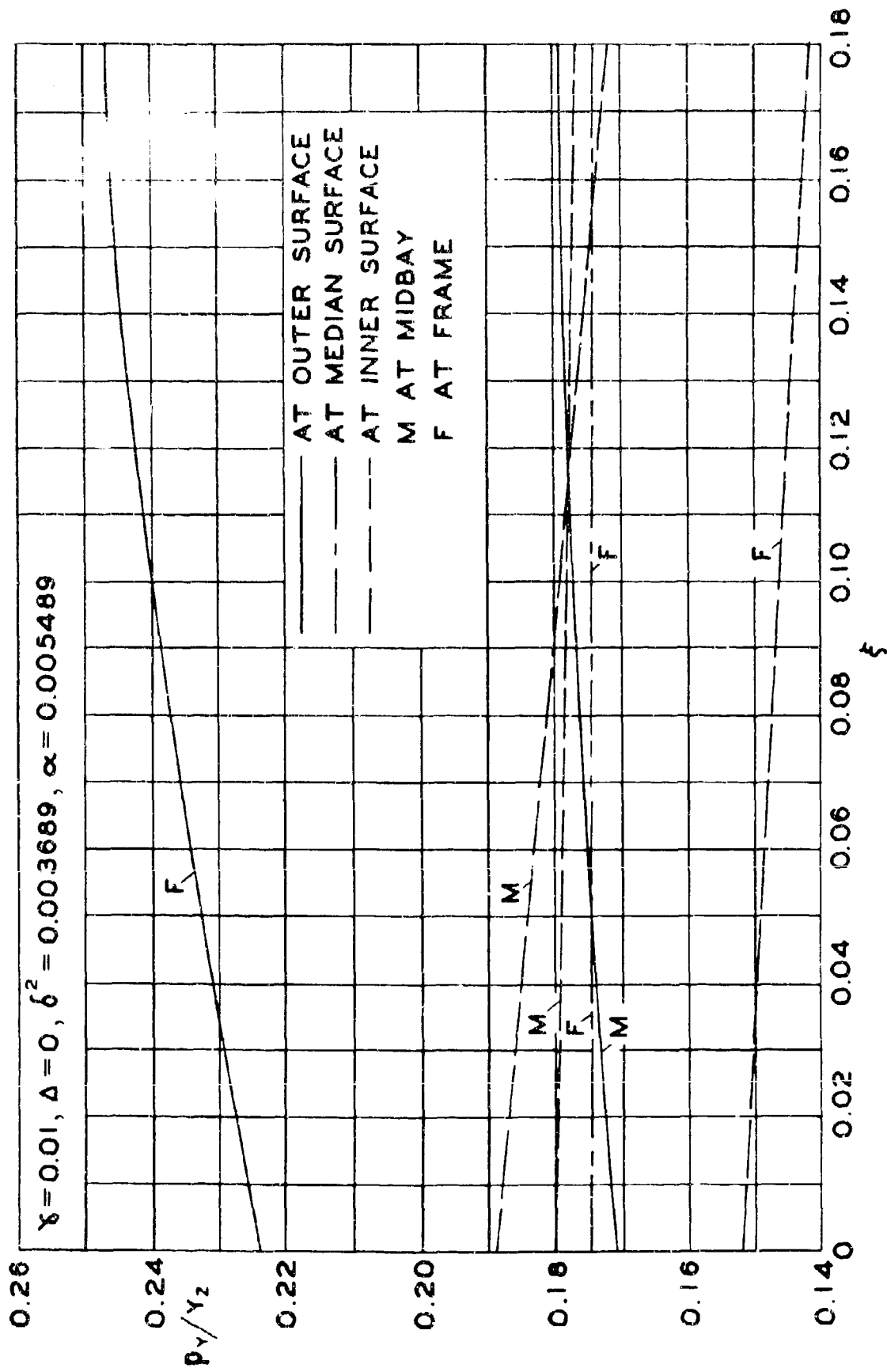


FIG. 16 EFFECTS OF TRANSVERSE SHEAR DEFORMATIONS ON YIELD PRESSURE

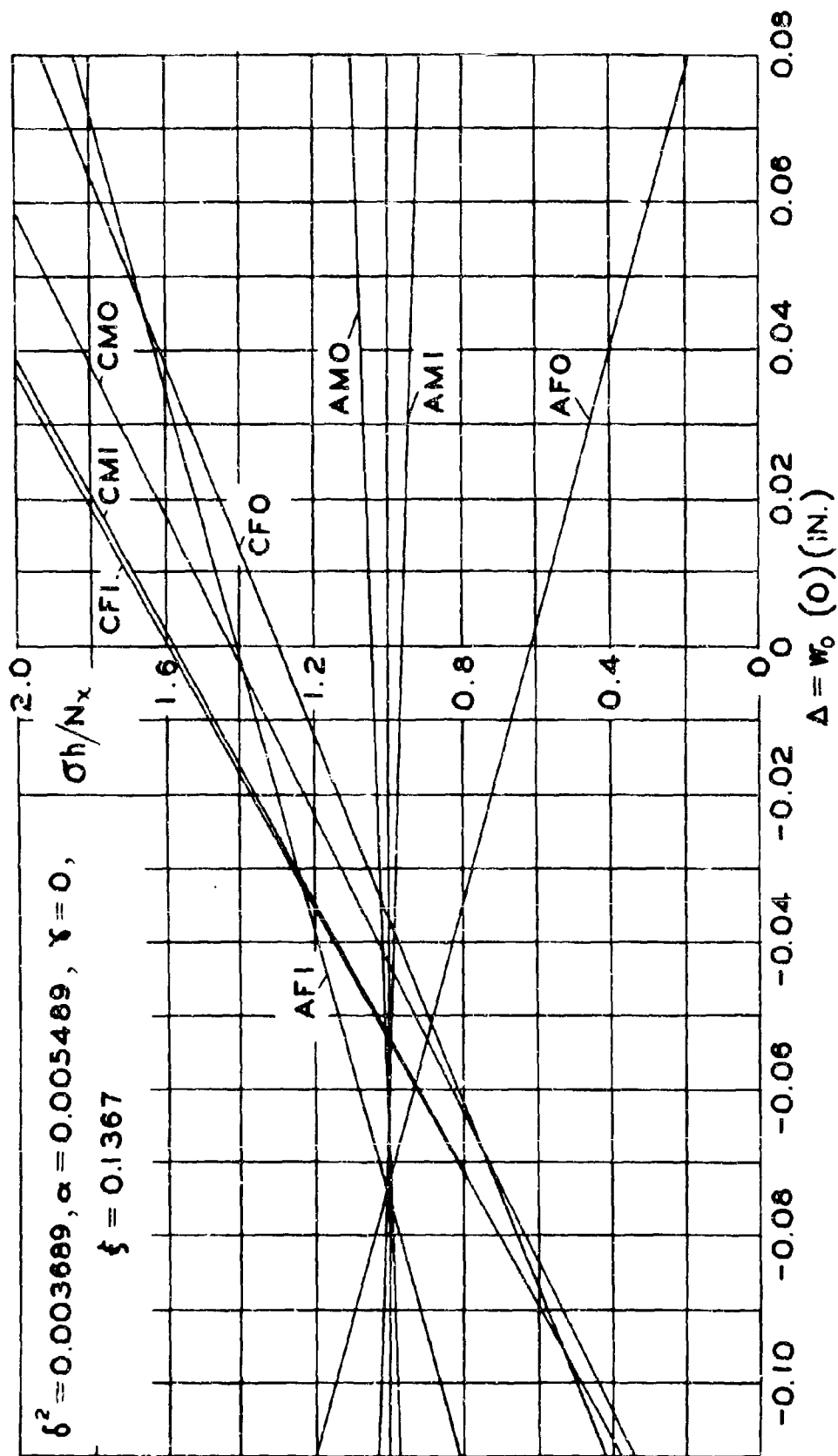


FIG. 17 EFFECTS OF INITIAL DEFLECTION ON STRESSES

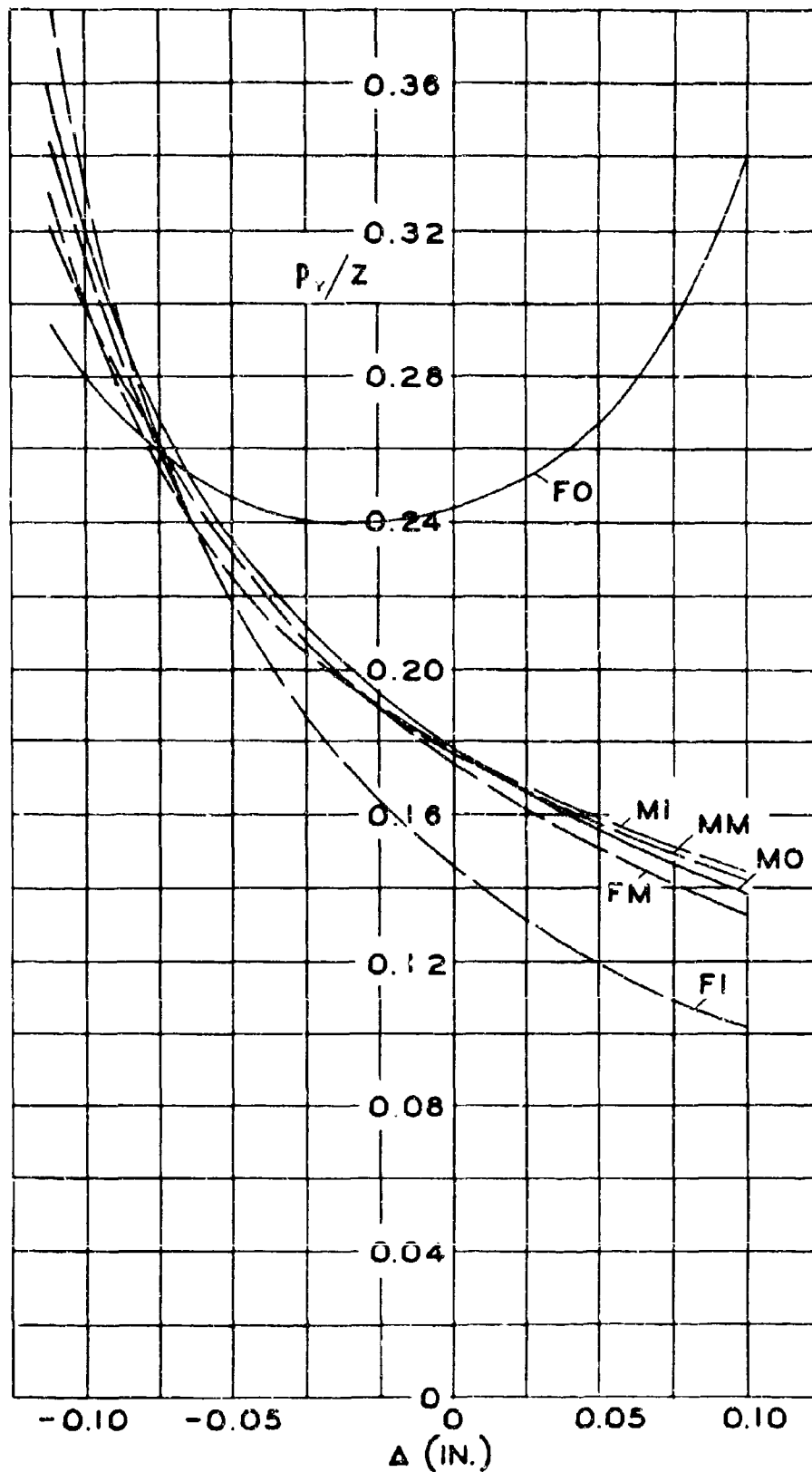


FIG. 18 EFFECTS OF INITIAL DEFLECTION
ON YIELD PRESSURE

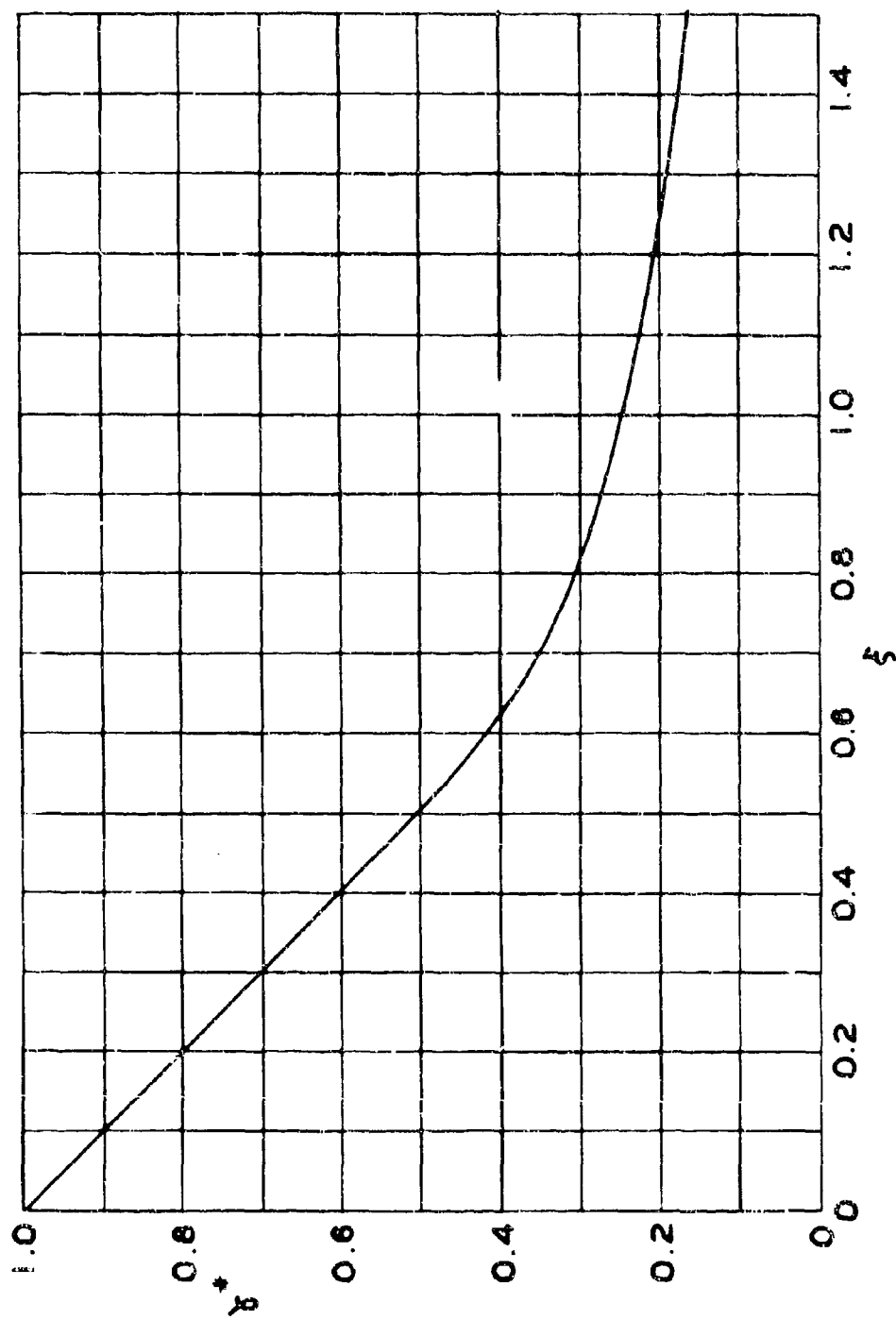


FIG. 19
BUCKLING LOAD OF INFINITE, AXIALLY COMPRESSED
CYLINDER VS TRANSVERSE SHEAR PARAMETER

UNCLASSIFIED

Security Classification

DOCUMENT CONTROL DATA - R & D

(Security classification of title, body of abstract and indexing annotation must be entered when the overall report is classified)

1. ORIGINATING ACTIVITY (Corporate, author) Polytechnic Institute of Brooklyn Dept. Aerospace Engineering & Applied Mechanics 333 Jay Street, Brooklyn, N.Y. 11201		2a. REPORT SECURITY CLASSIFICATION UNCLASSIFIED	
3. REPORT TITLE RING-STIFFENED ORTHOTROPIC CIRCULAR CYLINDRICAL SHELL UNDER HYDROSTATIC PRESSURE		2b. GROUP --	
4. DESCRIPTIVE NOTES (Type of report and inclusive dates) Research Report			
5. AUTHOR(S) (First name, middle initial, last name) Joseph Kempner; A. P. Misovec; F.C. Herzner			
6. REPORT DATE May 1968		7a. TOTAL NO. OF PAGES 128	7b. NO. OF REFS 19
8a. CONTRACT OR GRANT NO. Nonr 839(39)		9a. ORIGINATOR'S REPORT NUMBER(S) PIBAL Report No. 68-10	
b. PROJECT NO. NR 064-167		9b. OTHER REPORT NO(S) (Any other numbers that may be assigned this report)	
10. DISTRIBUTION STATEMENT ONR & DDC Distribution of this document is unlimited			
11. SUPPLEMENTARY NOTES ---		12. SPONSORING MILITARY ACTIVITY Office of Naval Research Washington, D.C.	
13. ABSTRACT A ring-reinforced, orthotropic circular cylindrical shell subjected to external hydrostatic pressure loading is investigated. The stresses and deflections throughout the shell are determined by a shell theory which considers the combined and separate effects of large rotations, transverse shear deformation, initial deflections and Flugge type thickness terms. The ring deformations are described by both a deep ring theory and a plane strain analysis. The results are used in the development of pertinent design formulae. Numerical results applicable to a typical glass-reinforced-plastic shell indicate that the nonlinear effects may be accurately provided for by using a perturbation solution. Hill's criterion for yielding of an orthotropic material as well as an analysis to approximate the actual stresses in the constituent materials of a nonhomogeneous shell are also applied.			

UNCLASSIFIED

Security Classification

14	KEY WORDS	LINK A		LINK B		LINK C	
		ROLE	WT	ROLE	WT	ROLE	WT
	orthotropic shell filament wound composite shell ring-reinforced shell hydrostatic pressure shear deformation						

UNCLASSIFIED

Security Classification

AD 670 519

POLYTECHNIC INSTITUTE OF BROOKLYN

E R R A T A

RING-STIFFENED ORTHOTROPIC CIRCULAR CYLINDRICAL SHELL UNDER
HYDROSTATIC PRESSURE

by

Joseph Kempner, A. P. Misovec and F. C. Herzner
May 1968

p. 90 Replace Table 3 by the enclosed

Fig. 12 Replace by the enclosed

PIBAL REPORT NO. 68-10

Reprinted by the
CLEARINGHOUSE
for Federal Scientific & Technical
Information Springfield, Va. 22151

TABLE 3. TRANSVERSE SHEAR DEFORMATION AND BEAM COLUMN EFFECTS

$\bar{\nu} = 0.2$		$\nu = 0$		$\nu = 0.2$	
		MIDBAY	FRAME	MIDBAY	FRAME
$\frac{E_x w}{N_x}$		- 8.194 ^{***} - 8.319 ^{**}	- 8.011 - 7.921	- 8.200 - 8.792	- 8.008 - 8.372
$\frac{\sigma_x h}{N_x}$	MEMBRANE	0.9972 0.9990	1.006 1.007	0.9970 0.9985	1.006 1.008
	BENDING	\pm 0.128 \pm 0.0385	\pm 0.292 \pm 0.380	\pm 0.136 \pm 0.064	\pm 0.300 \pm 0.394
$\frac{\sigma_y h}{N_x}$	MEMBRANE	1.463 1.483	1.436 1.423	1.465 1.557	1.436 1.493
	BENDING	\pm 0.0525 \pm 0.0730	\pm 0.128 \pm 0.143	\pm 0.0345 \pm 0.0730	\pm 0.129 \pm 0.150
$\frac{\sigma_z h}{N_x}$	INNER SURFACE	1.525 1.562	1.509 1.570	1.524 1.636	1.570 1.648
	OUTER SURFACE	1.412 1.416	1.313 1.284	1.415 1.490	1.311 1.349
$\frac{\sigma_x h}{N_x}$	INNER SURFACE	0.8697 0.9614	1.297 1.388	0.8610 0.9353	1.307 1.402
	OUTER SURFACE	1.126 1.038	0.7157 0.6280	1.134 1.063	0.7063 0.6146
$\frac{\tau_{xz} h}{N_x}$	MEDIAN SURFACE	0 0	0.1291 0.1265	0 0	0.1290 0.1245
$\frac{P_y}{Y_z}$	INNER SURFACE	0.1883 0.1769	0.1517 0.1465	0.1893 0.1752	0.1511 0.1424
	MEDIAN SURFACE	0.1794 0.1780	0.1744 0.1752	0.1794 0.1738	0.1744 0.1715
	OUTER SURFACE	0.1717 0.1787	0.2236 0.2413	0.1709 0.1721	0.2253 0.2379

^{***} $\xi = 0$ $p_c/p = 1.036$, 1.036

^{**} $\xi = 0.1367$, $p_c/p = 1.028$, 1.023

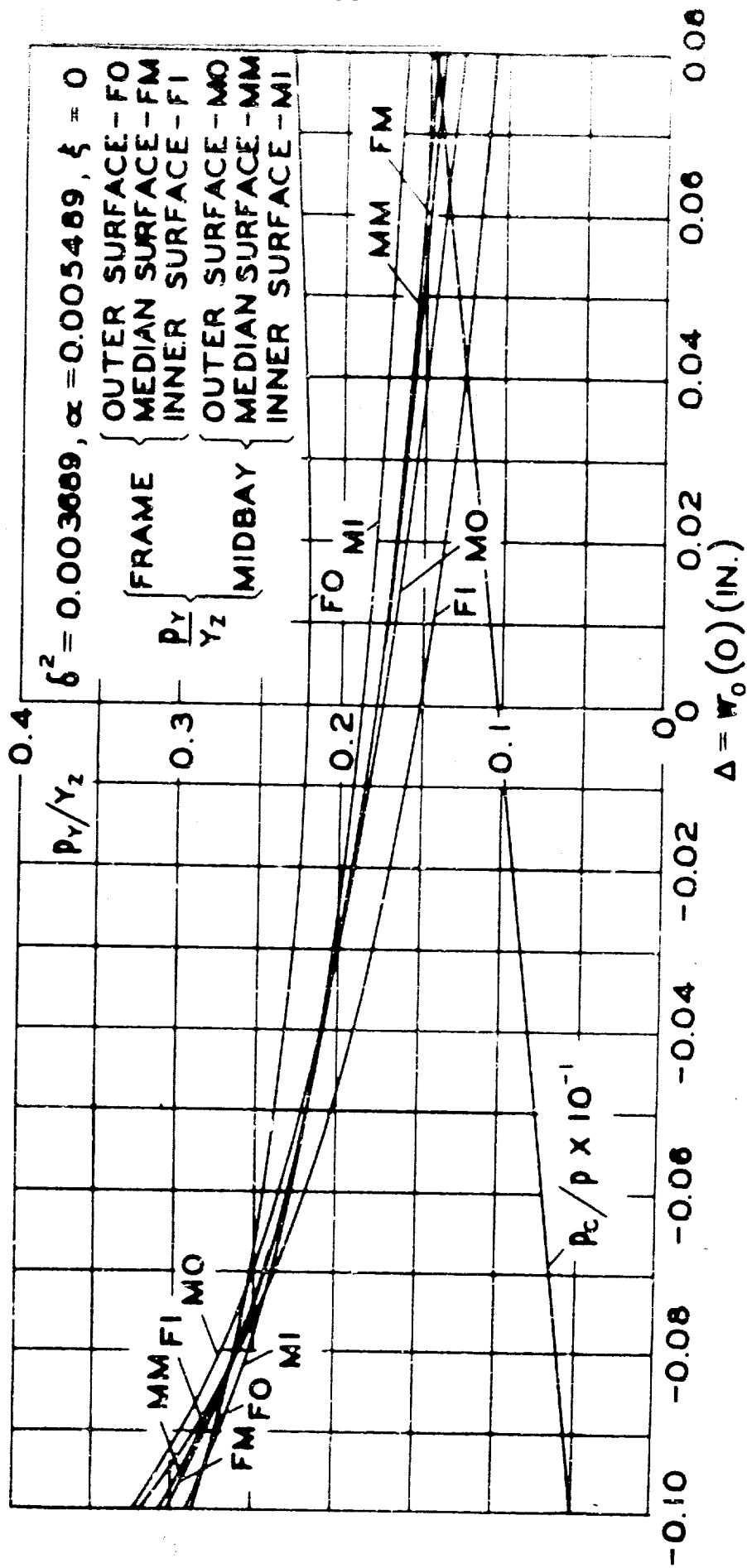


FIG. 12 EFFECT OF INITIAL DEFLECTION ON YIELD PRESSURE